University of Ljubljana

“Jožef Stefan” Institute

Introduction to Experimental Particle Physics

Peter Križan

University of Ljubljana and J. Stefan Institute

1st Nagoya Winter School, Ise-Shima, Februar 2009

Contents of this course

- Lecture 1: Introduction, experimental methods, detectors, data analysis
- Lecture 2: Selection of particle physics experiments

http://www-f9.ijs.si/~krizan/sola/nagoya-ise/

- Slides
- Literature

Contents

Introduction

Experimental methods

Accelerators

Spectrometers

Particle detectors

Analysis of data

Particle physics experiments

Accelerate elementary particles, let them collide → energy released in the collision is converted into mass of new particles, some of which are unstable

Two ways how to do it:

Fixed target experiments

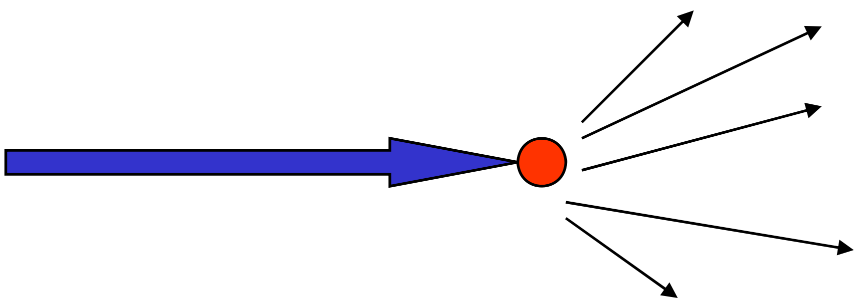

Collider experiments

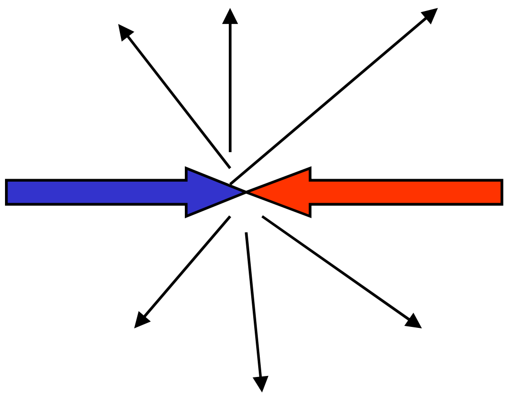

How to accelerate charged particles?

- Acceleration with electromagnetic waves (typical frequency is 500 MHz – mobile phones run at 900, 1800, 1900 MHz)
- Waves in a radiofrequency cavity: $c<c_0$

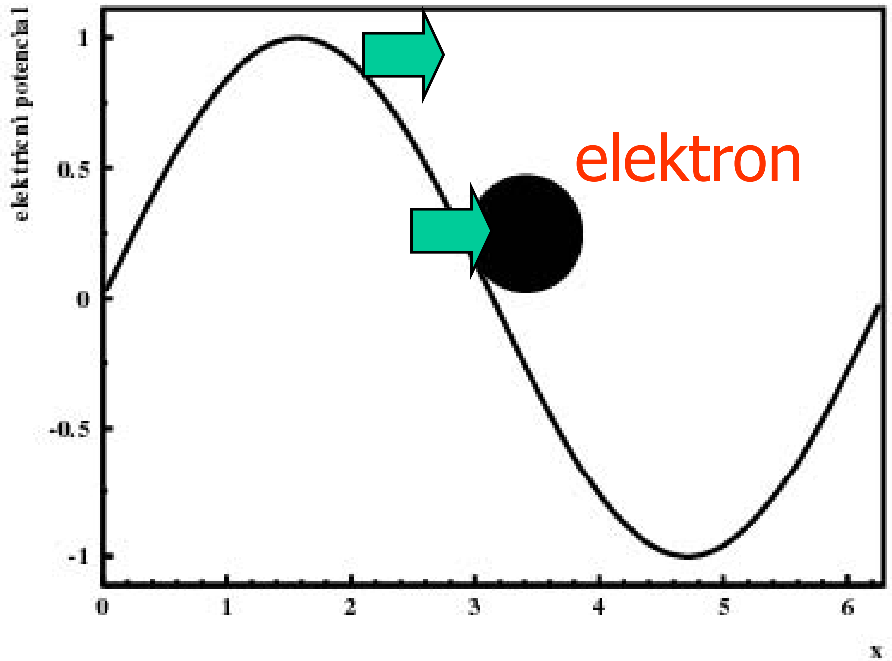

... Similar to surfing the waves

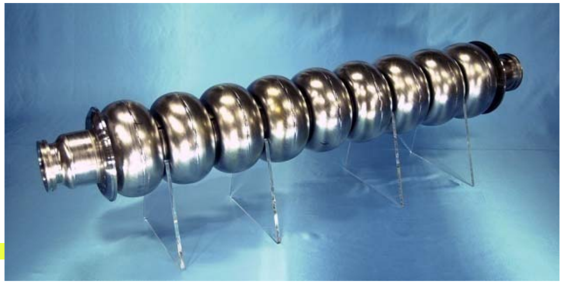

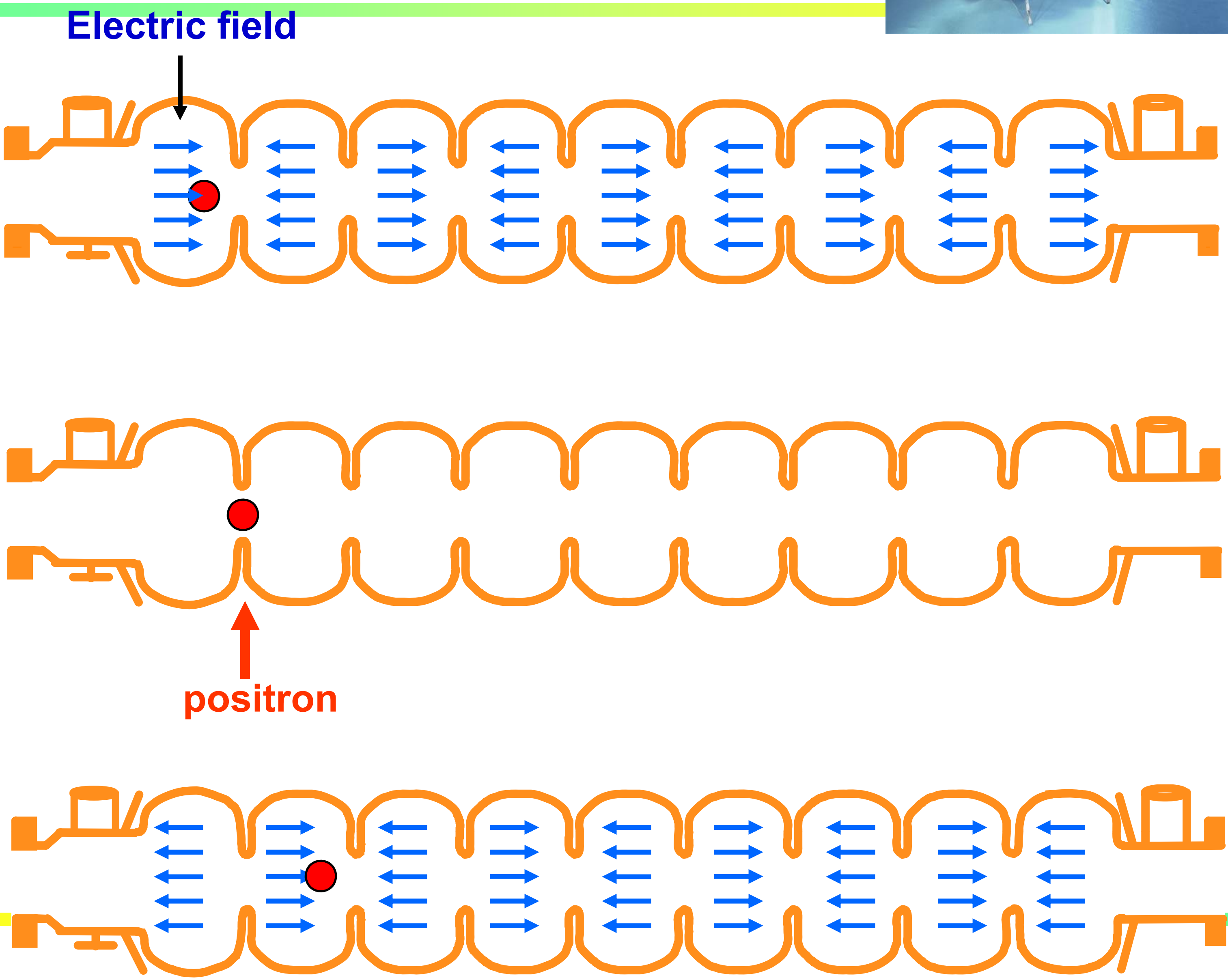

Electric field
positron

Stability of acceleration

- For a synchronous particles (A): energy loss = energy received from the RF field
- A particle that comes too late (B), gets more energy, the one that is too fast (C), gets less →

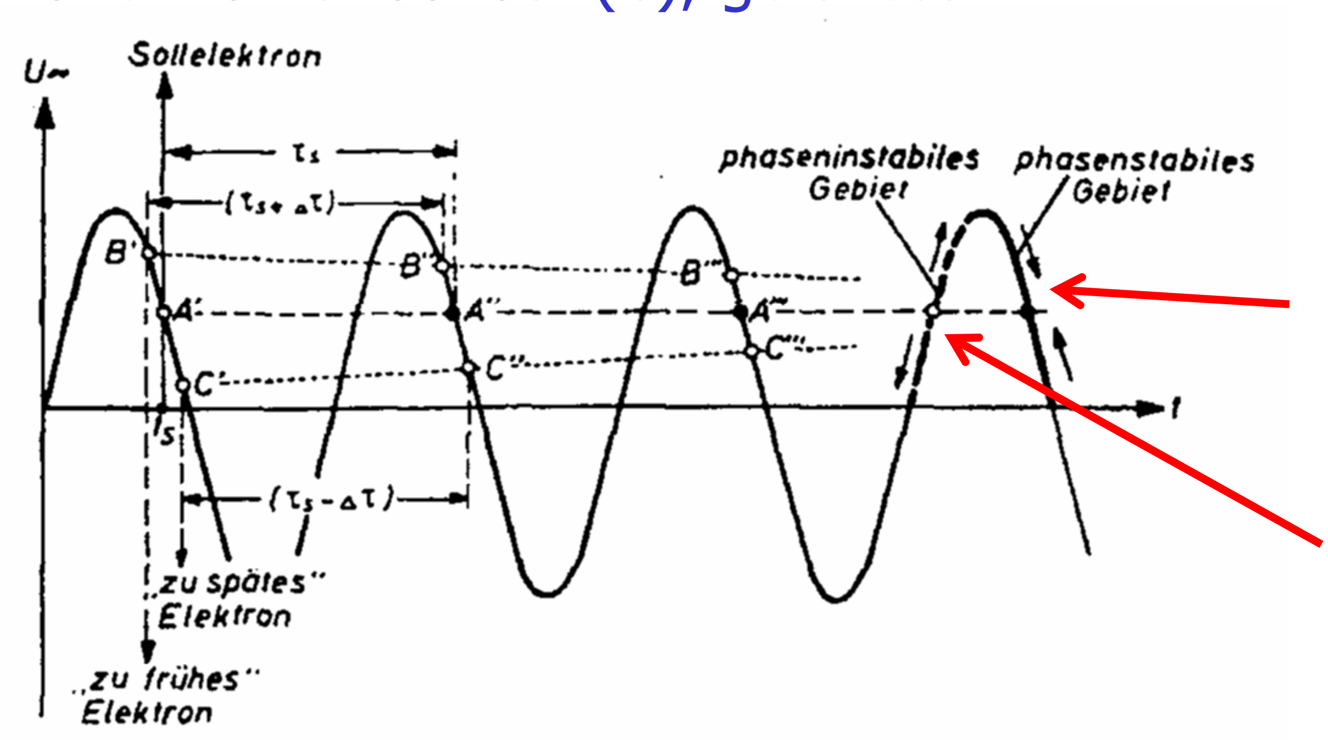

- OK if particle ~ in phase→ stable orbit
- Not OK if too far away

Synchrotron

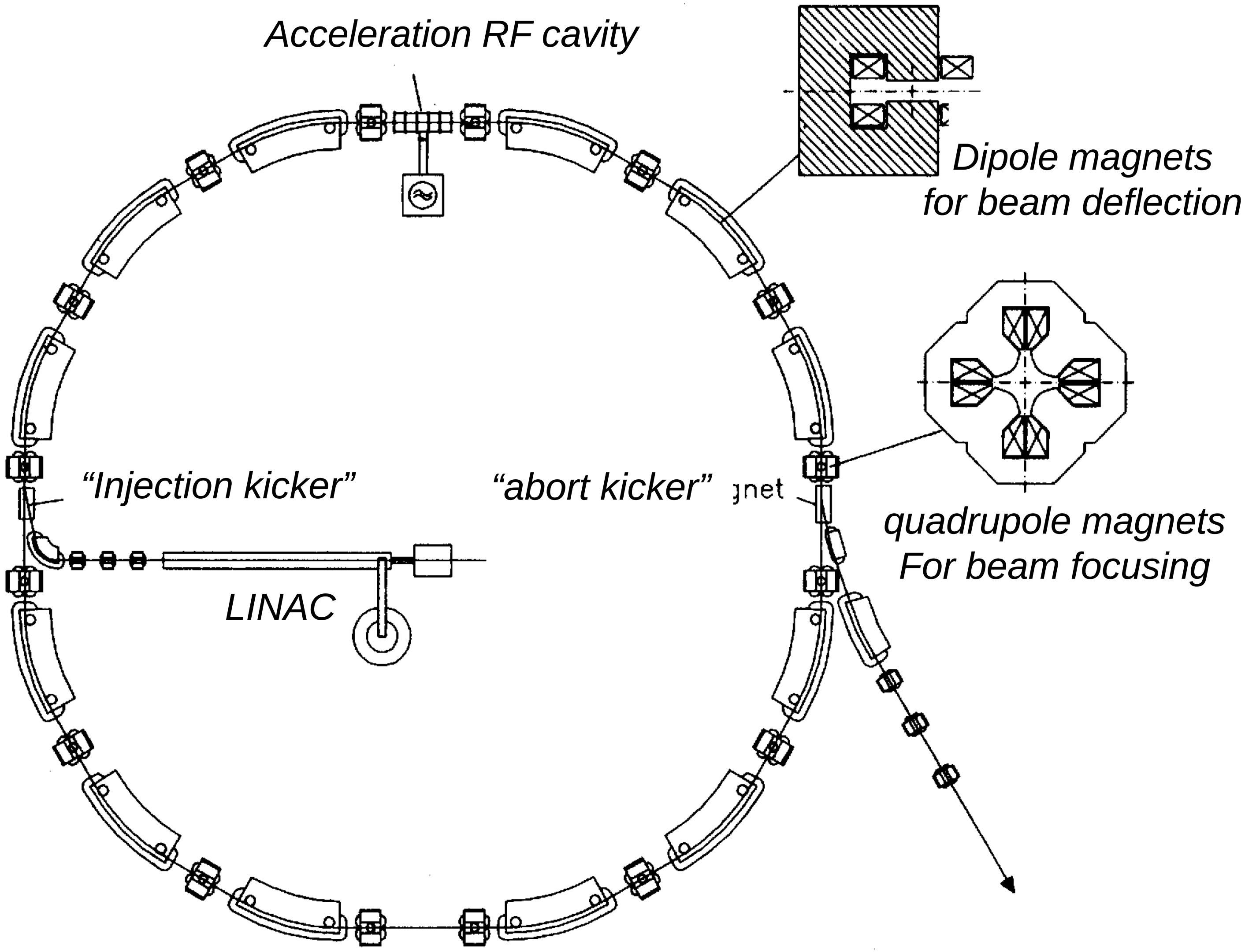

Electron position collider: KEK-B

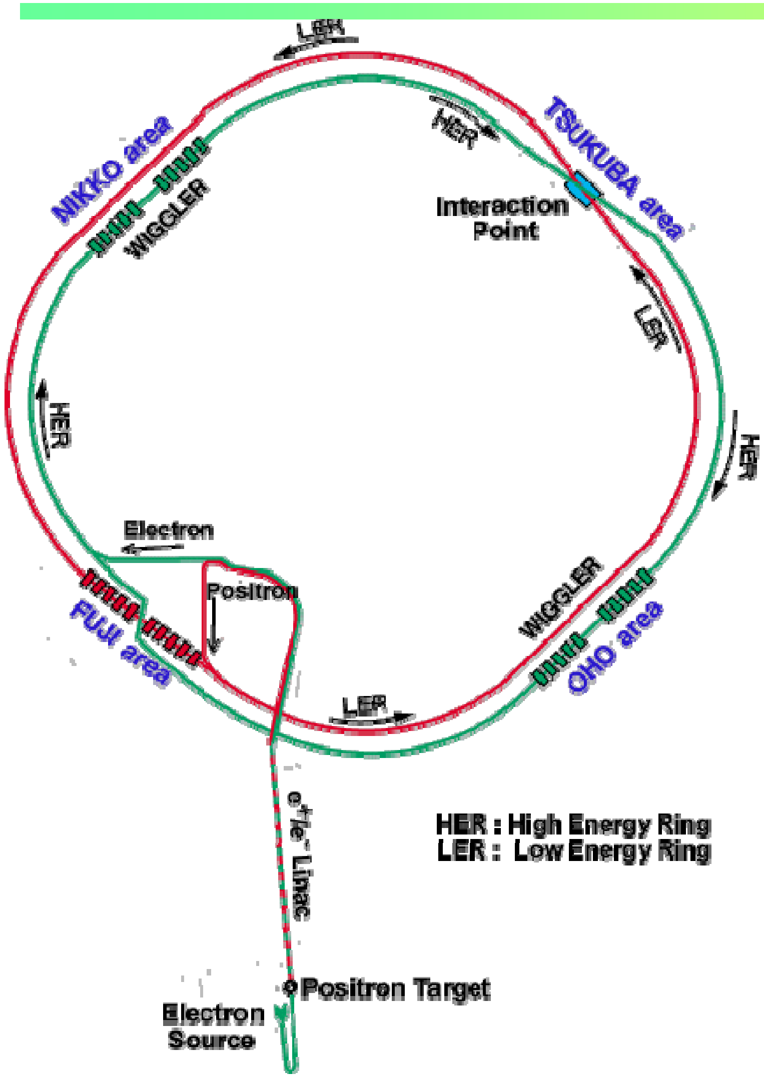

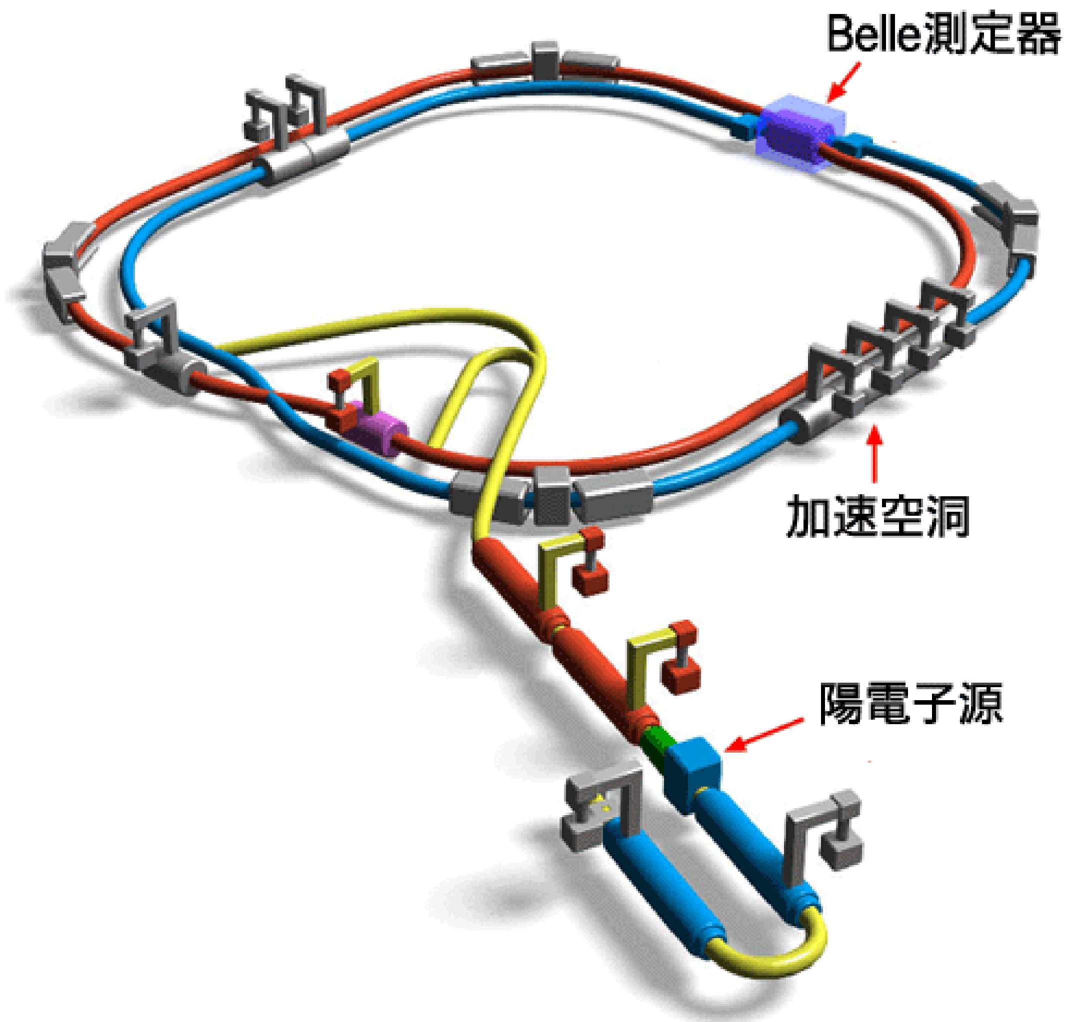

Large hadron collider

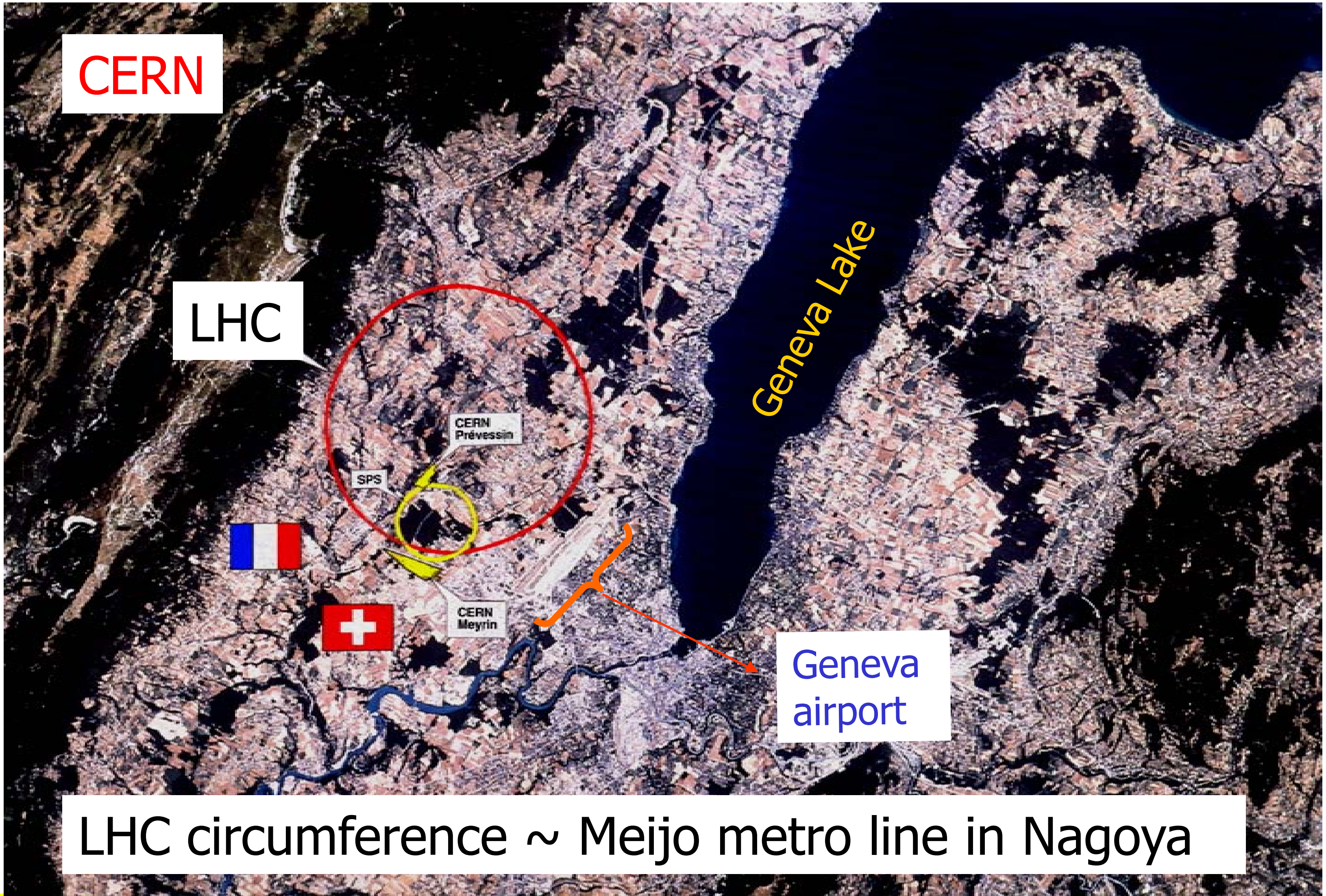

Interaction region: BaBar

Head-on collisions

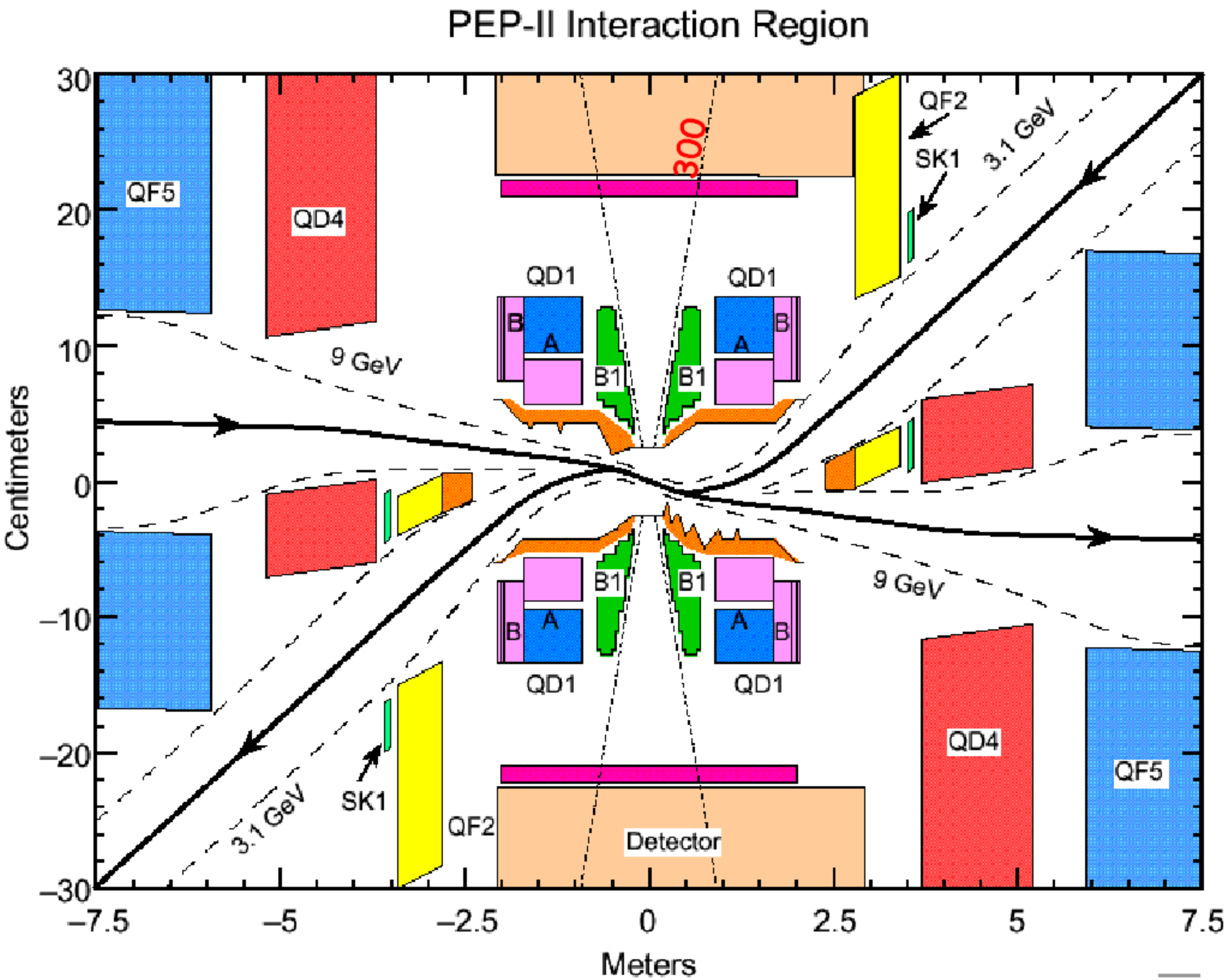

Interaction region: Belle

Collisions at a finite angle +-11mrad

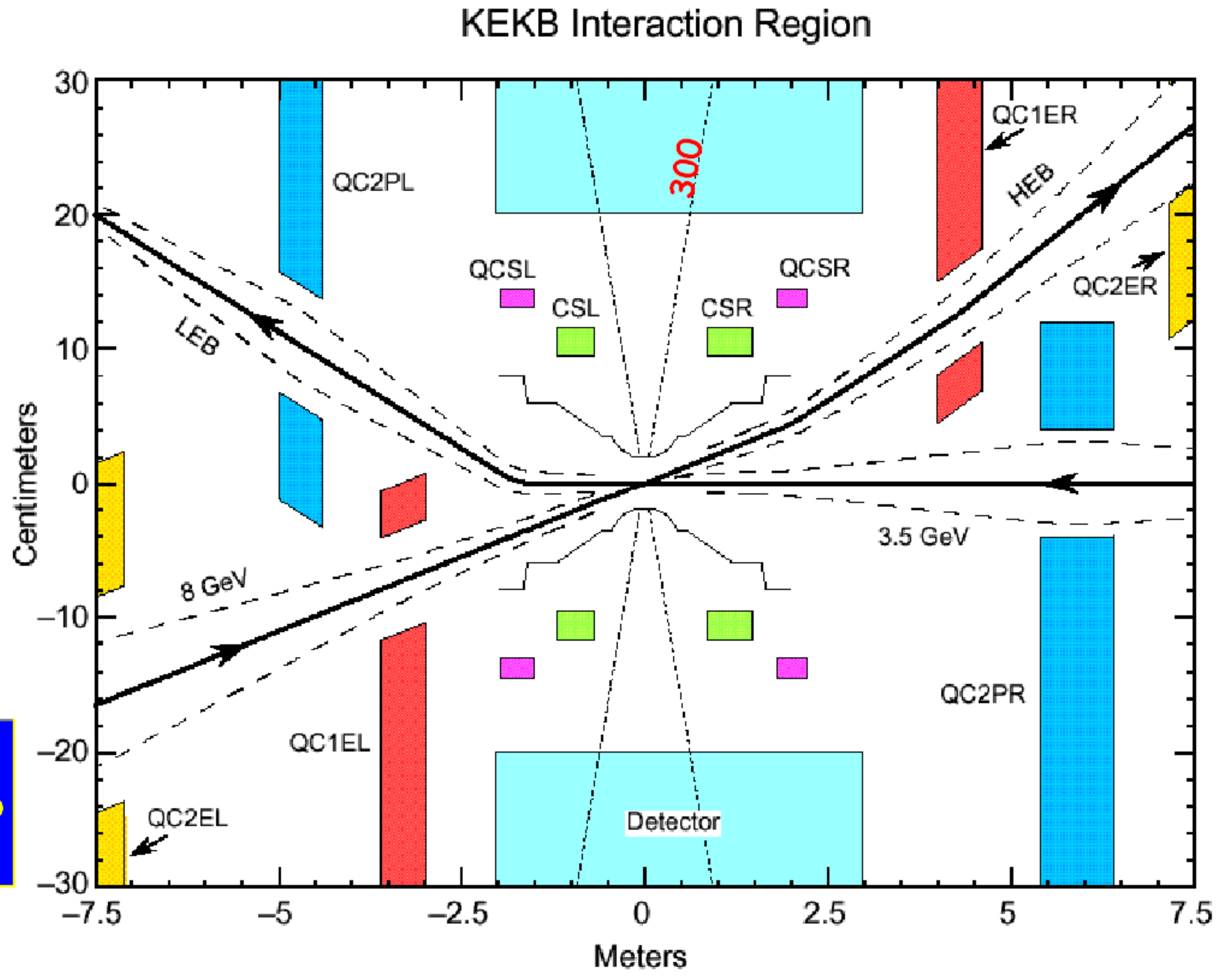

Accelerator figure of merit 1: Center-of-mass energy

If there is enough energy available in the collission, new, heavier particles can be produced.

$E_{CMS} > mc^2$

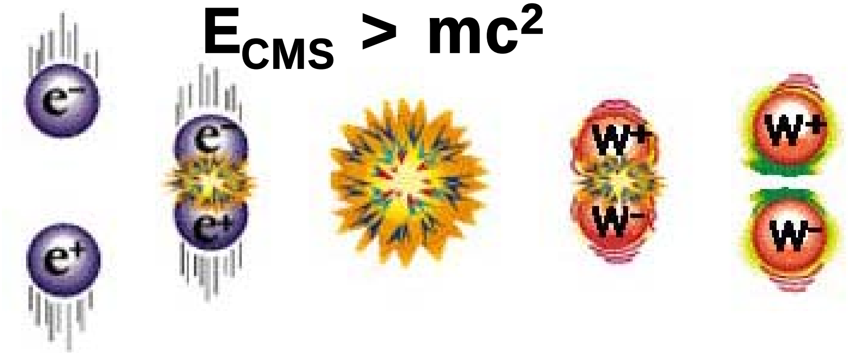

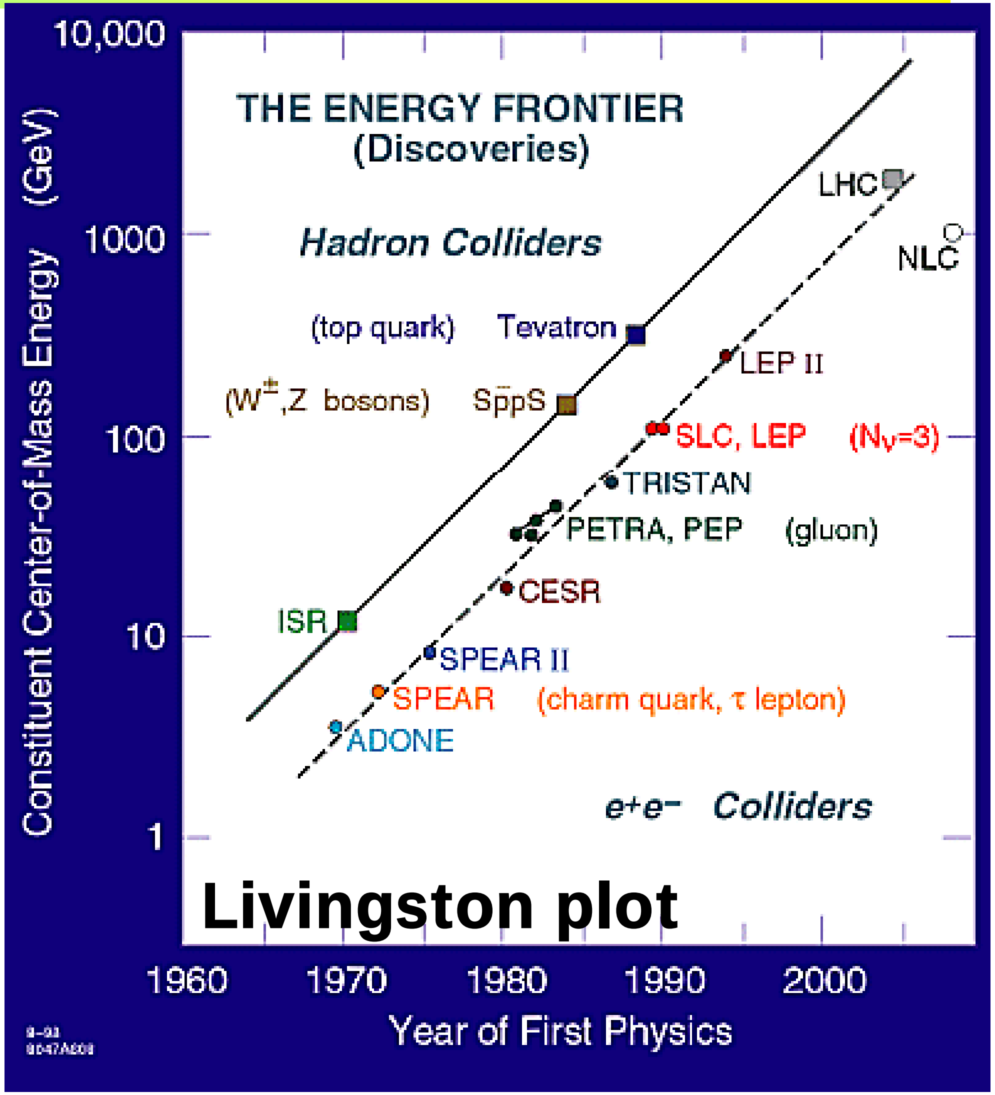

e.g. LHC, CERN, Tevatron: search for Higgs bosons, $m_{Higgs} > 100GeV$

Accelerator figure of merit 2: Luminosity

Observed rate of events = Cross section x Luminosity

$$\frac{dN}{dt} = L\sigma$$

Accelerator figures of merit: luminosity ***L***

and integrated luminosity

$$L_{\text{int}} = \int L(t)dt$$

Luminosity vs time

$$R = \mathcal{L}\sigma$$

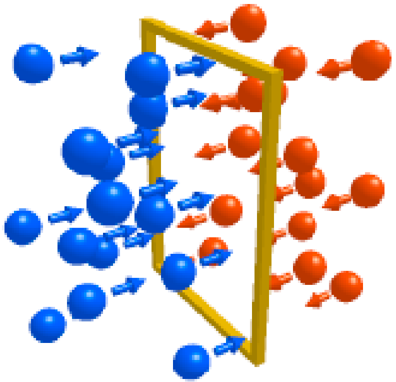

(number of events/unit time)

= (cross section) X (luminosity)

$$\mathcal{L} = \frac{I_{LER}\, I_{HER}}{e^2 f_{rev}\, N_{bunch}\, A_{eff}}$$

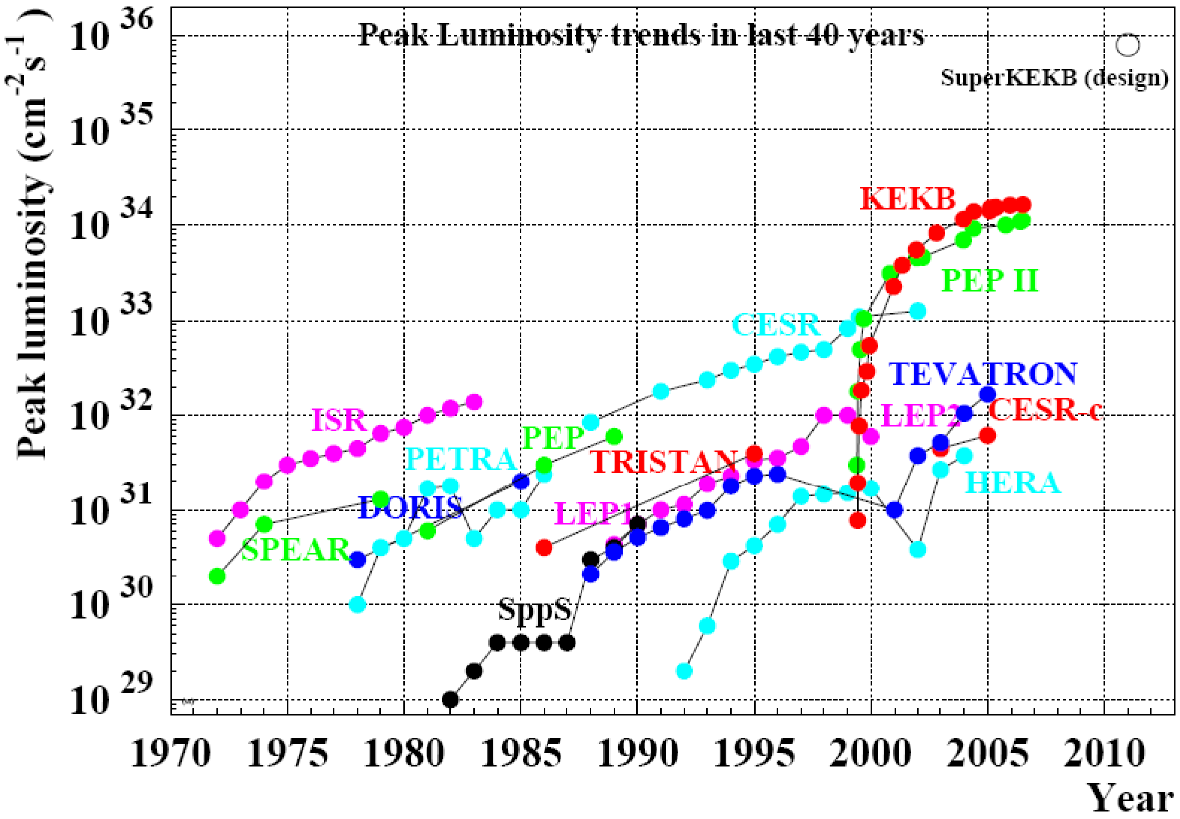

A high luminosity is needed for studies of rare processes.

Luminosity: improvement in time

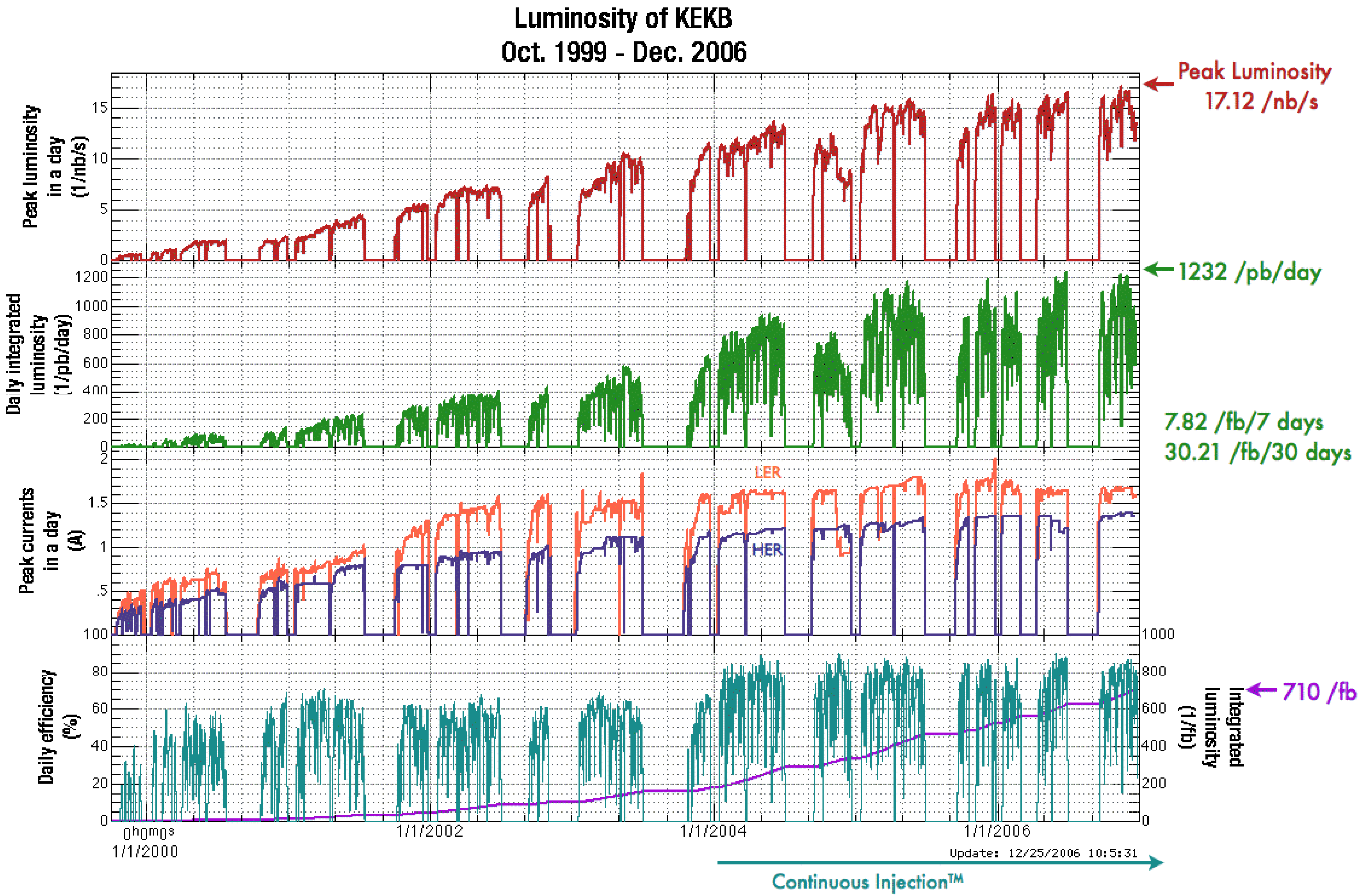

How to understand what happened in a collision?

- Measure the coordinate of the point ('vertex') where the reaction occured, and determine the positions and directions of particles that have been produced
- Measure momenta of stable charged particles by measuring their radius of curvature in a strong magnetic field (~1T)
- Determine the identity of stable charged particles (e, μ, π, K, p)
- Measure the energy of high energy photons γ

How to understand what happened in a collision?

Illustration on an example:

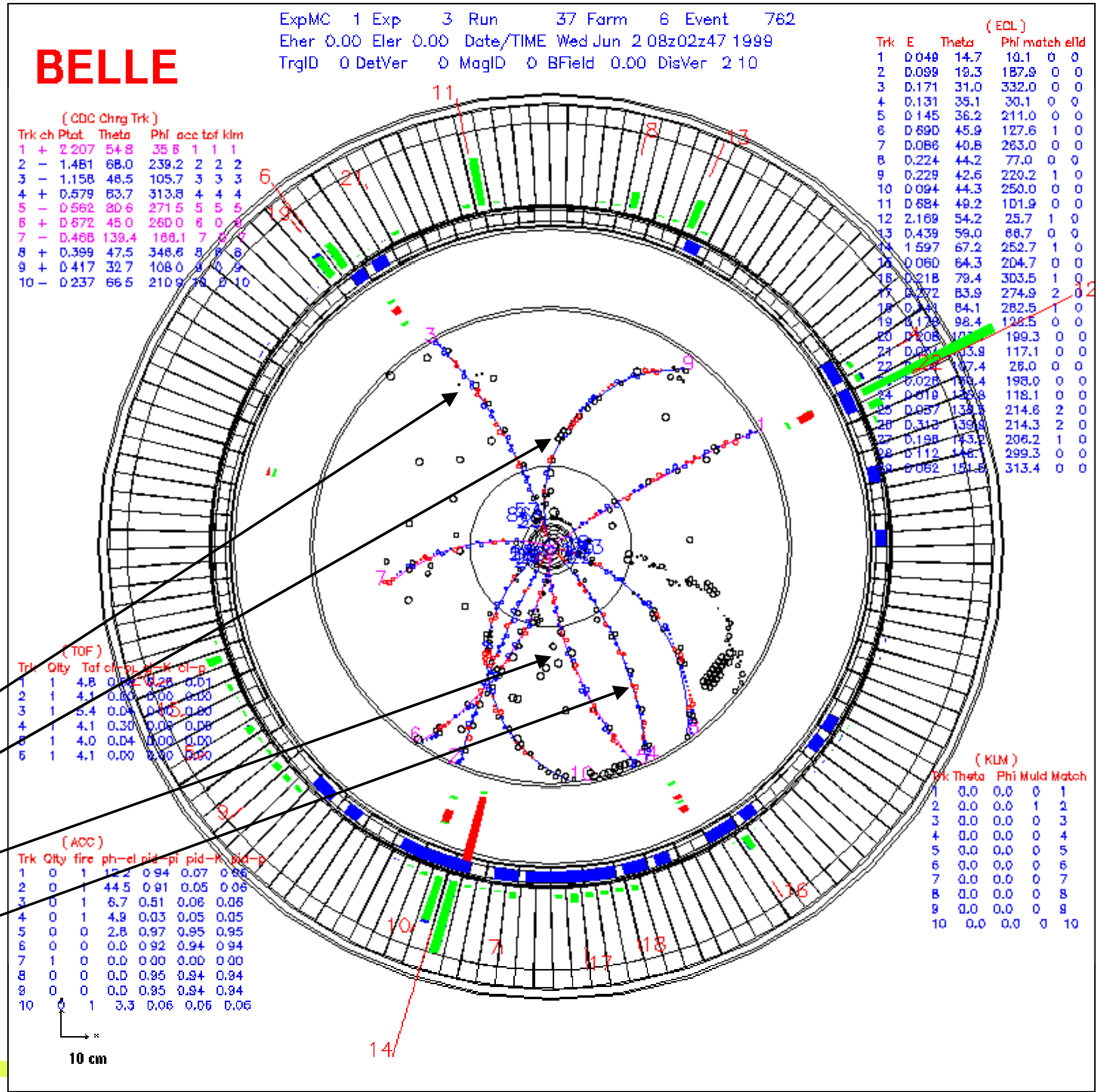

$B^0 \rightarrow K^0_S\, J/\psi$

$K^0_S \rightarrow \pi^- \pi^+$

$J/\psi \rightarrow \mu^- \mu^+$

Search for particles which decayed close to the production point

How do we reconstructing final states which decayed to several stable particles (e.g., 1,2,3)?
From the measured tracks calculate the invariant mass of the system (i= 1,2,3):

$$M = \sqrt{(\sum E_i)^2 - (\sum \vec{p}_i)^2}$$

The candidates for the X→123 decay show up as a peak in the distribution on (mostly combinatorial) background.
The name of the game: have as little background under the peak as possible without loosing the events in the peak (=reduce background and have a small peak width).

How do we know it was precisely this reaction?

$B^0 \rightarrow K^0_S\, J/\psi$

$K^0_S \rightarrow \pi^- \pi^+$

$J/\psi \rightarrow \mu^- \mu^+$

← detect

For $\pi^- \pi^+$ in $\mu^- \mu^+$ pairs we calculate the invariant mass:

$M^2c^4=(E_1+ E_2)^2- (p_1+ p_2)^2$

Mc^2 must be for K^0_S close to 0.5 GeV,

for J/ψ close to 3.1 GeV.

Rest in the histrogram: random coincidences ('combinatorial background')

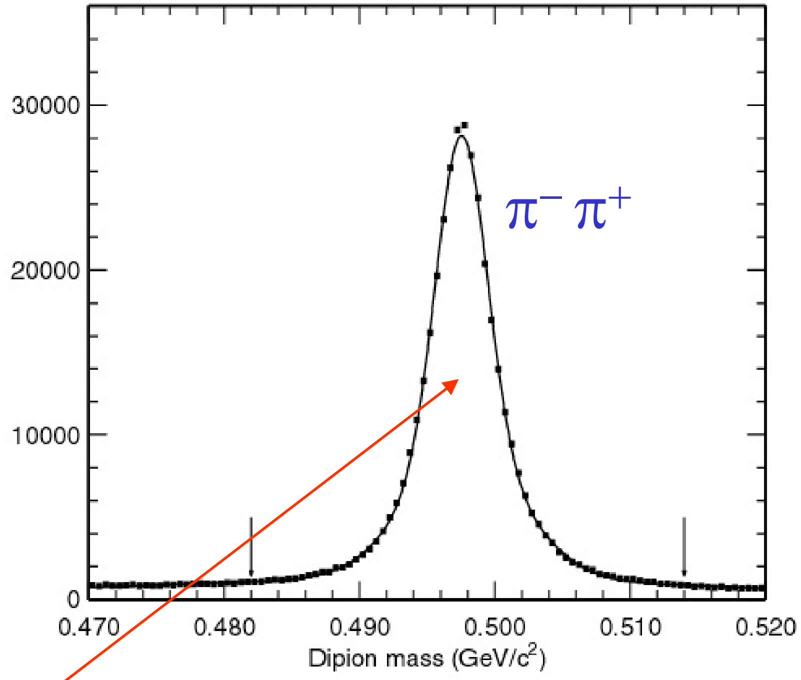

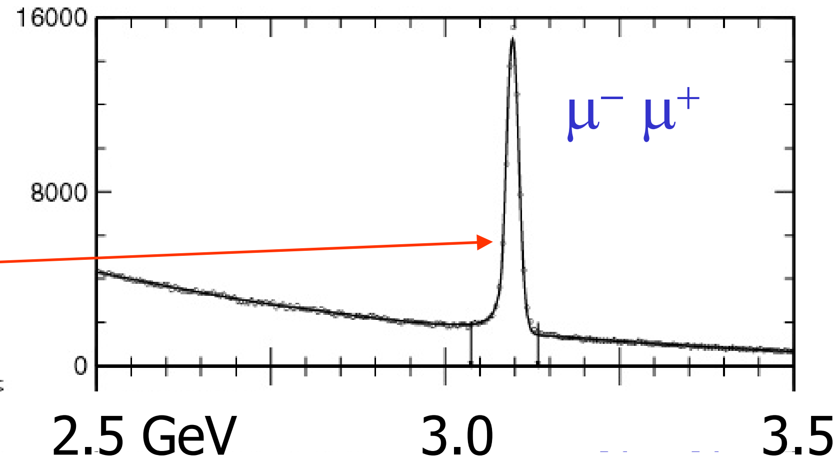

Experimental aparatus

Detector form: symmetric for colliders with symmetric energy beams; extended in the boost direction for an asymmetric collider; very forward oriented in fixed target experiments.

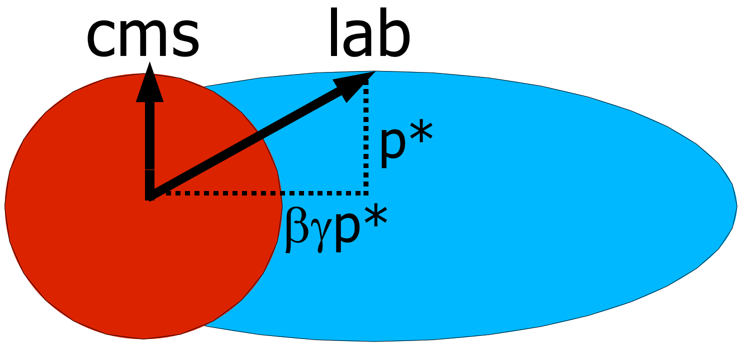

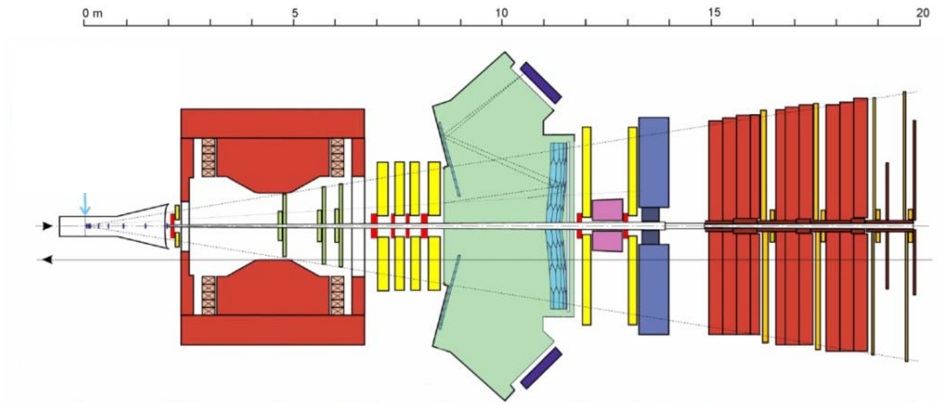

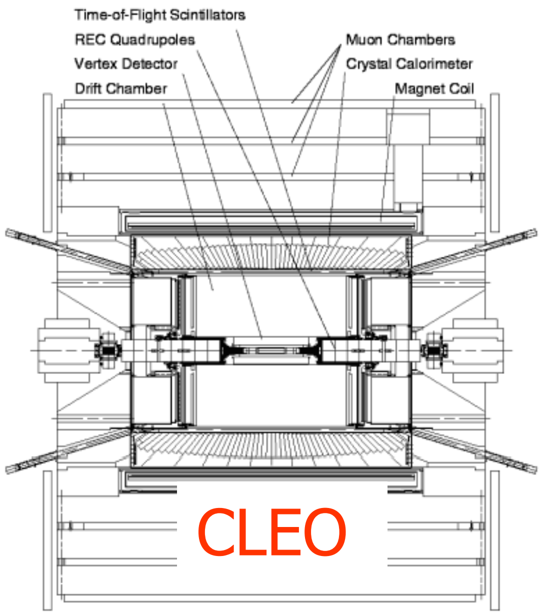

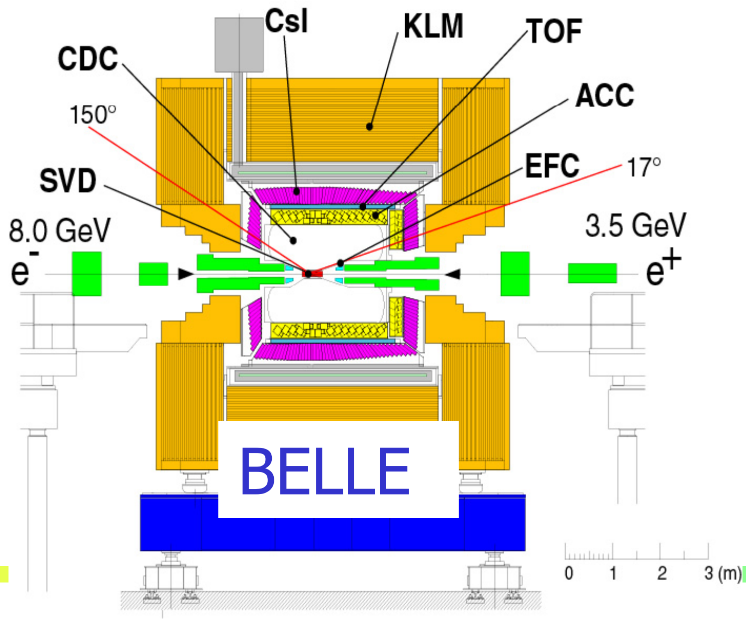

Example of a fixed target experiment: HERA-B

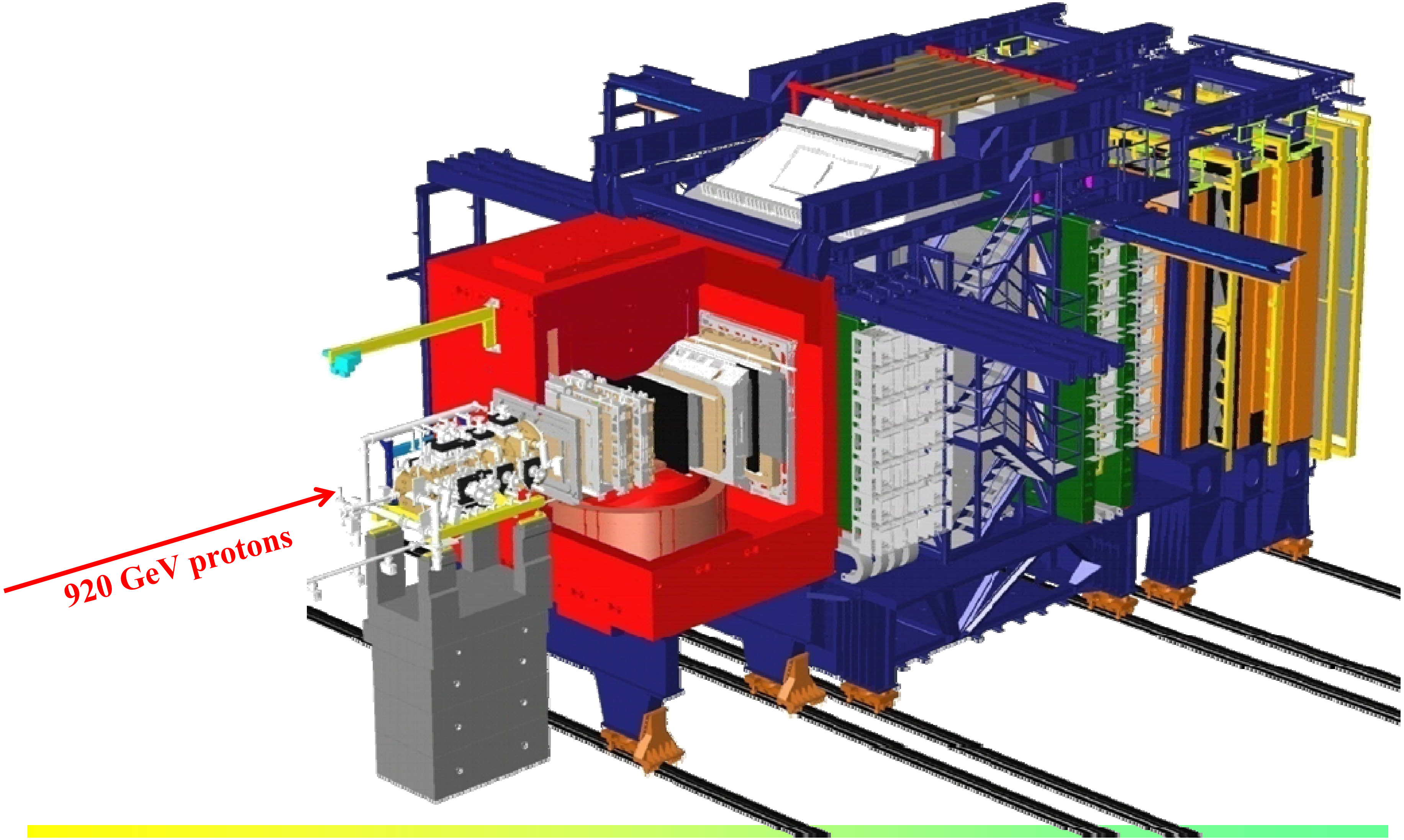

Belle spectrometer at KEK-B

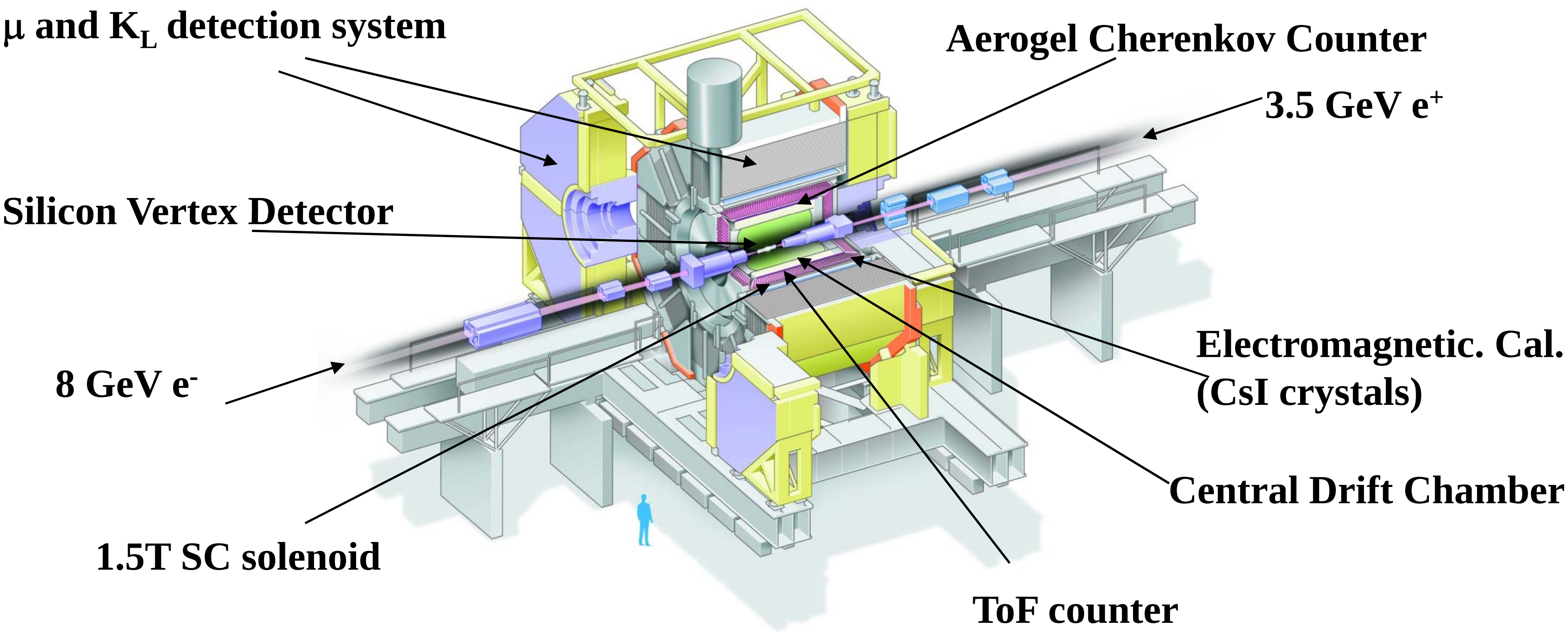

ATLAS at LHC

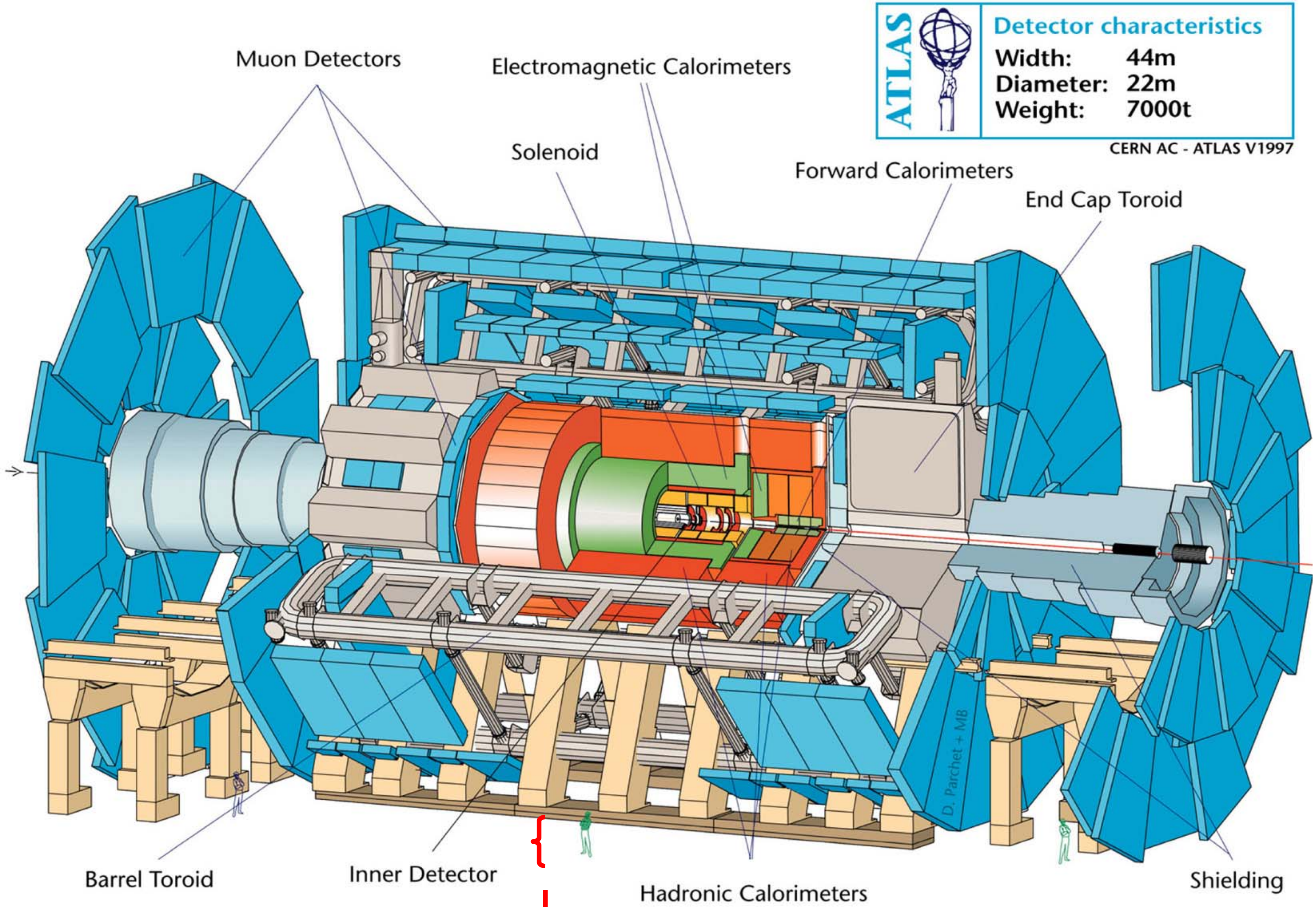

A physicist...

Components of an experimental apparatus (‘spectrometer’)

- Tracking and vertexing systems
- Particle identification devices
- Calorimeters (measurement of energy)

Components of an experimental apparatus (‘spectrometer’)

- Tracking and vertexing systems
- Particle identification devices
- Calorimeters (measurement of energy)

Silicon vertex detector (SVD)

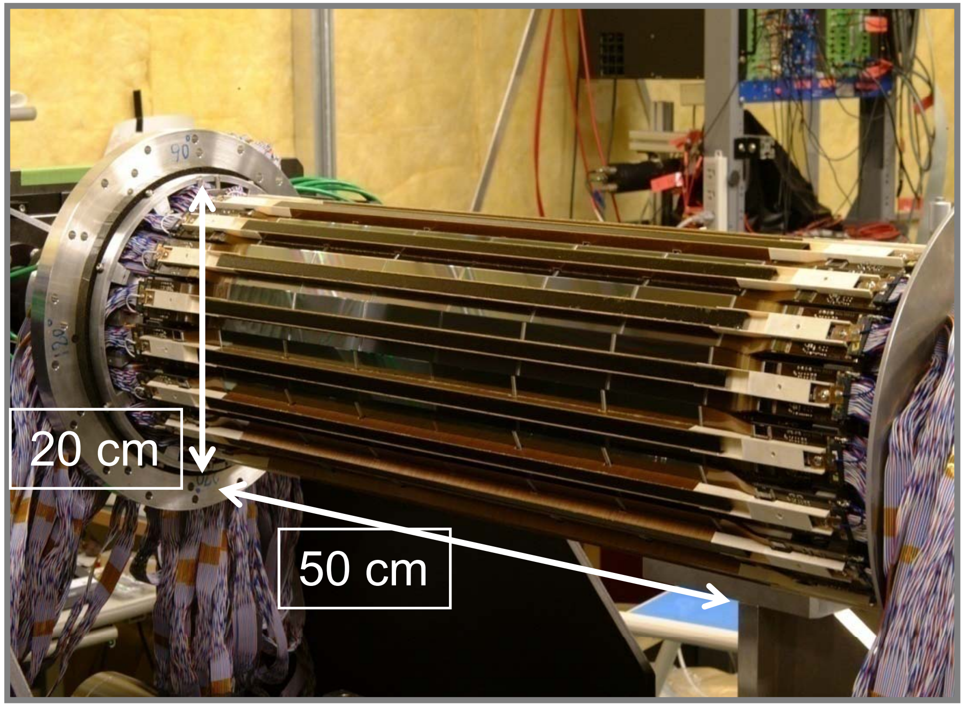

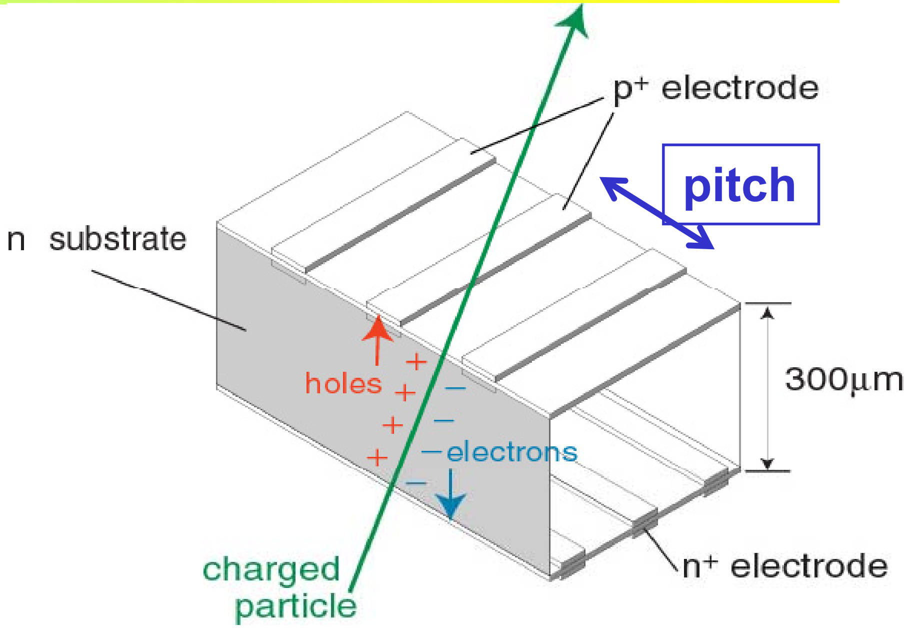

Two coordinates measured at the same time

Typical strip pitch ~50μm, resolution about ~15 μm

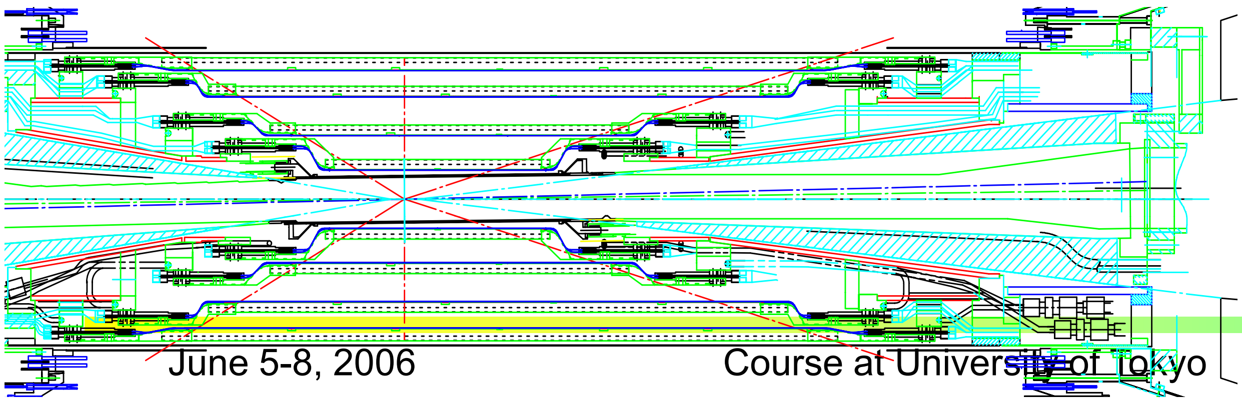

Interaction of charged particles with matter

Energy loss due to ionisation: depends on βγ, typically about 2 MeV/cm ρ/(g cm^{-3}).

Liquids, solids: few MeV/cm

Gases: few keV/cm

Minimum ionizing particles (MIP)

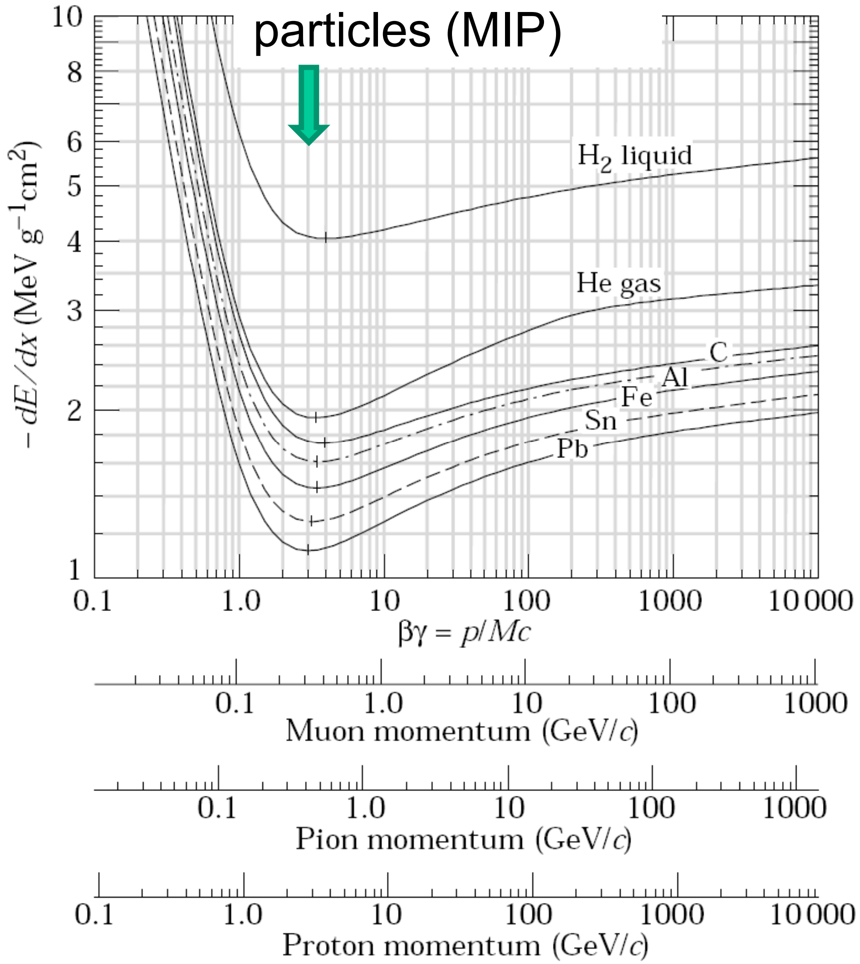

Primary ionisation: charged particle kicks electrons from atoms.

In addition: excitation of atoms (no free electron), on average need W_i (>ionisation energy) to create e-ion pair.

W_i typically 30eV → per cm of gas about 2000eV/30eV=60 e-ion pairs

Ionisation

n_{prim} is typically 20-50 /cm

(average value, Poisson like distribution – used in measurements of n_{prim})

The primary electron ionizes further: secondary e-ion pairs, typically about 2-3x more.

Finally: 60-120 electrons /cm

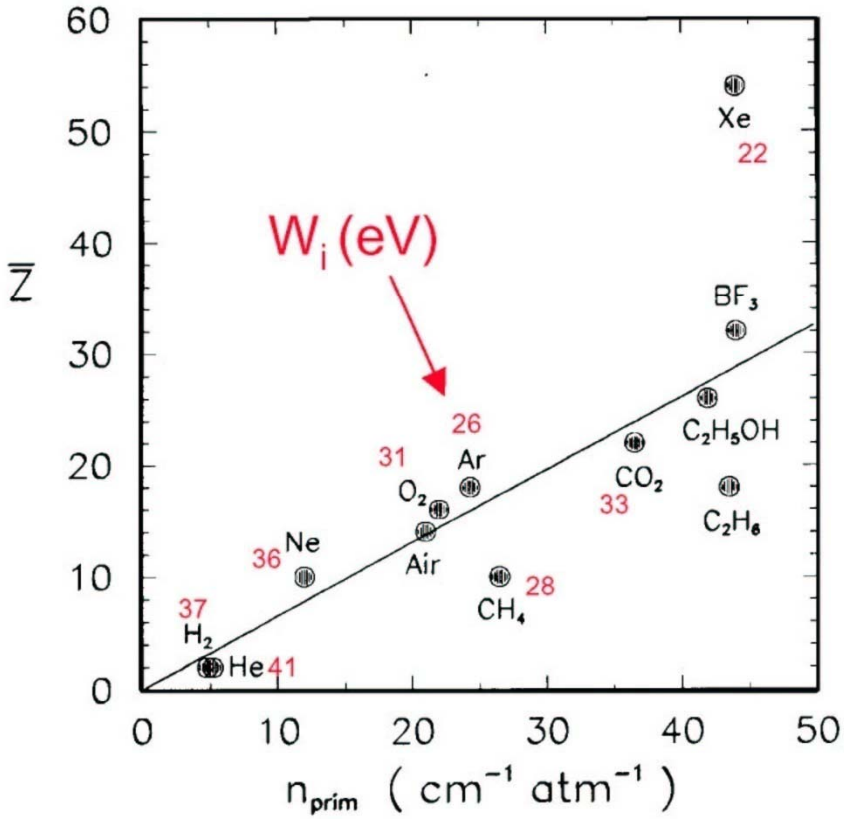

Can this be detected? 120 e-ion pairs make a pulse of V=ne/C=2mV (at typical C=10pF) → NO

-> Need multiplication

Multiplication in gas

Simplest example: cylindrical counter, radial field, electrons drift to the anode in the center

$E = E(r) \propto 1/r$

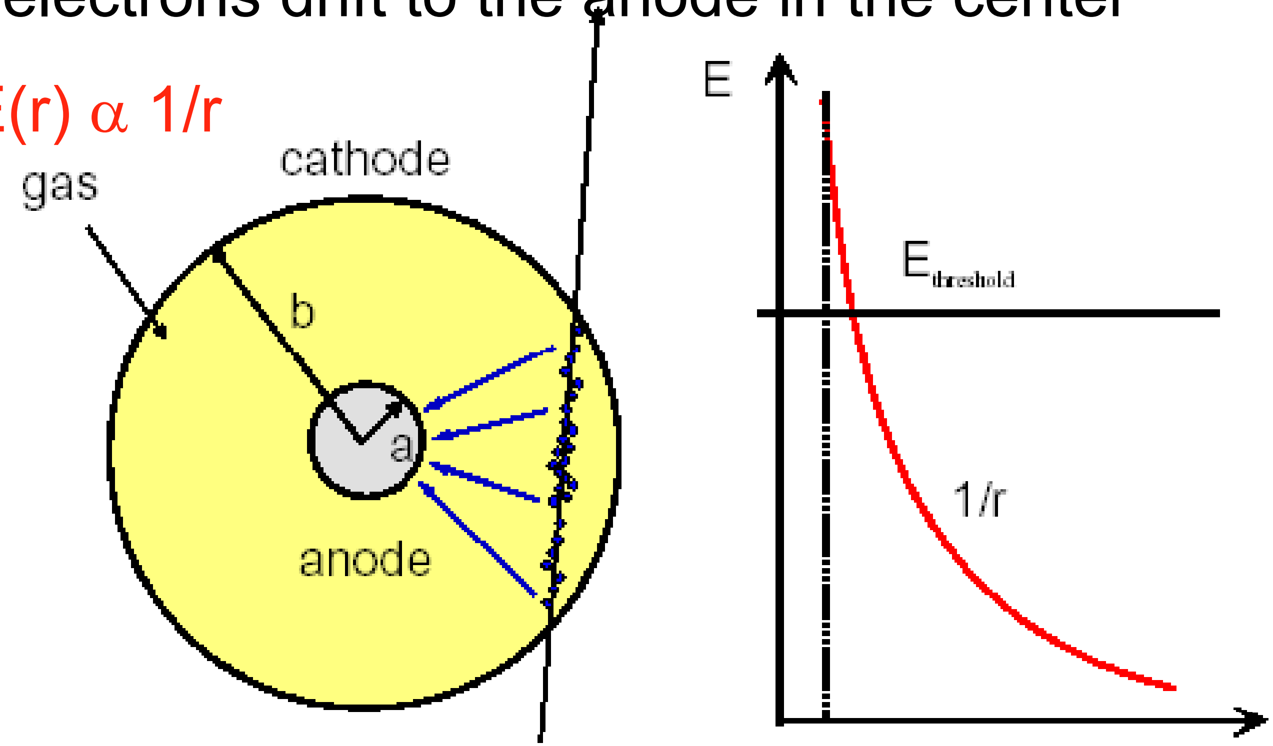

If the energy eEd gained over several mean free paths (d around 10mm) exceeds the ionisation energy → new electron

Electric field needed → E = I/ed = 10V/mm = 10kV/cm

Diffusion and mobility of ions

Diffusion: ions loose their enegy in collisions with the gas molecules, thermalize quickly (mean free path around 0.1μm) ; Maxwellian energy distribution.

Localized charge distribution diffuses: fraction of charges in dx after time t

$$\frac{dN}{N} = \frac{1}{\sqrt{4\pi Dt}} e^{-\frac{x^2}{4Dt}} dx$$

D, diffusion coefficient: typically around 0.05 cm^2/s

The r.m.s. of the distribution for 1D and 3D cases:

$$\sigma_x = \sqrt{2Dt}, \sigma_V = \sqrt{6Dt}$$

Electric field: the Maxwellian distribution changes by very little, ions drift in electric field with an average net (drift) velocity (not instant velocity!) depending linearly on the electric field:

$$\mathbf{v_D^+ = \mu^+ (E/p)}$$

μ^+: mobility, related to D, $D^+/\mu^+ = kT/e = 0.026$V

Typical values for μ^+: 1-2 cm^2 atm/Vs; at 1kV/cm: 1cm/ms

Drift velocity of electrons

No simple relation to E field, typical value 5cm/μs

Few examples:

Argon changes drastically with additives

Methane, ethane, CO_2

Methylal, Ethylene

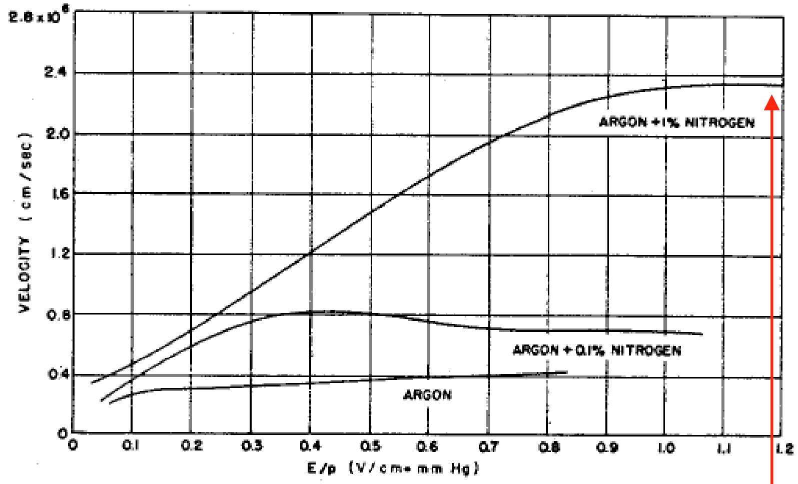

Fig. 25 Drift velocity of electrons in pure argon, and in argon with small added quantities of nitrogen. The very large effect on the velocity for small additions is apparent[22].

Very useful: in some gas mixtures v_D gets saturated

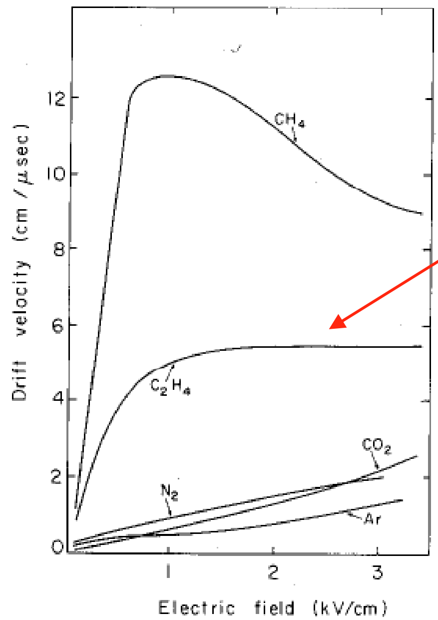

Fig. 26 Drift velocity of electrons in several gases at normal conditions[12,22,23]

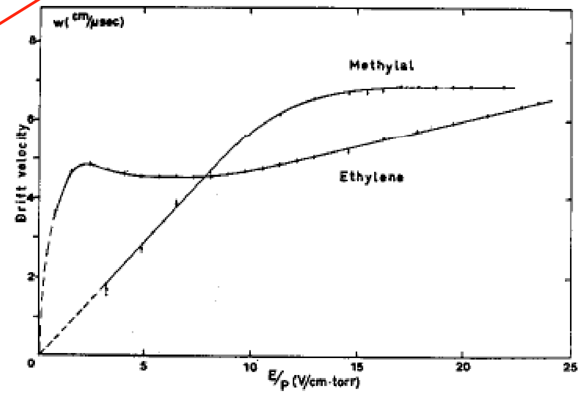

Fig. 27 Drift velocity of electrons in methylal $[(OCH_3)_2CH_2]$ and in ethylene (C_2H_4)[24]

Multiplication in gas

Electron travels (drifts) towards the anode (wire); close to the wire the electric field becomes high enough (several kV/cm), the electron gains sufficient energy between two subsequent collisions with the gas molecules to ionize -> start of an avalanche.

(F. Sauli, CERN 77-09)

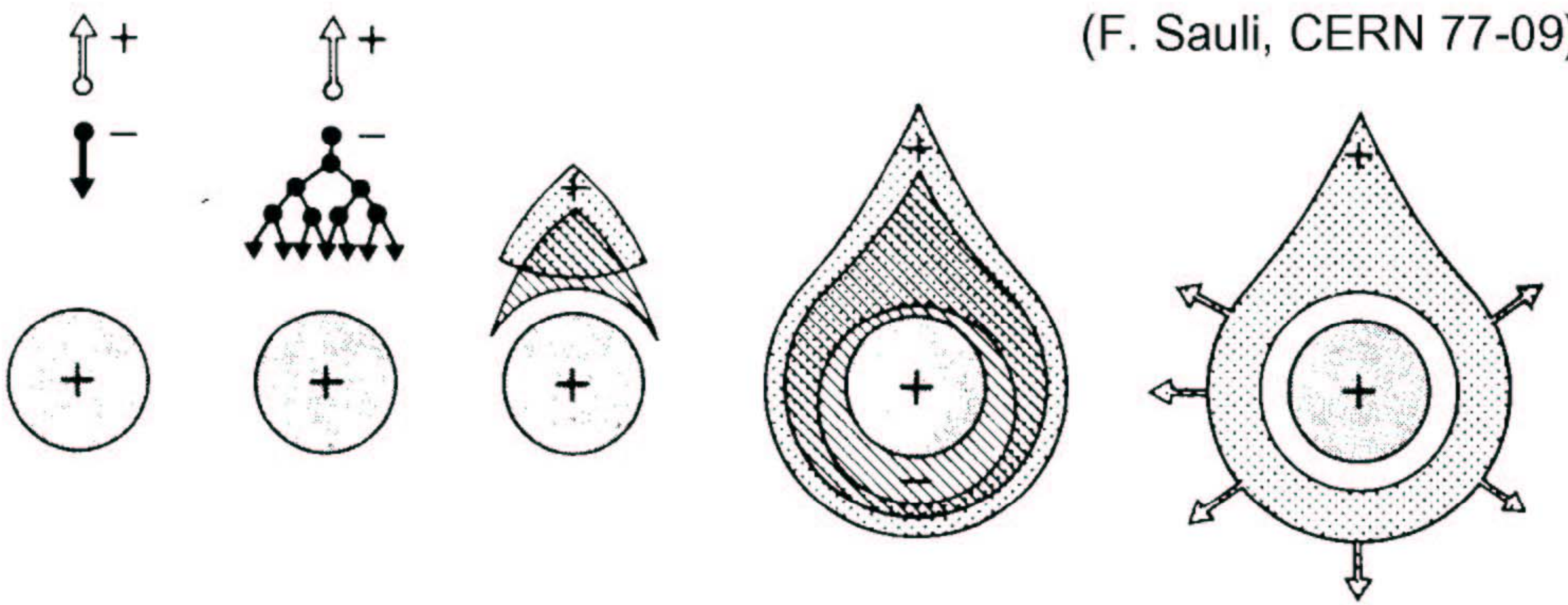

a b c d e

Signal development 2

$$QEdr = -U_0 Cldu$$

The work of the electric force on the ions drifting in the electric field, *Qedr*, is supplied by the generator: charge *Cldu* flows through the HV source with high voltage U_0 (C = cap. per unit length).

$$E = \frac{U_0 C}{2\pi\varepsilon_0}\frac{1}{r}$$

$$Q = nMe_0$$

$$u(t) = \int_0^t du = -\frac{Q}{2\pi\varepsilon_0 l}\ln\frac{r(t)}{a}$$

$$\frac{dr}{dt} = v = \mu^+\frac{E}{p} = \frac{\mu^+}{p}\frac{U_0 C}{2\pi\varepsilon_0}\frac{1}{r}$$

$$\int_a^r r dr = \frac{\mu^+}{p}\frac{U_0 C}{2\pi\varepsilon_0}\int_0^t dt$$

$$r(t) = \sqrt{a^2 + \frac{\mu^+}{p}\frac{U_0 C}{\pi\varepsilon_0}t} = a\sqrt{1+\frac{t}{t_0}}$$

$$t_0 = \frac{\pi\varepsilon_0 p}{\mu^+ U_0 C}(b^2 - a^2) \approx 500\mu s$$

$$u(t) = -\frac{Q}{4\pi\varepsilon_0 l}\ln(1+\frac{t}{t_0})$$

Note: Electrons are produced very close to the anode, drift over a small potential difference -> contribute very little to the signal (1%)

Signal development 3

Time evolution of the signal

$$u(t) = -\frac{Q}{4\pi\varepsilon_0 l}\ln(1+\frac{t}{t_0})$$

with no RC filtering (τ = inf.) and with time constants 10μs and 100μs.

If faster signals are needed → smaller time constants→ smaller signals

e.g. τ =40ns: max u(t) is about ¼ of the τ = inf. case

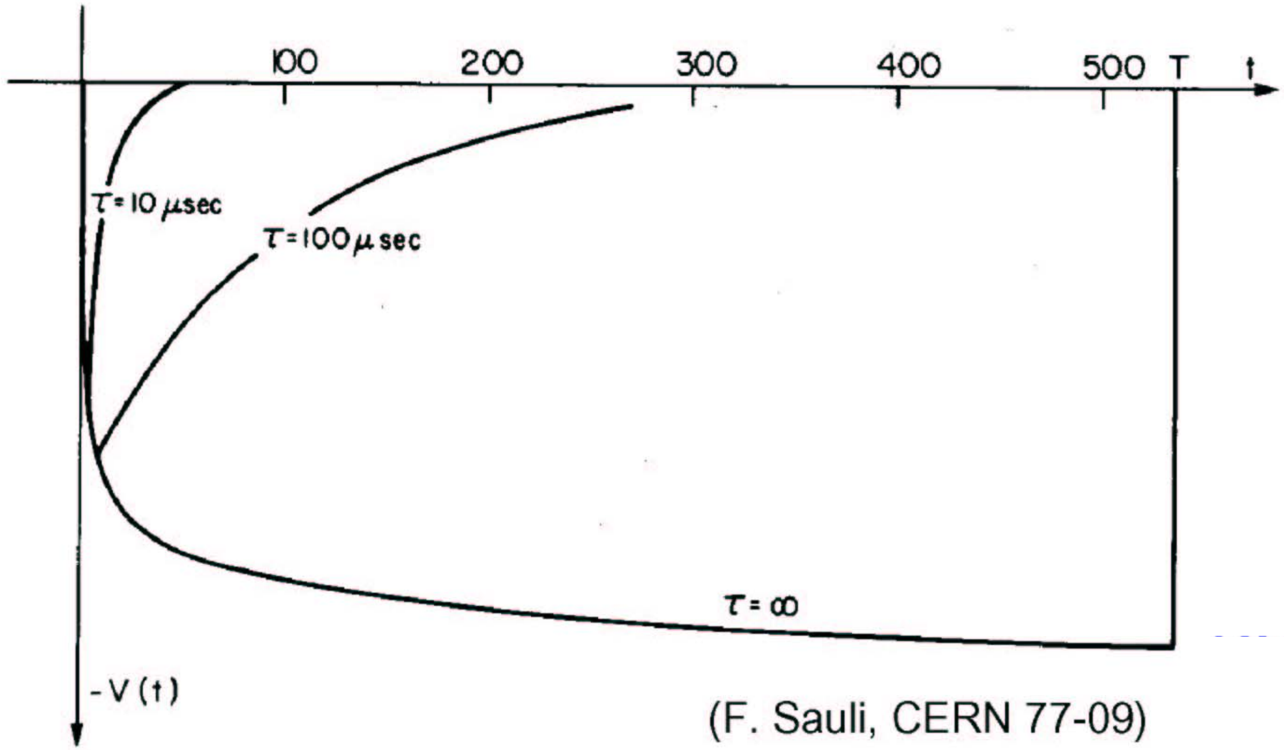

(F. Sauli, CERN 77-09)

Multiwire proportional chamber (MWPC)

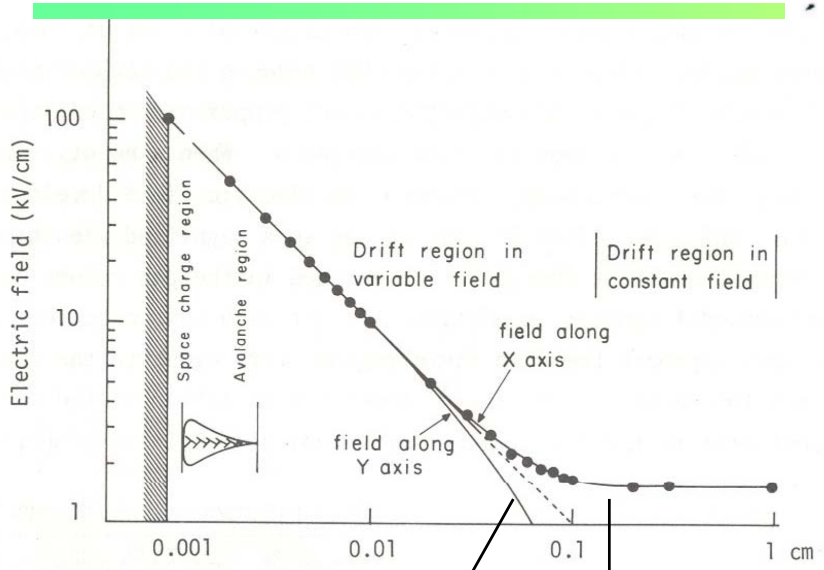

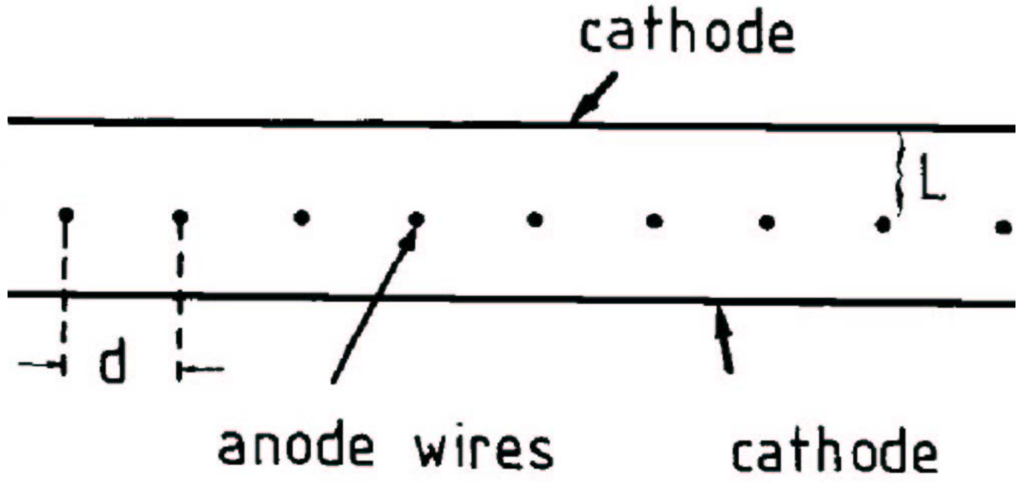

Typical parameters:

L=5mm, d=1-2mm,

wire radius =20 mm

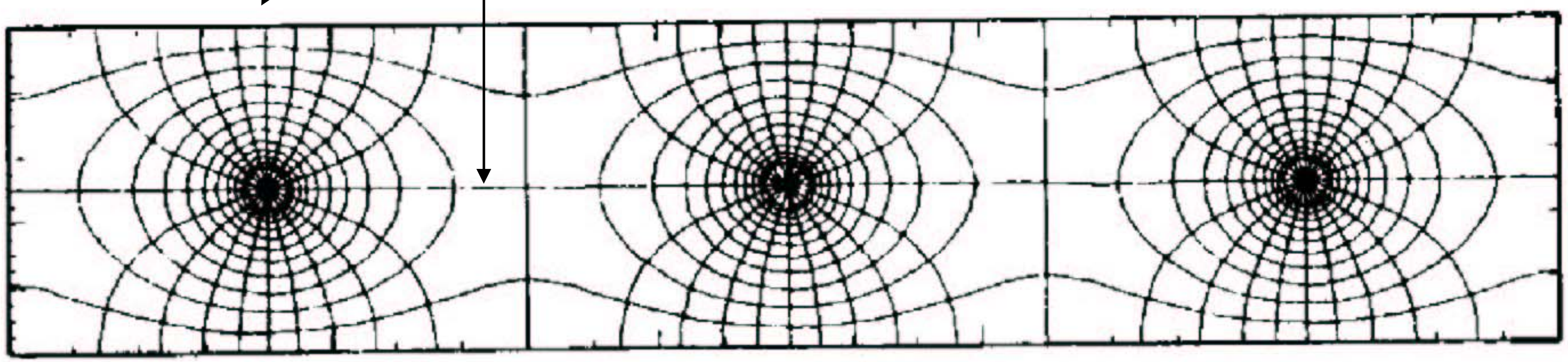

Multiwire proportional chamber (MWPC)

The address of the fired wire gives only 1-dimensional information.

Normally digital readout: spatial resolution limited to

$\sigma = d/\sqrt{12}$

for d=1mm → σ =300 mm

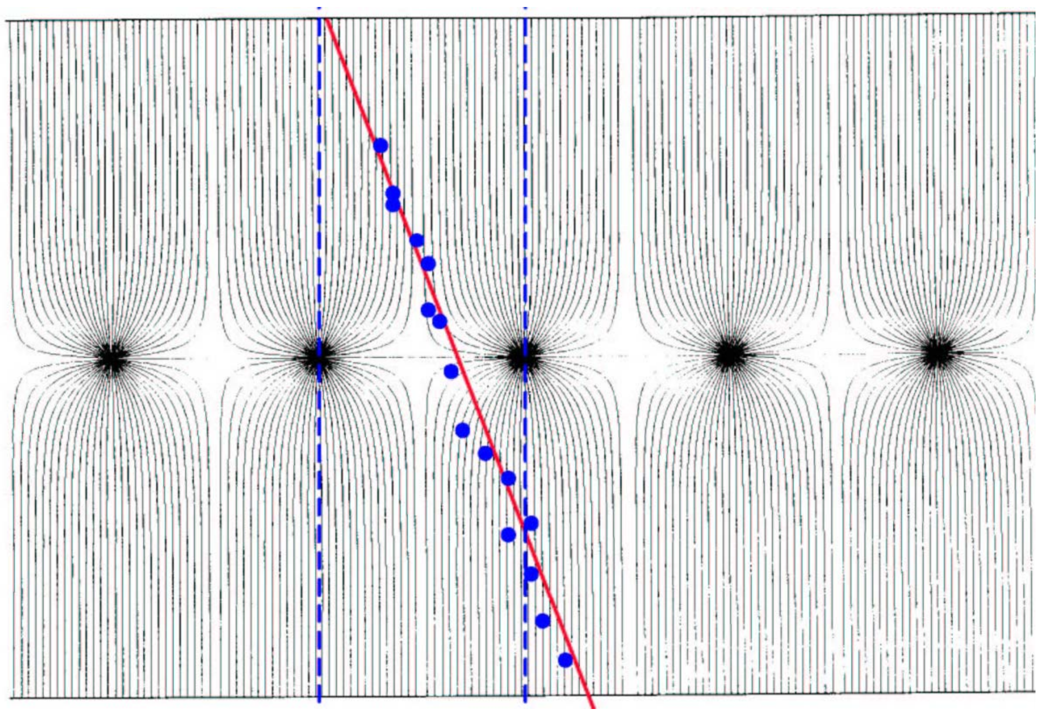

Revolutionized particle physics experiments
→ Nobel prize for G. Charpak

CENTER OF GRAVITY OF INDUCED CHARGE

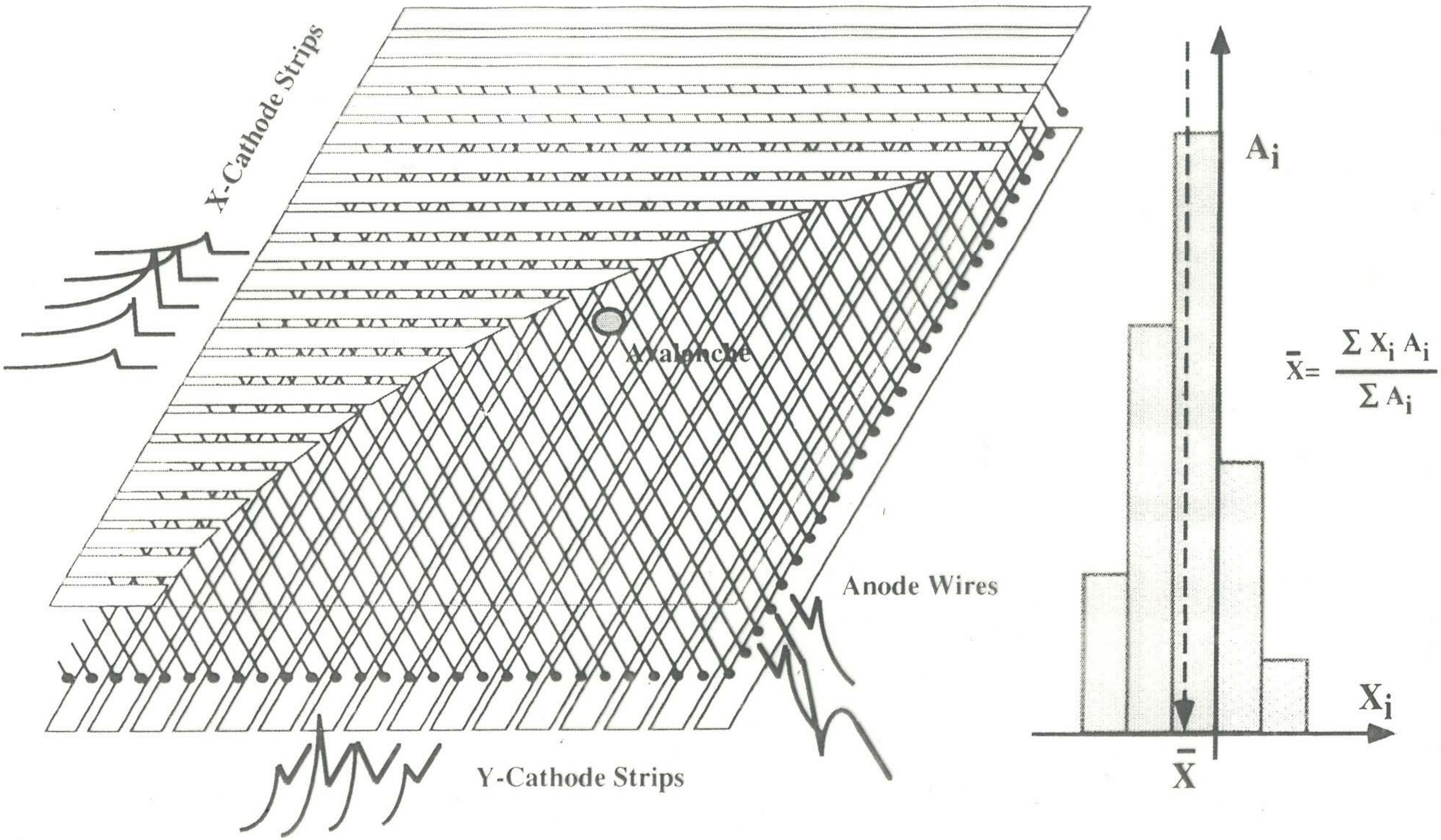

Drift chamber

Improve resolution by measureing the drift time of electrons

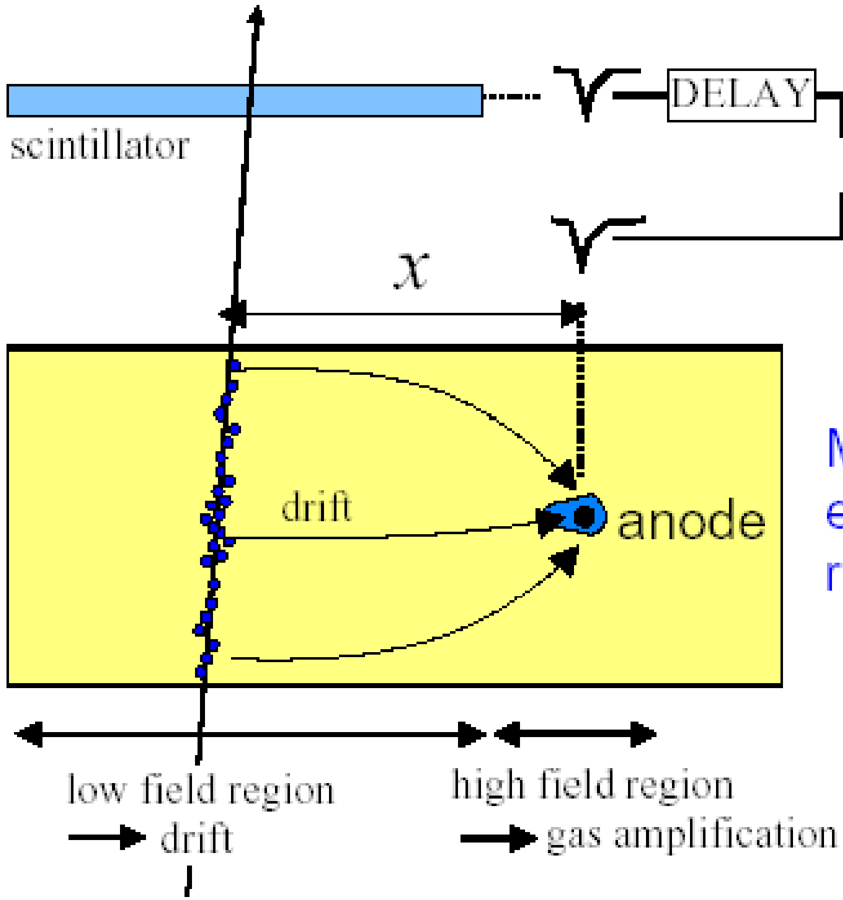

Measure arrival time of electrons at sense wire relative to a time t_0.

$$x = \int v_D(t)dt$$

Drift chamber: resolution

Resolution determined by

- diffusion,
- primary ionisation statistics,
- electronics,
- path fluctuations.

Resolution as a function of drift distance

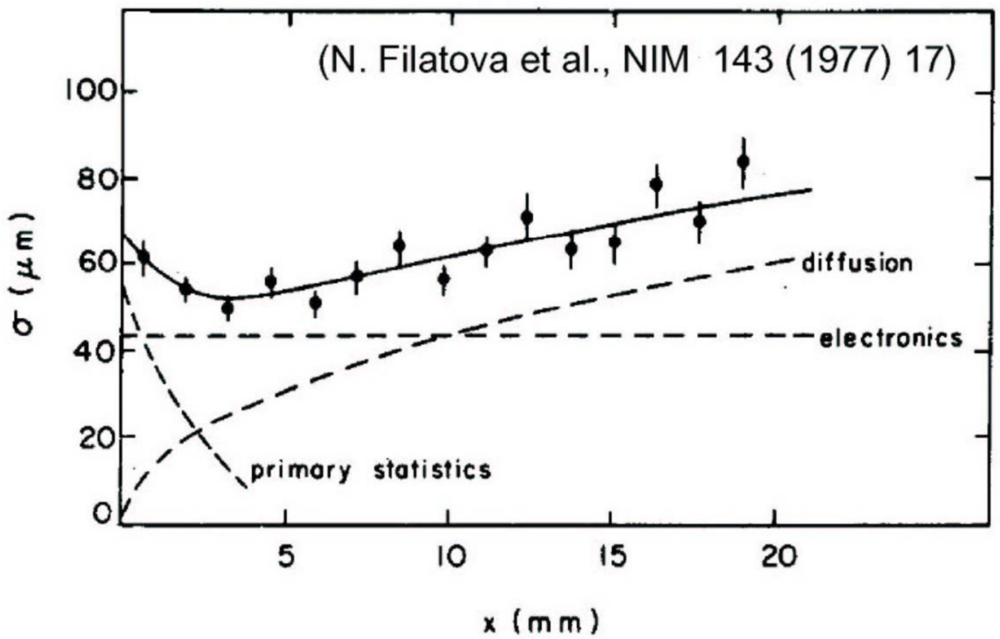

Diffusion: $\sigma_x \propto \sqrt{Dt} \propto \sqrt{x}$

Primary ionisation statistics: if e-ion pairs are produced over distance L, the probability that the first one is produced at x from the wire is $e^{-nx/L}$

Drift chamber with small cells

One big gas volume, small cells defined by the anode and field shaping (potential) wires

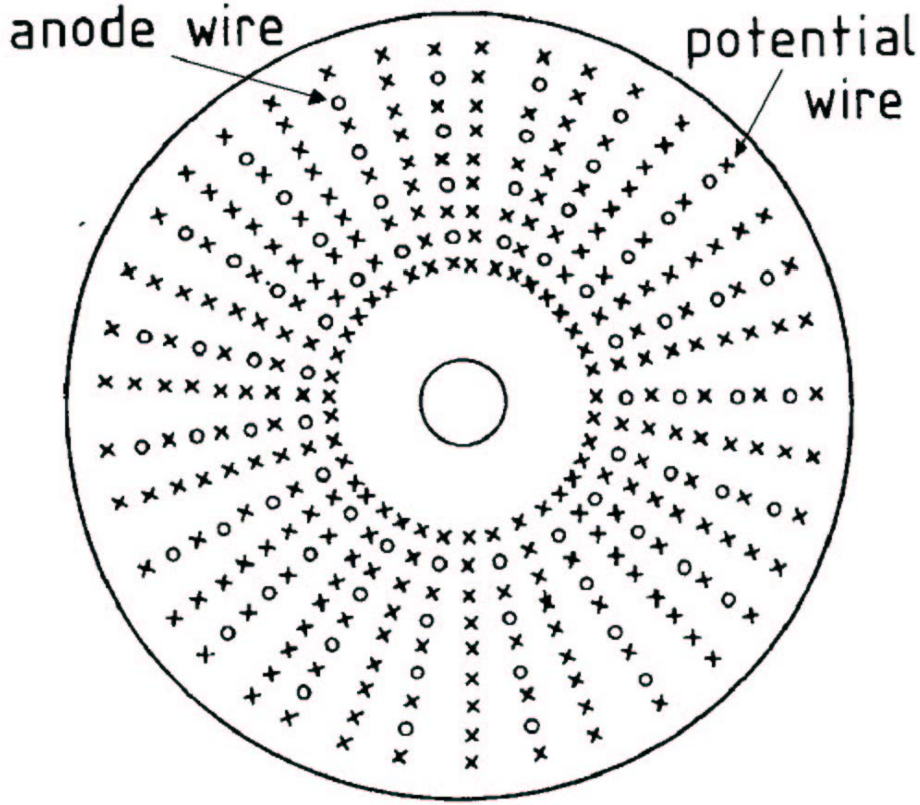

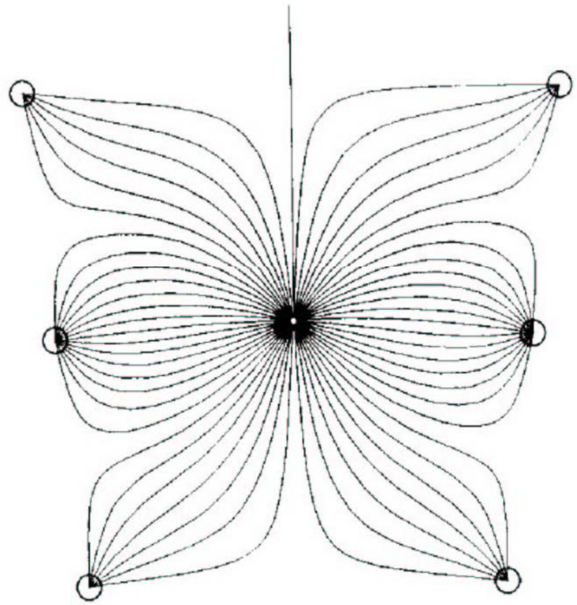

Drift chamber with small cells

Example: ARGUS drift chamber with axial and 'stereo' wires (at an angle to give the hit position along the main axis)

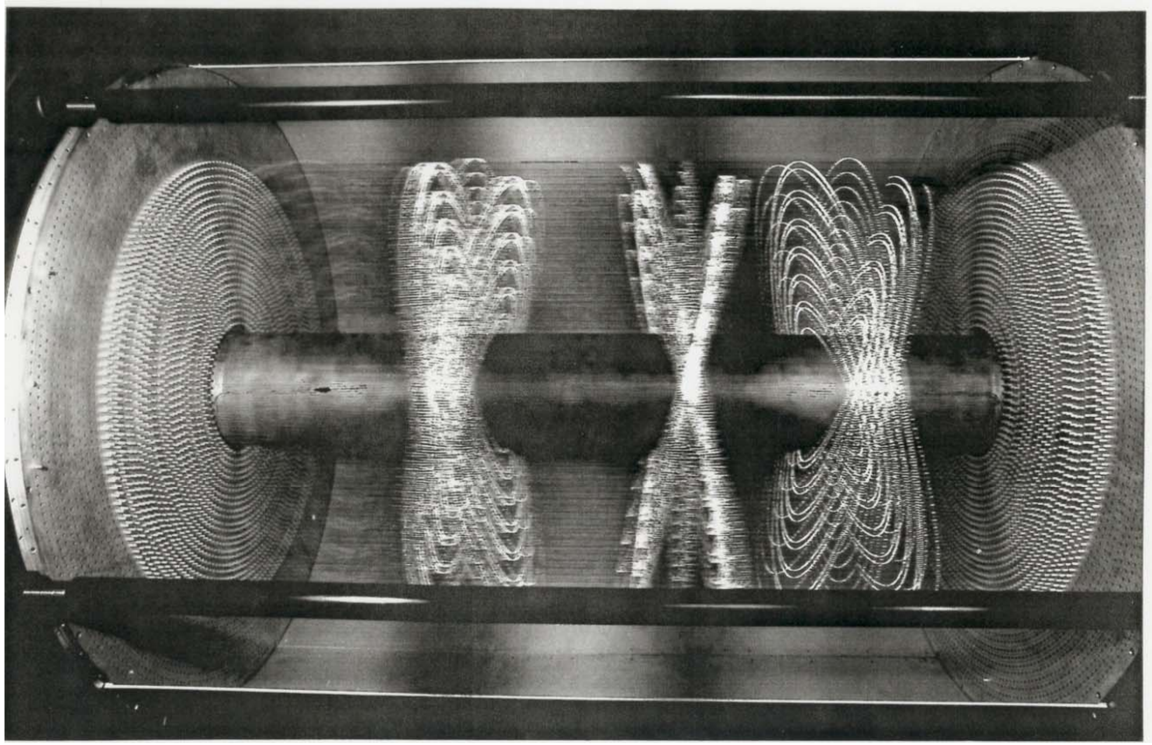

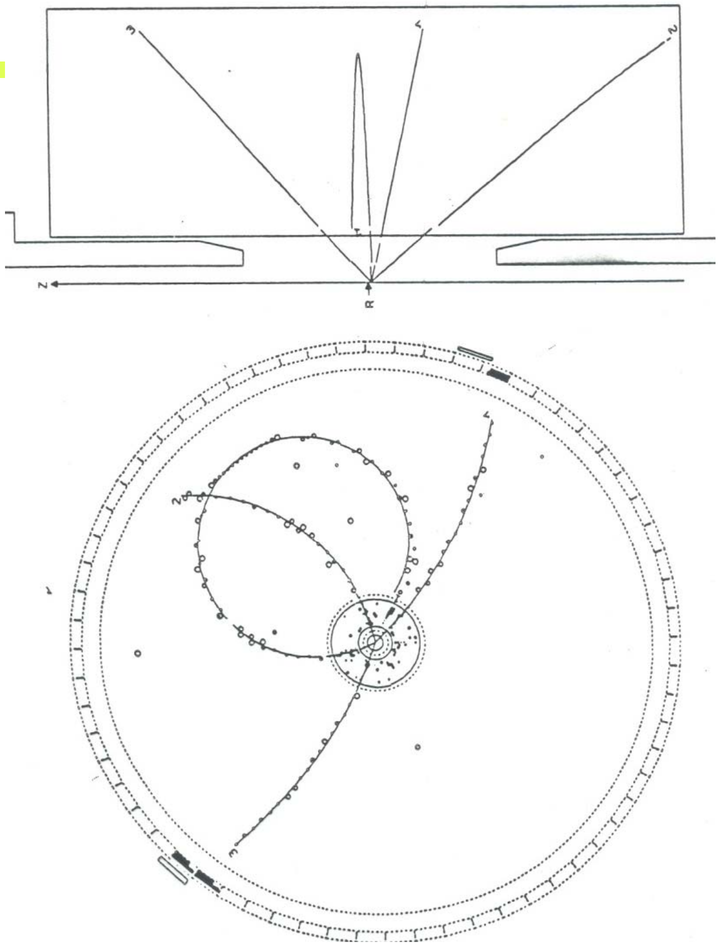

Typical event in two projections

Single cell drift chamber

Simplify manufacturing: put each wire in a tube (straw or hexagonal); useful for large areas.

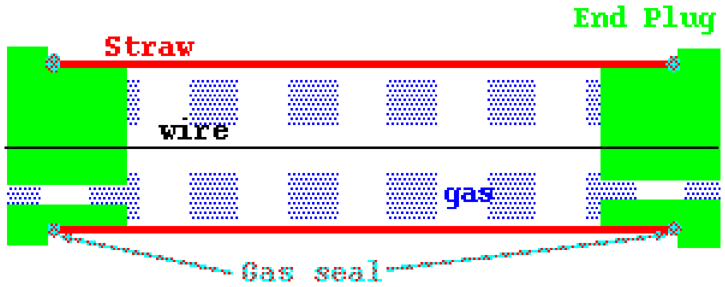

Cells can be several meters long!

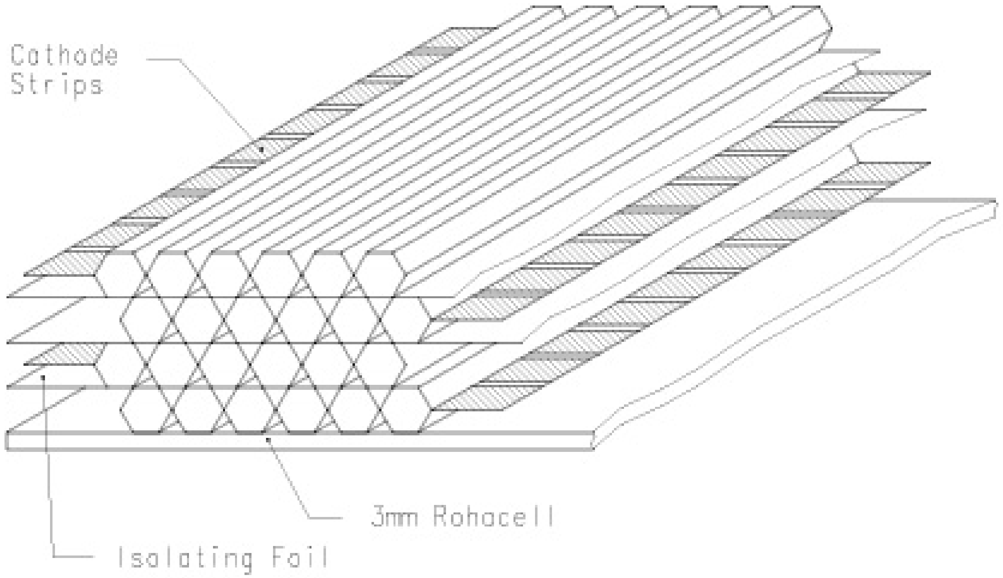

Diffusion and mobility of electrons in magnetic field

E perpendicular to B

Lorentz force perpendicular to B → net drift at an angle α to E

$tg\alpha = \omega\tau$

α: Lorentz angle

ω: cyclotron frequency, ω=eB/m

τ: mean time between collisions

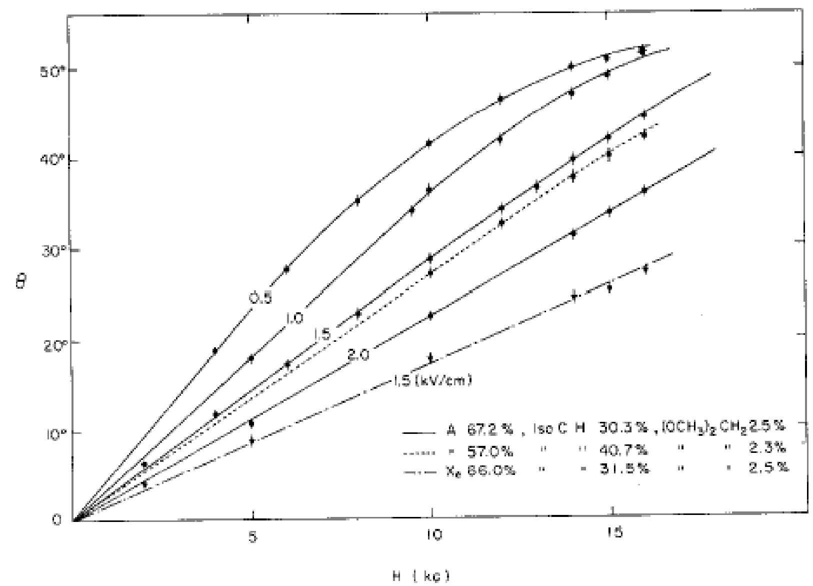

Fig. 38 Measured drift angle (angle between the electric field and the drift directions) as a function of electric and magnetic field strength[9].

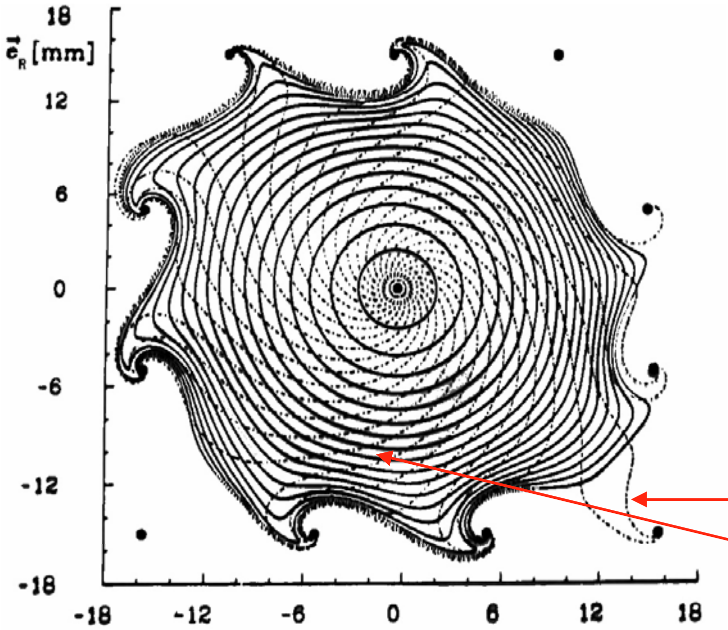

Drift lines in a radial E field (dash-dotted)

Isochrones (full lines)

Diffusion and mobility of electrons in magnetic field 2

E and B parallel:

drift along E, diffusion in the transverse direction reduced! – departing electrons get curled back:

$$D_T(B) = D_0/(1 + \omega^2\tau^2)$$

→ Less diffusion in the tranversal direction!

σ (μm) for 15cm drift distance

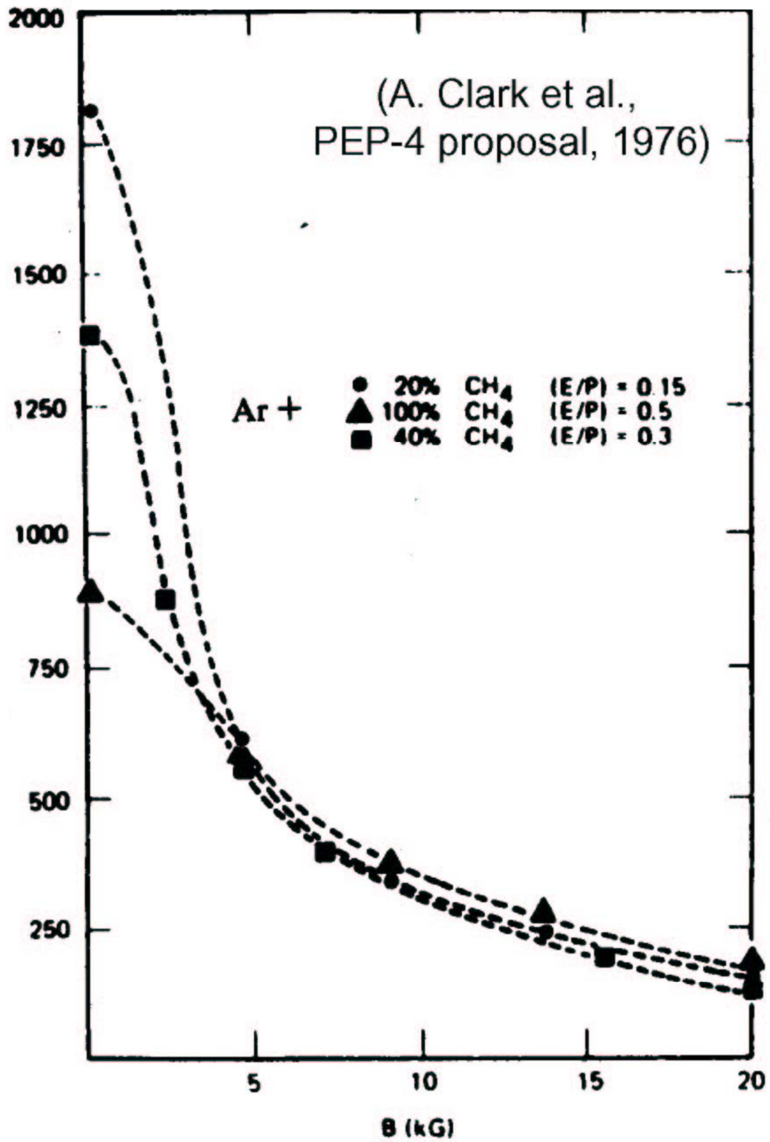

Drift chamber: TPC – time projection chamber

3-dimensional information: drift over a large distance,
2 dim. read-out at one side

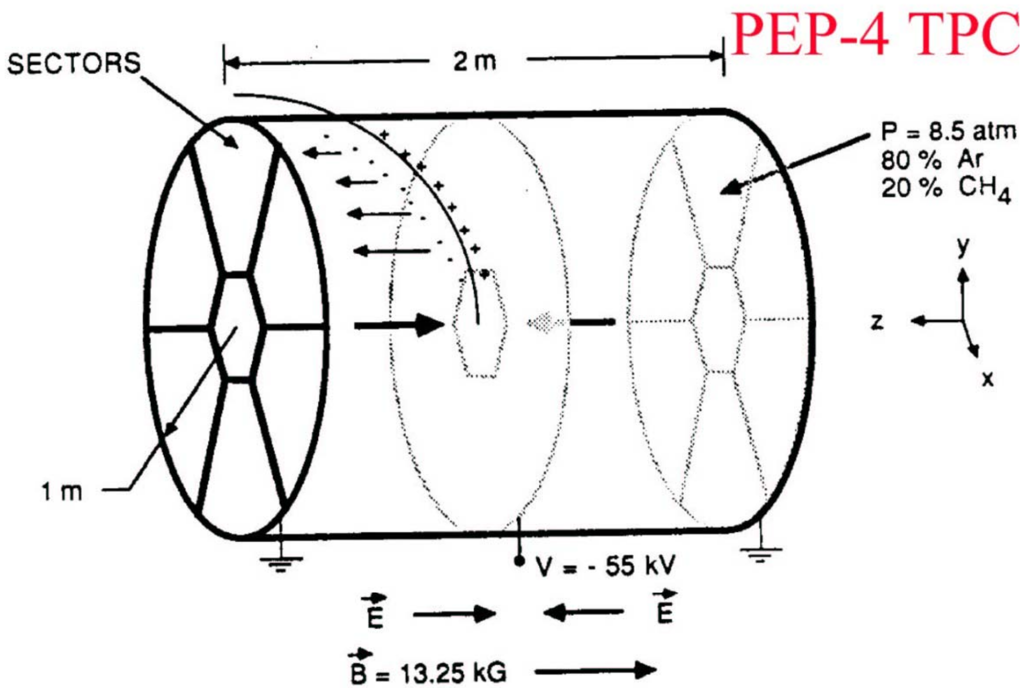

Diffusion: no problem for the tranverse coordinate in spite of the very long drift distance because B parallel to E (drift direction).

Drift chamber: TPC – time projection chamber

z coordinate (along the E, B field): from drift time

2 dim. read-out at one side:

- Anode wires and cathode pads
- Anode wires and cathode strips (perpendicular)

Resolutions for the ALEPH TPC (d=3.6m, L=4.4m):

in x,y: 173 mm, in z: 740 mm.

Potential problems:

- need an excellent drift velocity monitoring (long drift distance)
- high quality gas (long drift distance)
- space charge: ions drifting back to the cathode

Components of an experimental apparatus (‘spectrometer’)

- Tracking and vertexing systems
- Particle identification devices
- Calorimeters (measurement of energy)

Why Particle ID?

Particle identification is an important aspect of particle, nuclear and astroparticle physics experiments.

Some physical quantities in particle physics are only accessible with sophisticated particle identification (B-physics, CP violation, rare decays, search for exotic hadronic states).

Nuclear physics: final state identification in quark-gluon plasma searches, separation between isotopes

Astrophysics/astroparticle physics: identification of cosmic rays – separation between nuclei (isotopes), charged particles vs high energy photons

Introduction: Why Particle ID?

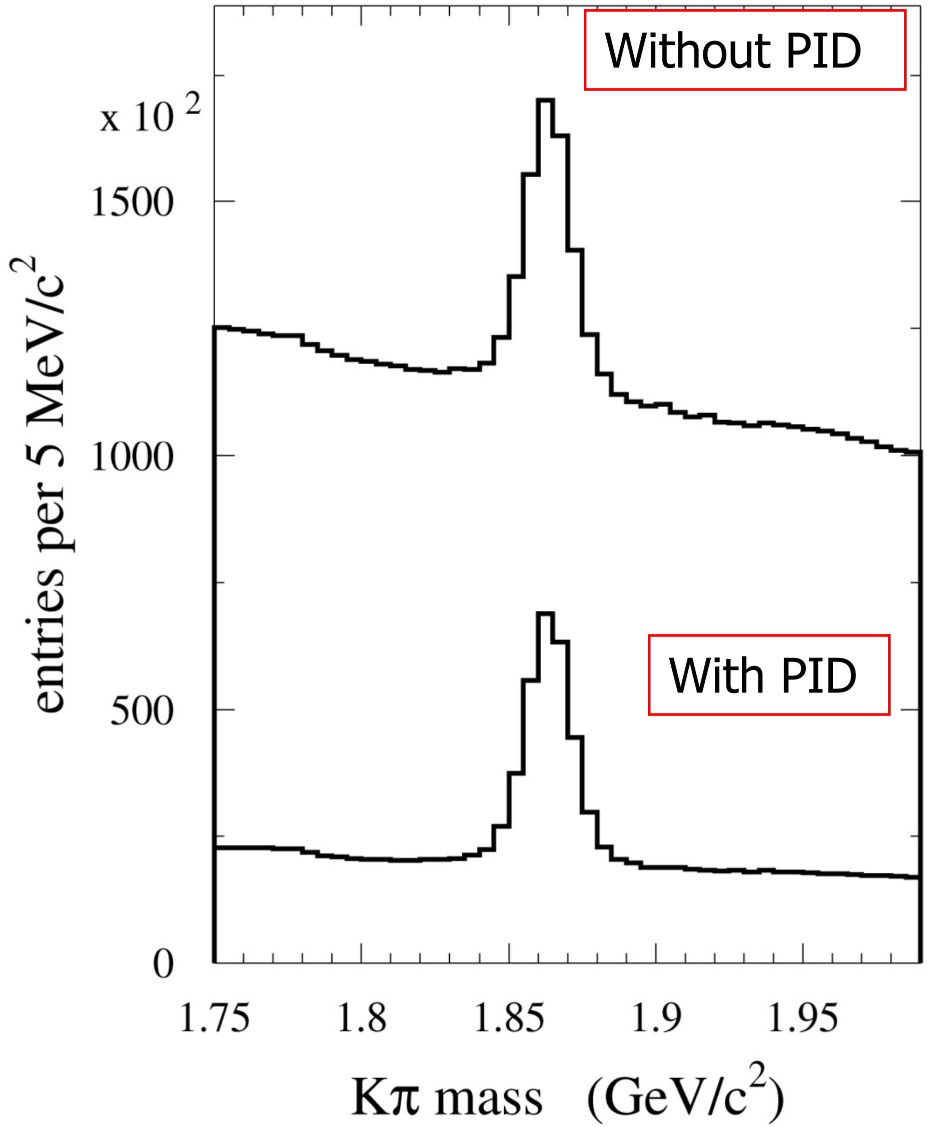

Example 1: B factories

Particle identification reduces combinatorial background by ~3x

Introduction: Why Particle ID?

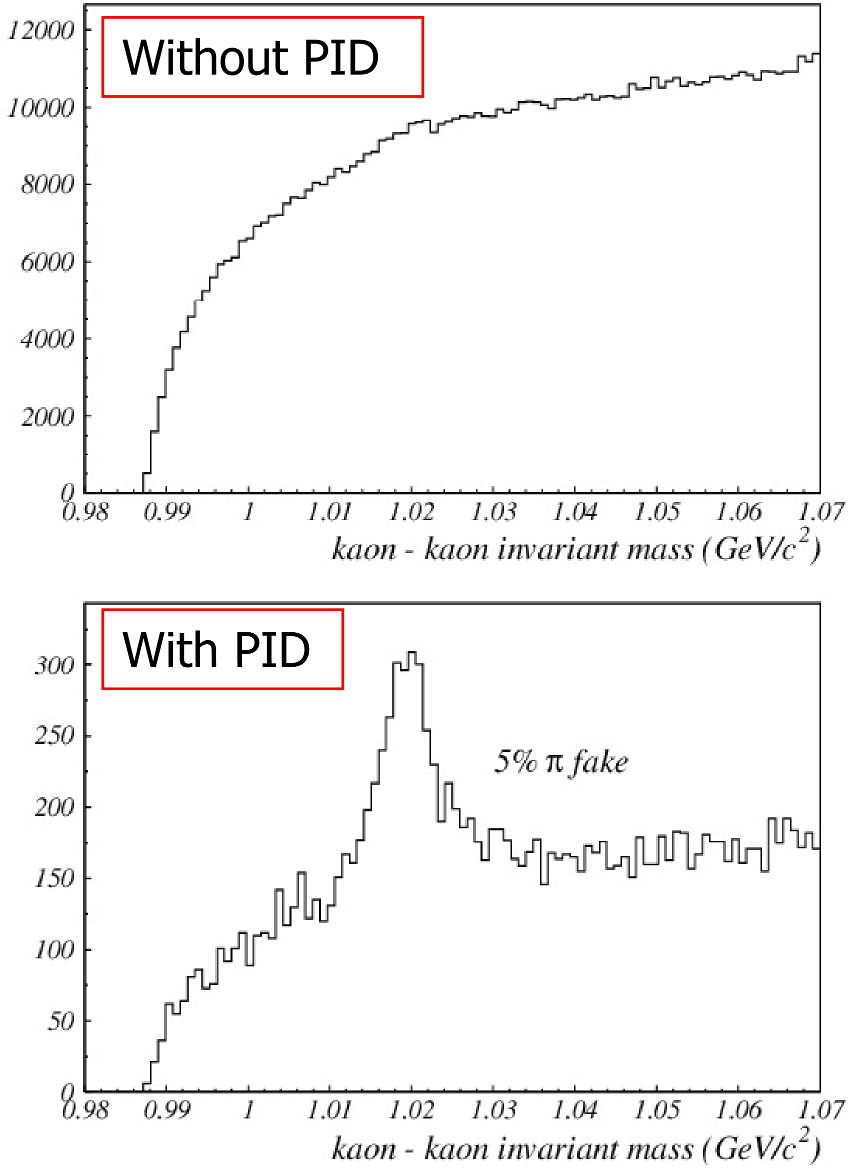

Example 2: HERA-B

K^+K^- invariant mass.

The $\phi \rightarrow K^+K^-$ decay only becomes visible after particle identification is taken into account.

Particle identification systems in Belle

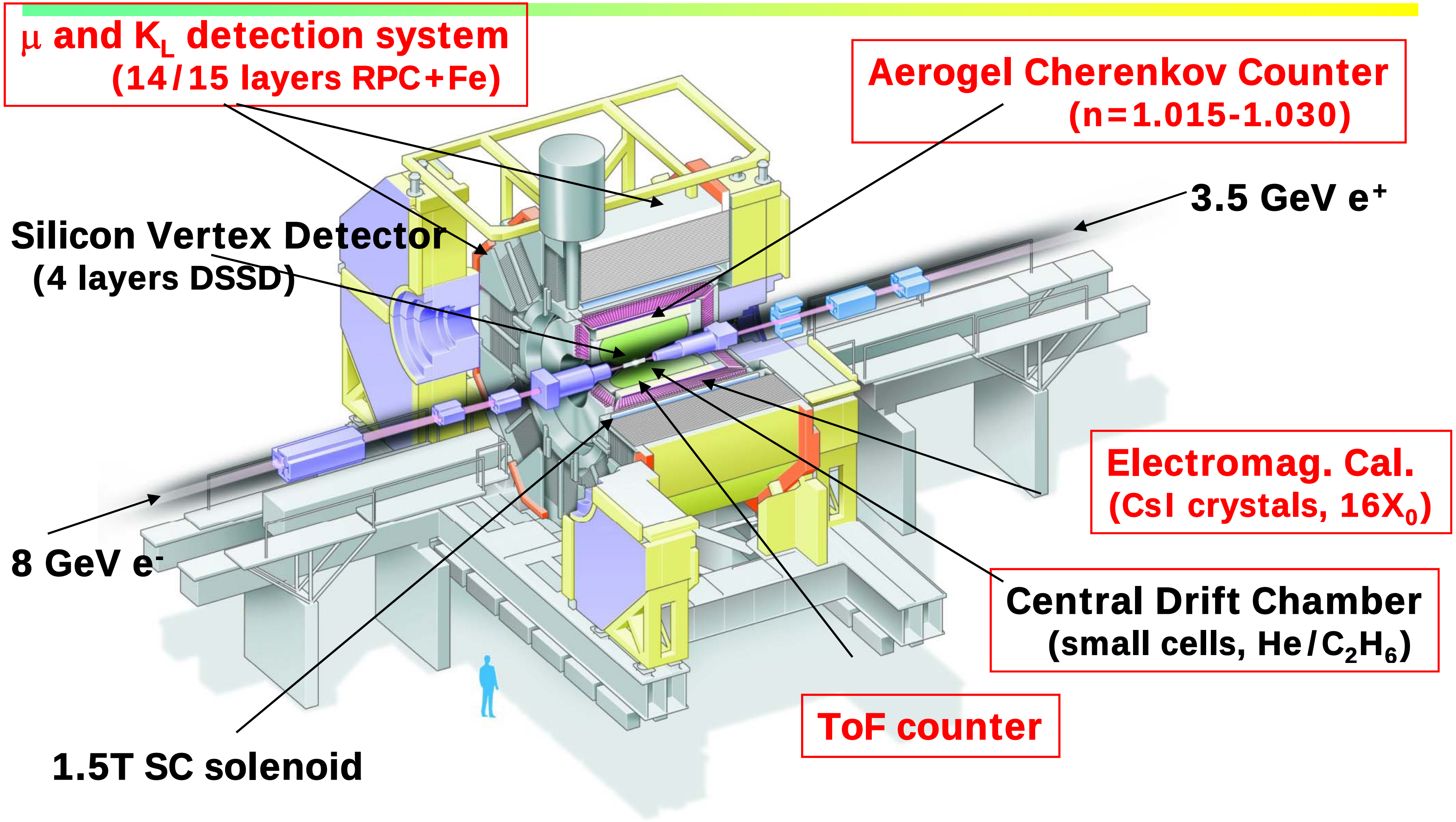

Efficiency and purity in particle identification

Efficiency and purity are tightly coupled!

Two examples:

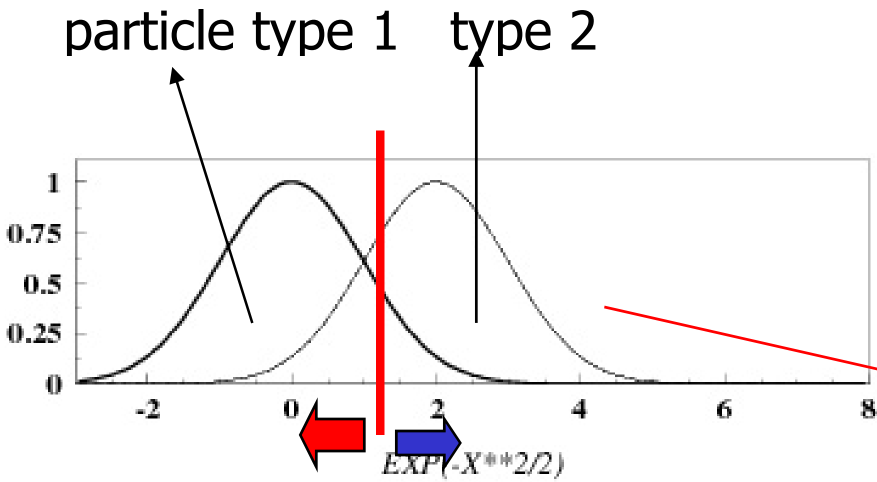

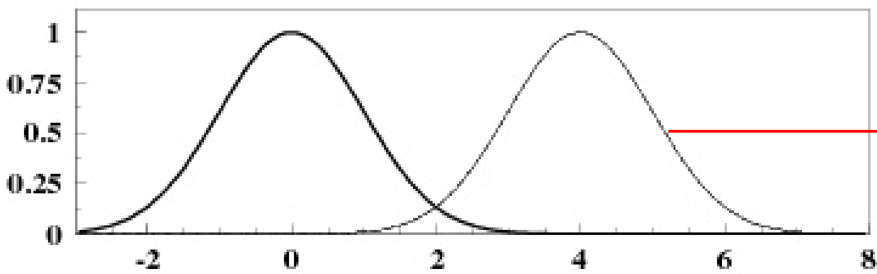

some discriminating variable

eff. vs fake probability

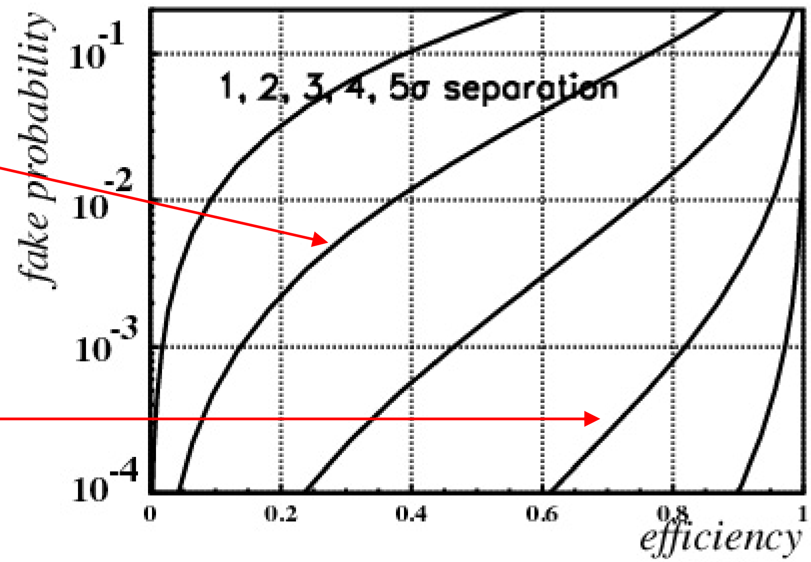

Identification of charged particles

Particles are identified by their mass or by the way they interact.

Determination of mass: from the relation between momentum and velocity, $p=\gamma mv$.

Momentum known (radius of curvature in magnetic field)

→Measure velocity:

time of flight

ionisation losses dE/dx

Cherenkov angle

transition radiation

Mainly used for the identification of hadrons.

Identification through interaction: electrons and muons

Time-of-flight measurement (TOF)

Measure time difference over a known distance, determine velocity

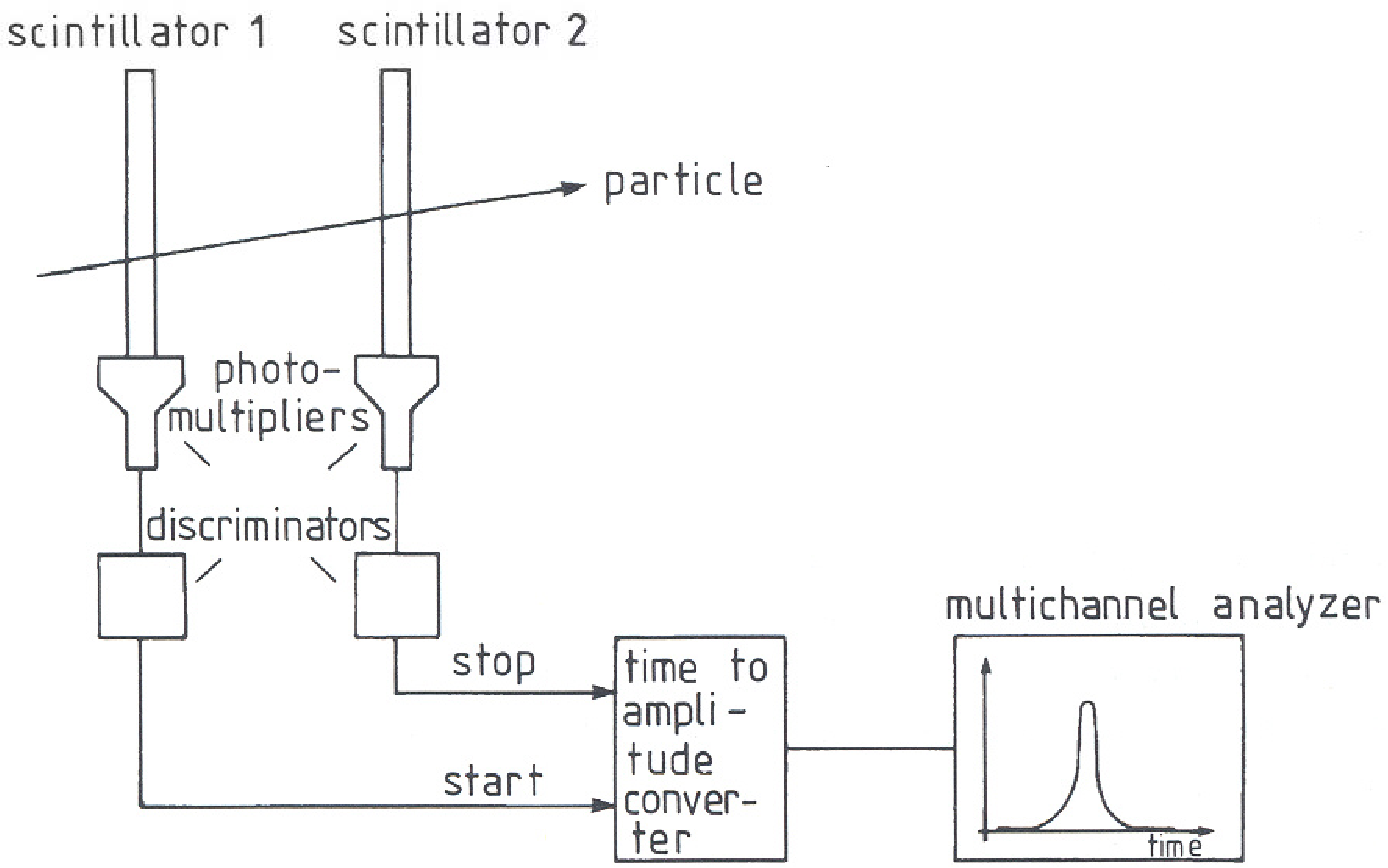

Fig. 6.5. Working principle of time-of-flight measurement.

Time-of-flight measurement 2

Time difference between two particle species for path length=1m

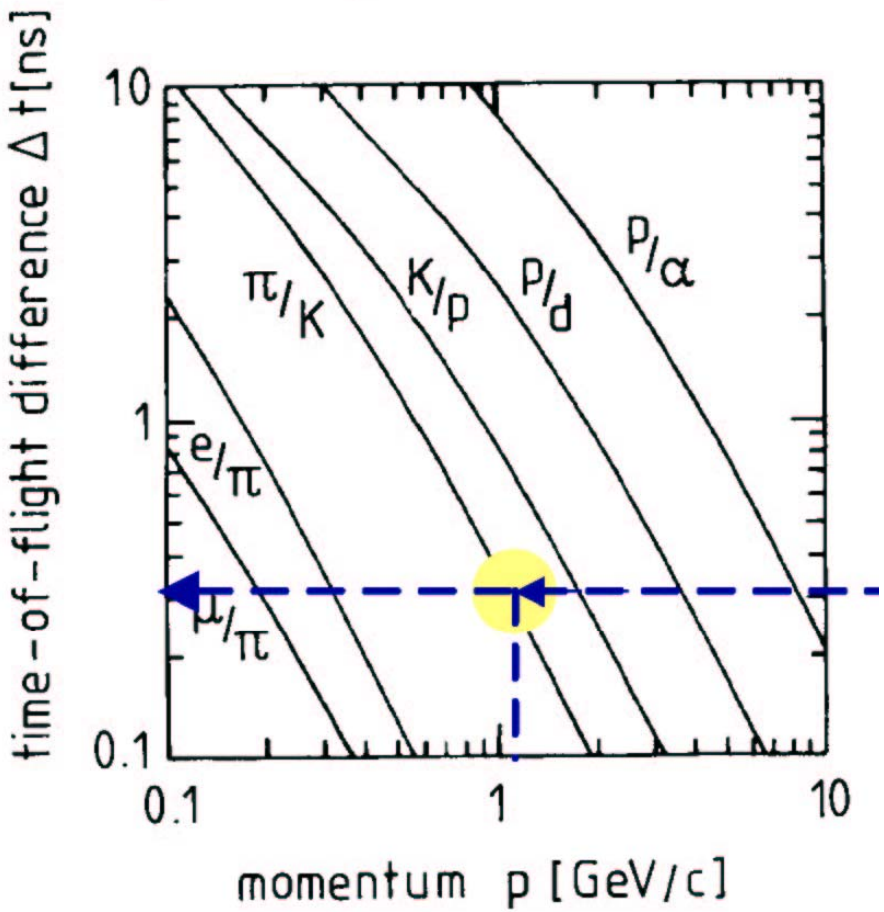

Required resolution, example:

π/K difference at 1GeV/c: 300ps

For a 3σ separation need σ(TOF)=100ps

Resolution contributions:

- PMT: transient time spread (TTS)
- Path length variation
- Momentum uncertainty

Very fast: MCP-PMT

Microchannel plate (MCP) PMT: multi-anode PMT with two MCP stages

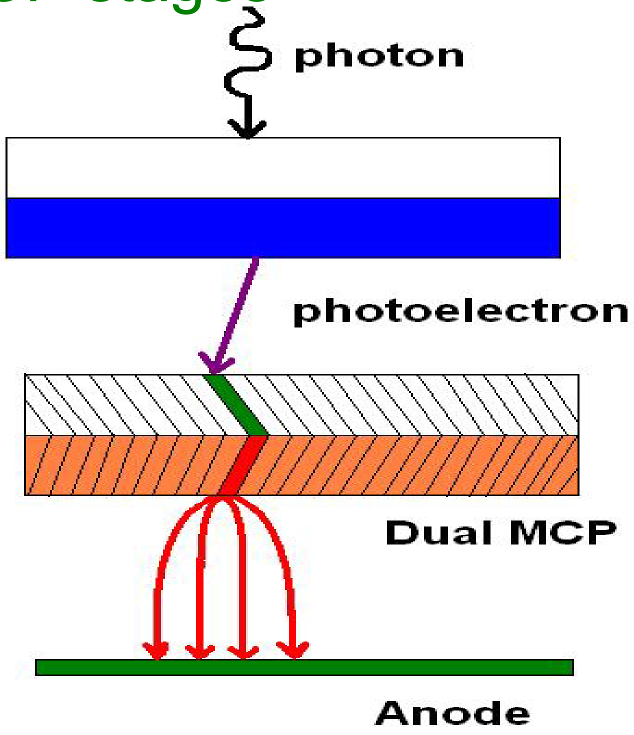

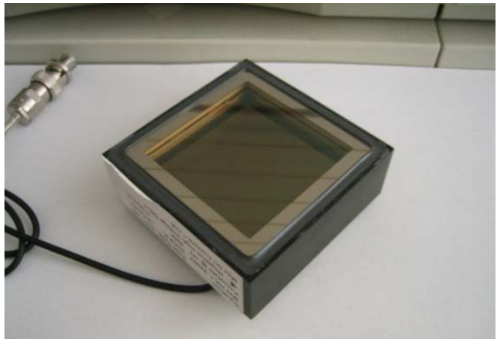

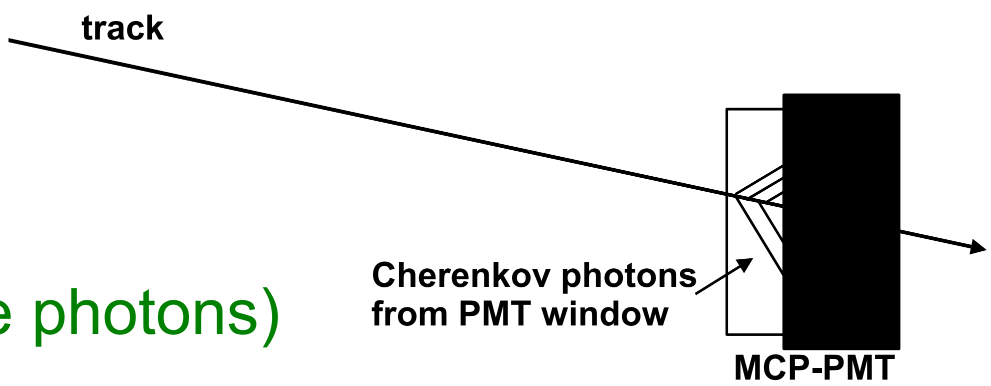

→ very fast (σ~40ps for single photons)

Identification with dE/dx measurement

dE/dx is a function of velocity.

For particles with different mass the Bethe-Bloch curve gets displaced → separation is possible if the resolution is good enough

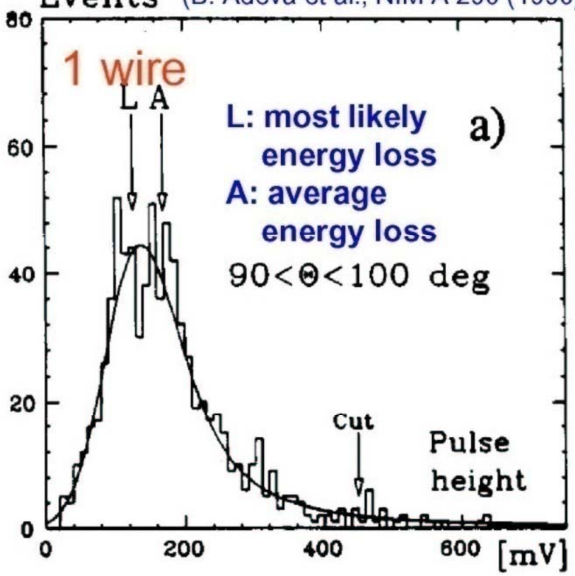

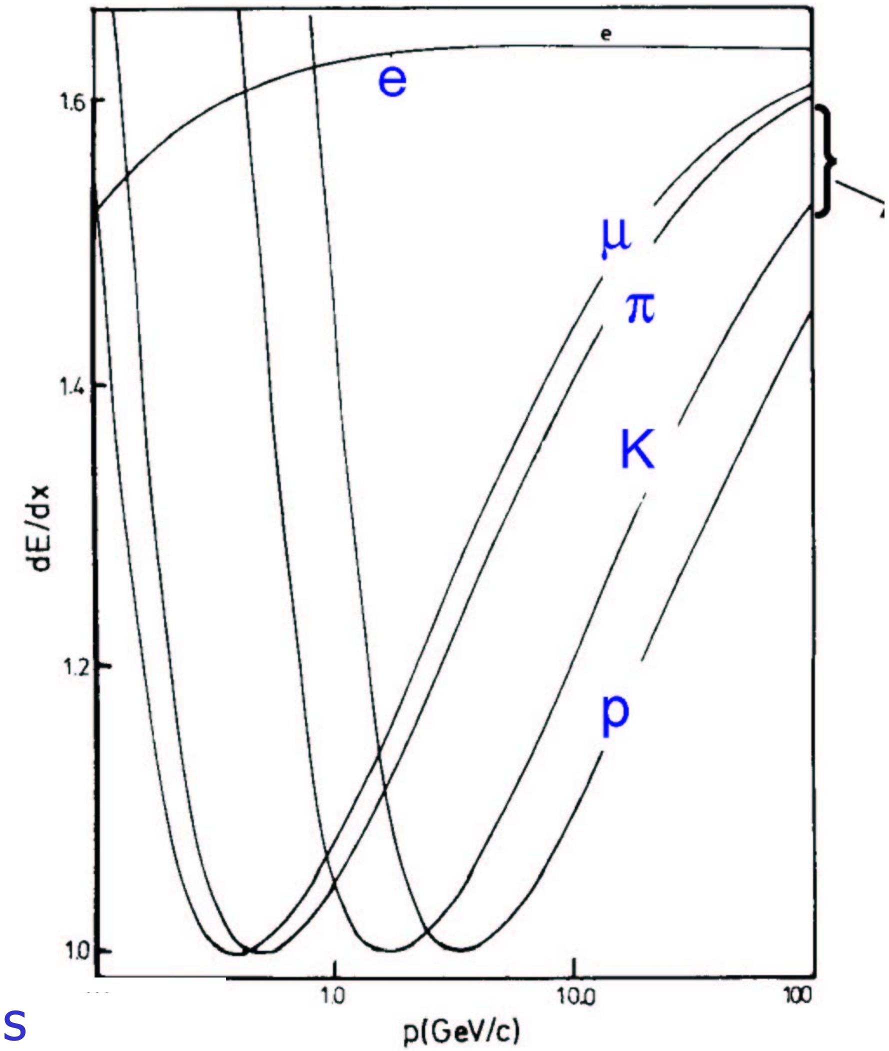

Problem: long tails (Landau distribution, not Gaussian)

Identification with dE/dx measurement

dE/dx performance in two large drift chambers.

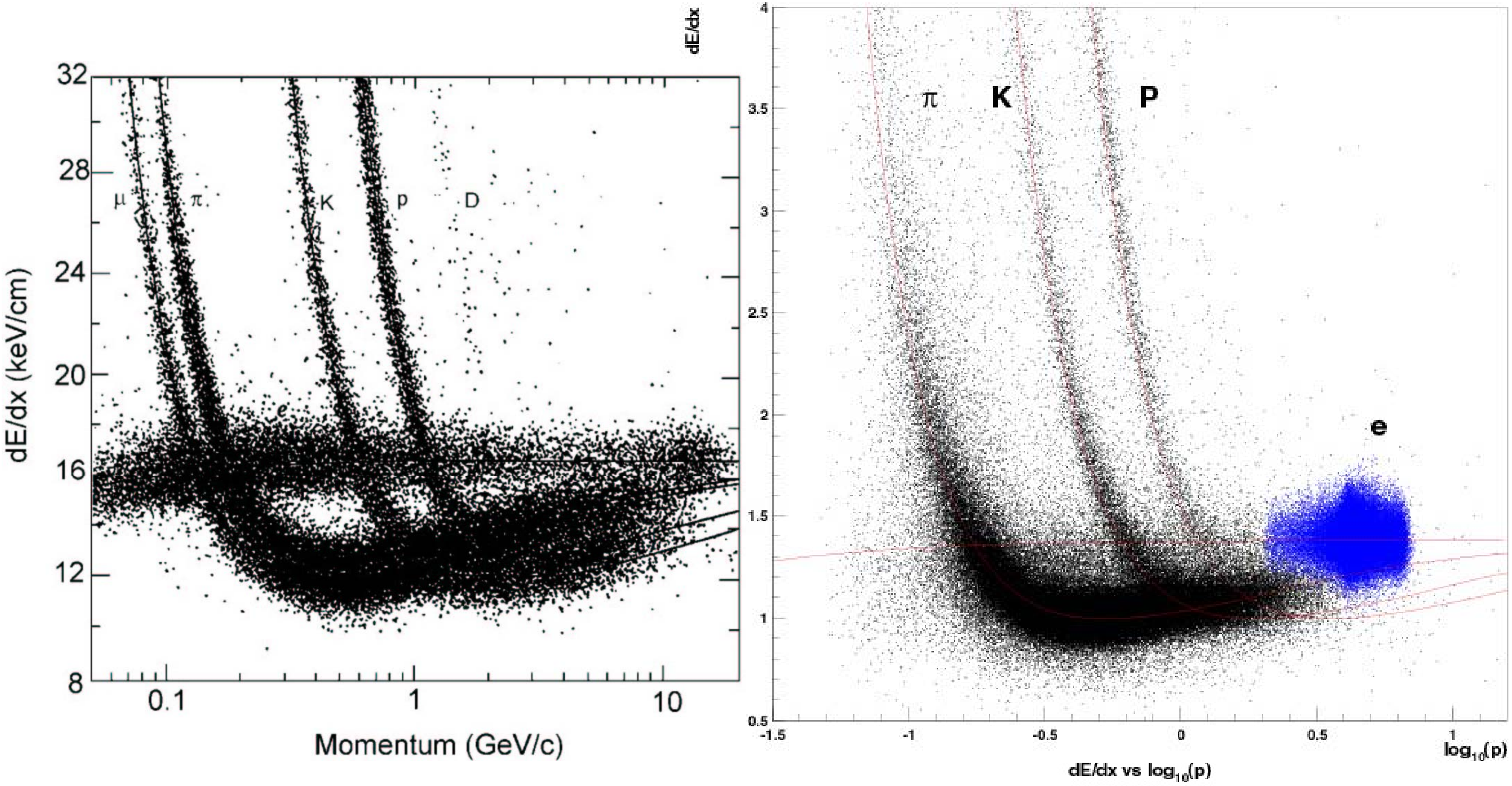

Čerenkov radiation

A charged track with velocity v=βc above the speed of light c/n in a medium with index of refraction n= √ε emits polarized light at a characteristic (Čerenkov) angle,

$\cos\theta = c / nv = 1/\beta n$

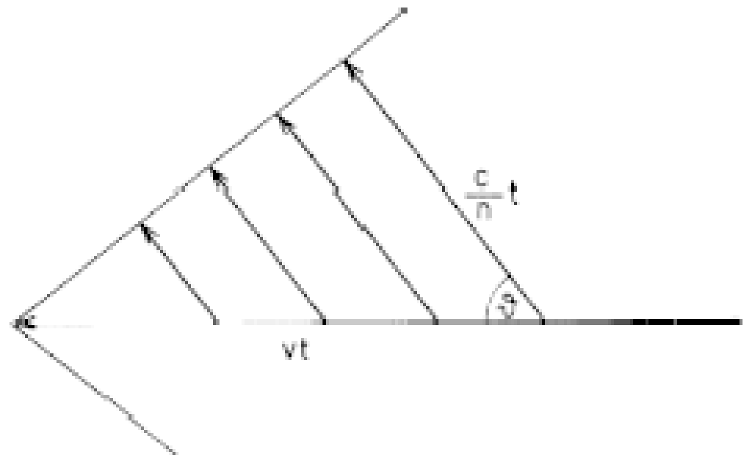

Two cases:

1) $\beta < \beta_t = 1/n$: below threshold no Čerenkov light is emitted.
2) $\beta > \beta_t$: the number of Čerenkov photons emitted over unit photon energy E=hν in a radiator of length L amounts to

$$\frac{dN}{dE} = \frac{\alpha}{\hbar c} L \sin^2\theta = 370 (cm)^{-1} (eV)^{-1} L \sin^2\theta$$

Number of detected photons

Example: in 1m of air (n=1.00027) a track with β=1 emits N=41 photons in the spectral range of visible light (ΔE ~ 2 eV).

If Čerenkov photons were detected with an average detection efficiency of ε=0.1 over this interval, N=4 photons would be measured.

In general: number of detected photons can be parametrized as

$N = N_0 L \sin^2\theta$

where N_0 is the figure of merit, $$N_0 = \frac{\alpha}{\hbar c}\int Q(E)T(E)R(E)dE$$

and Q T R is the product of photon detection efficiency, transmission of the radiator and windows and reflectivity of mirrors employed.

Typically: N_0 = 50 - 100/cm

Cherenkov counters

Threshold counters --> count photons to separate particles below and above threshold; for $\beta < \beta_t = 1/n$ (below threshold) no Čerenkov light is emitted

Ring Imaging (RICH) --> measure Čerenkov angle and count photons

Short historical excursion

- 1934 Čerenkov characterizes the radiation
- 1938 Frank, Tamm give the theoretical explanation
- 50-ties - 70-ties Čerenkov counters are developed and are being used in nuclear and particle physics experiments, as differential and threshold counters
- 1958: Nobel prize for Čerenkov
- 1977 Ypsilantis, Seguinot introduce the idea of a RICH counter with a large area wire chamber based photon detector
- 1981-83 first use of a RICH counter in a particle physics experiment (E605)
- 1992--> first results from the DELPHI RICH, SLD CRID, OMEGA RICH

Belle ACC (aerogel Cherenkov counter): threshold Čerenkov counter

K (below thr.) vs. π (above thr.): adjust n

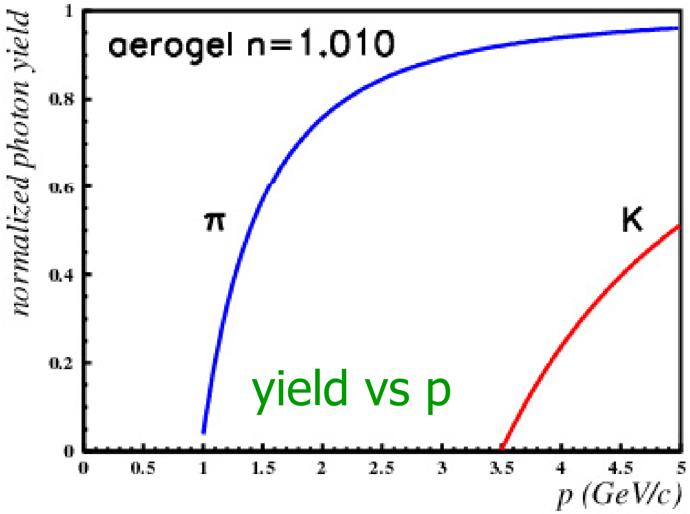

measured for 2 GeV < p < 3.5 GeV
expected, measured ph. yield

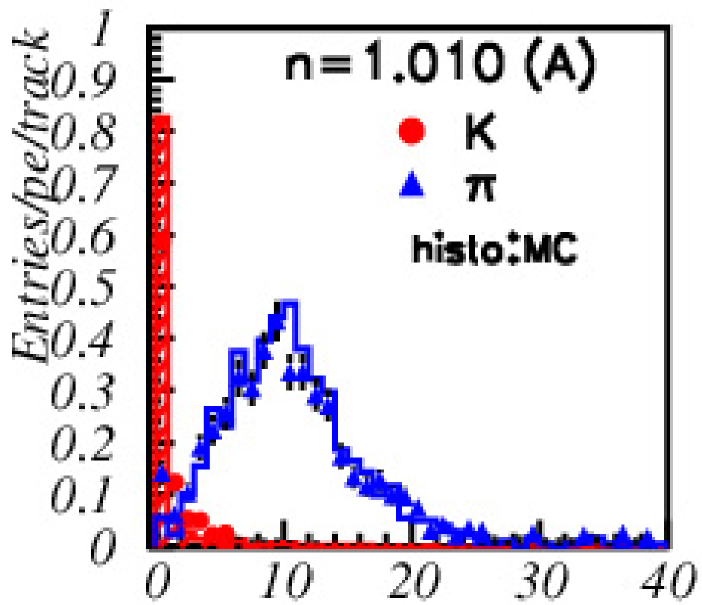

Detector unit: a block of aerogel and two fine-mesh PMTs

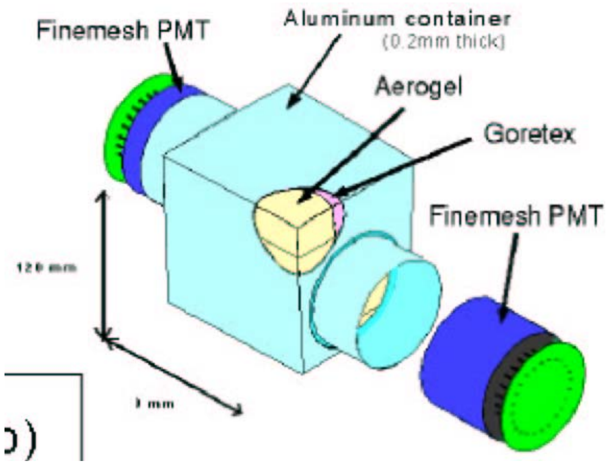

Belle ACC (aerogel Cherenkov counter): threshold Cherenkov counter

- K (below thr.) vs. π (above thr.): adjust n for a given angle kinematic region (more energetic particles fly in the 'forward region')

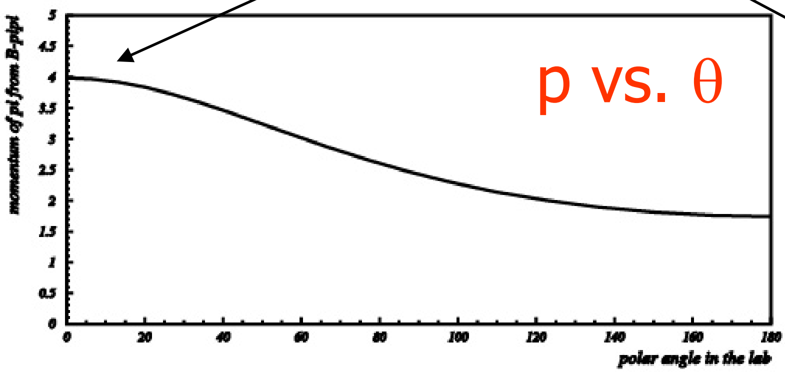

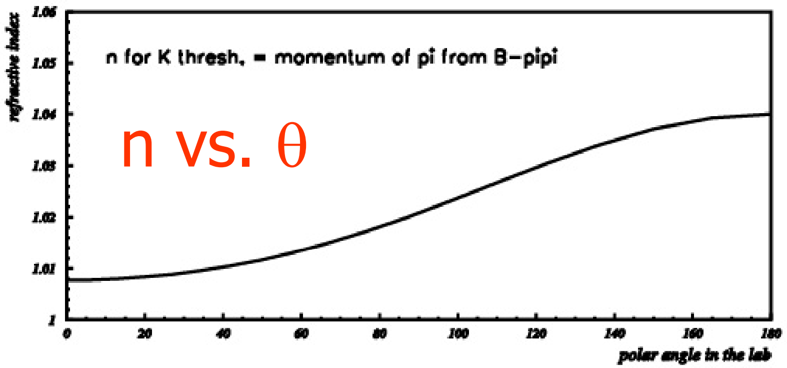

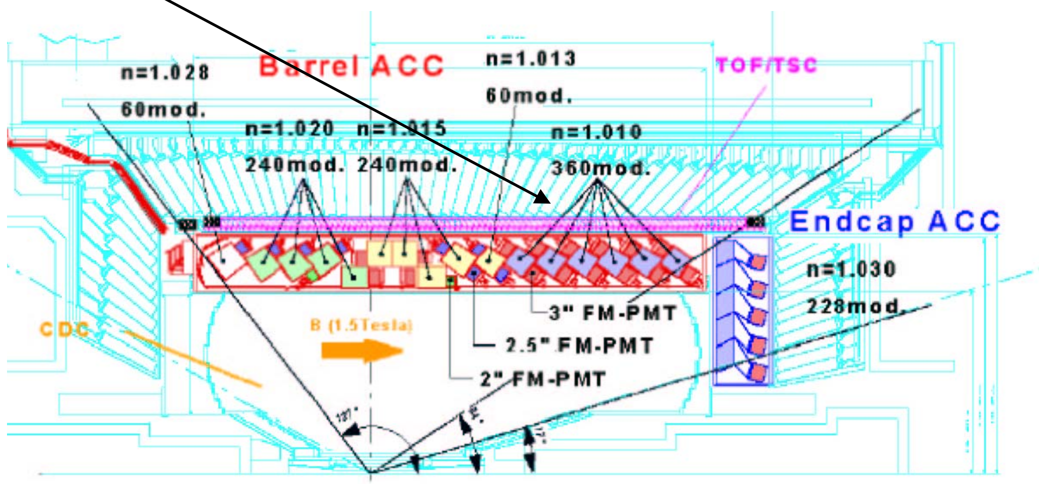

Measuring Cherenkov angle

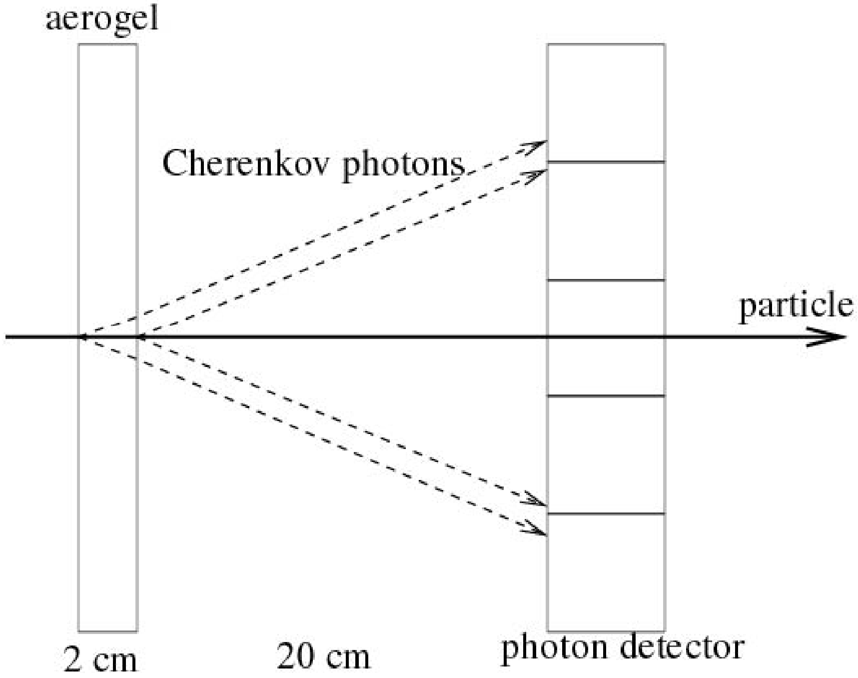

Proximity focusing RICH

Idea: transform the direction into a coordinate → ring on the detection plane

→ Ring Imaging CHerenkov

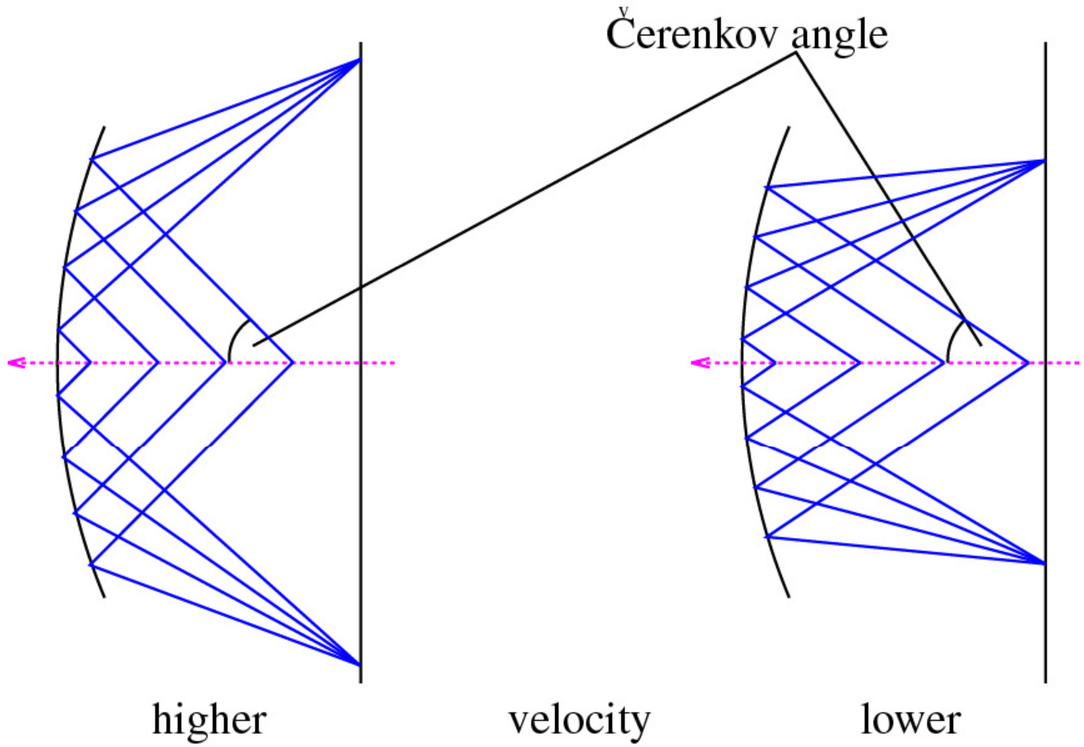

RICH with a focusing mirror

RICH counter 2

From the image on the photon detector, the Čerenkov angle of the track can be reconstructed, i.e. from the known track direction (ring center) and hit coordinate the angle is calculated and plotted for each individual photon

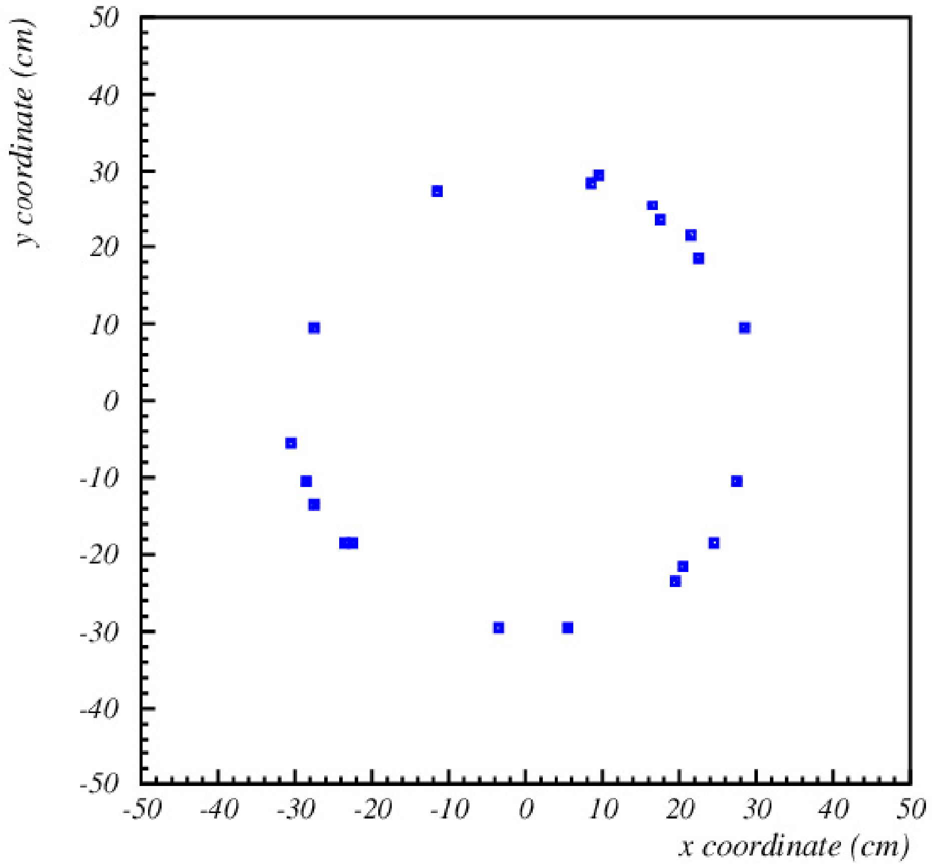

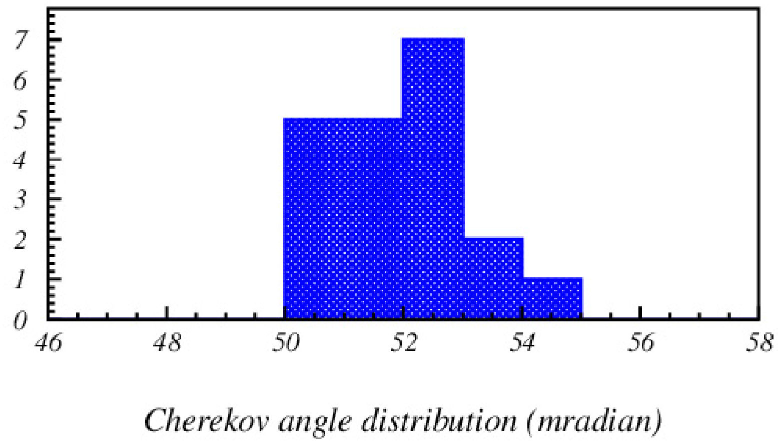

HERA-B RICH

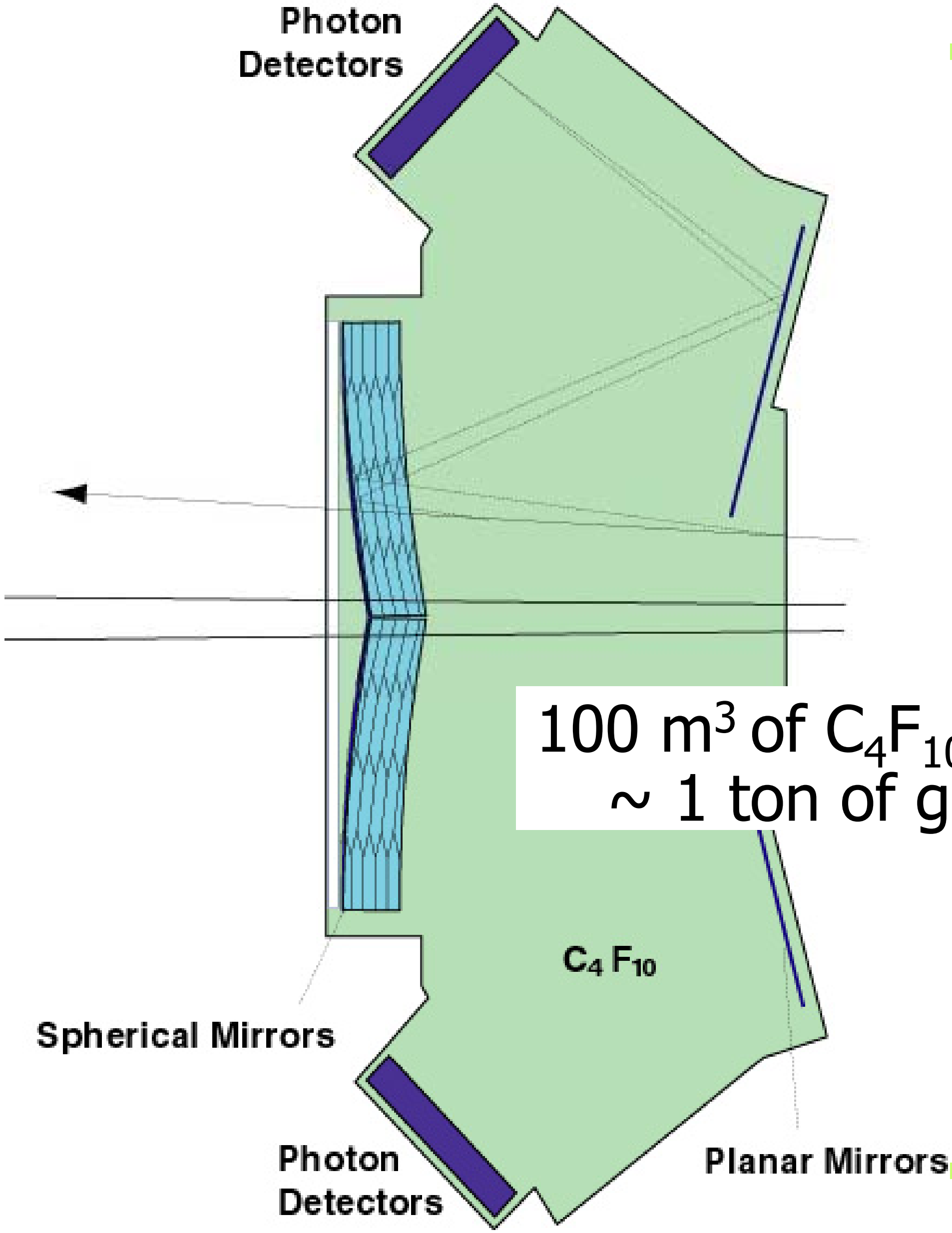

$100\ m^3$ of C_4F_{10}
~ 1 ton of gas

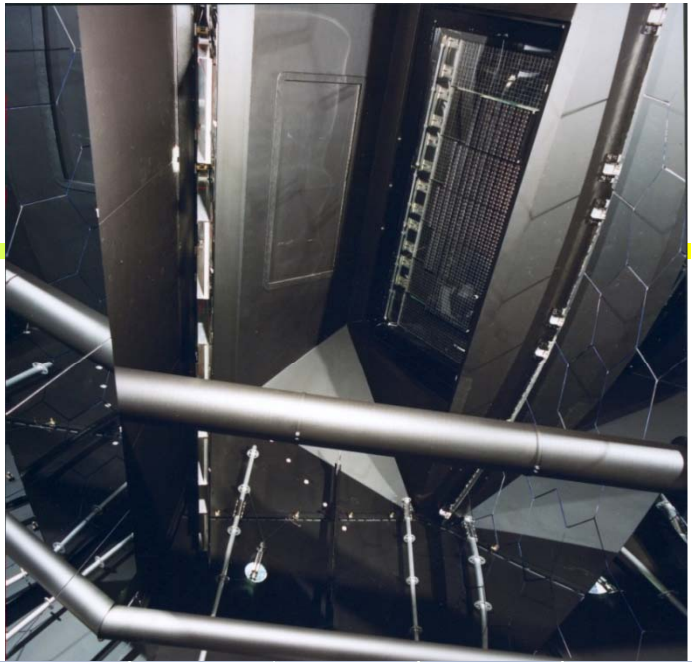

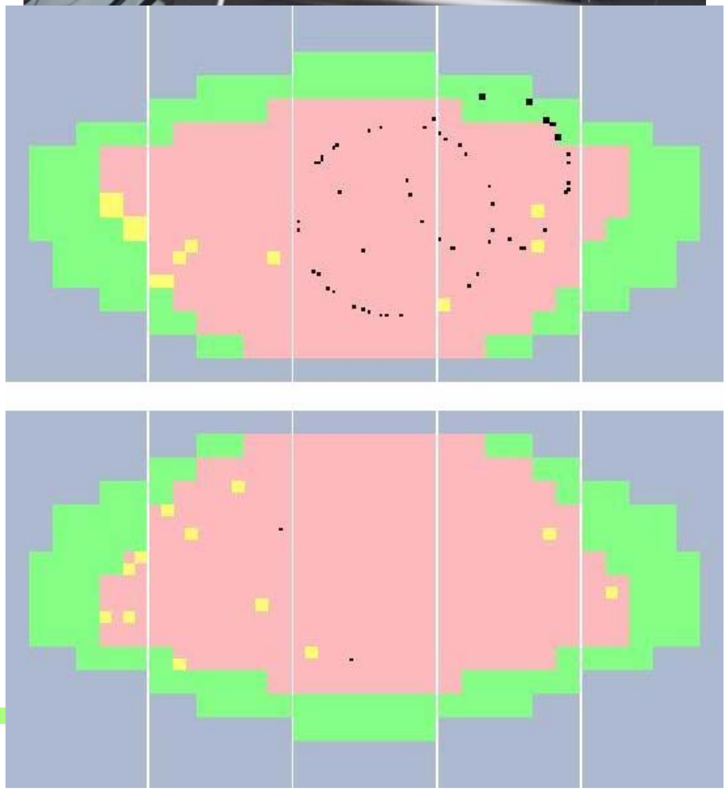

Photon detection in RICH counters

RICH counter: measure photon impact point on the photon detector surface

→ detection of single photons with

- sufficient spatial resolution
- high efficiency and good signal-to-noise ratio
- over a large area (square meters)

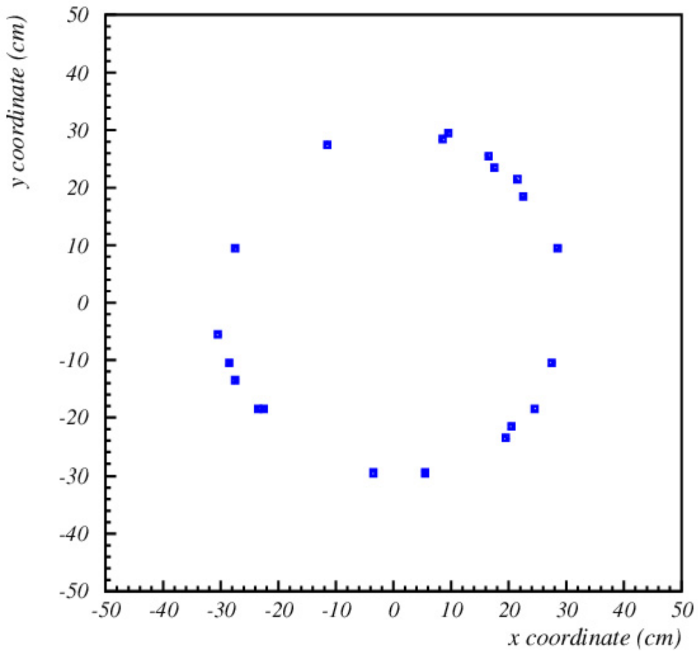

Special requirements:

- Operation in magnetic field
- High rate capability
- Very high spatial resolution
- Excellent timing (time-of-arrival information)

Multianode PMT
Hamamatsu R5900-M16

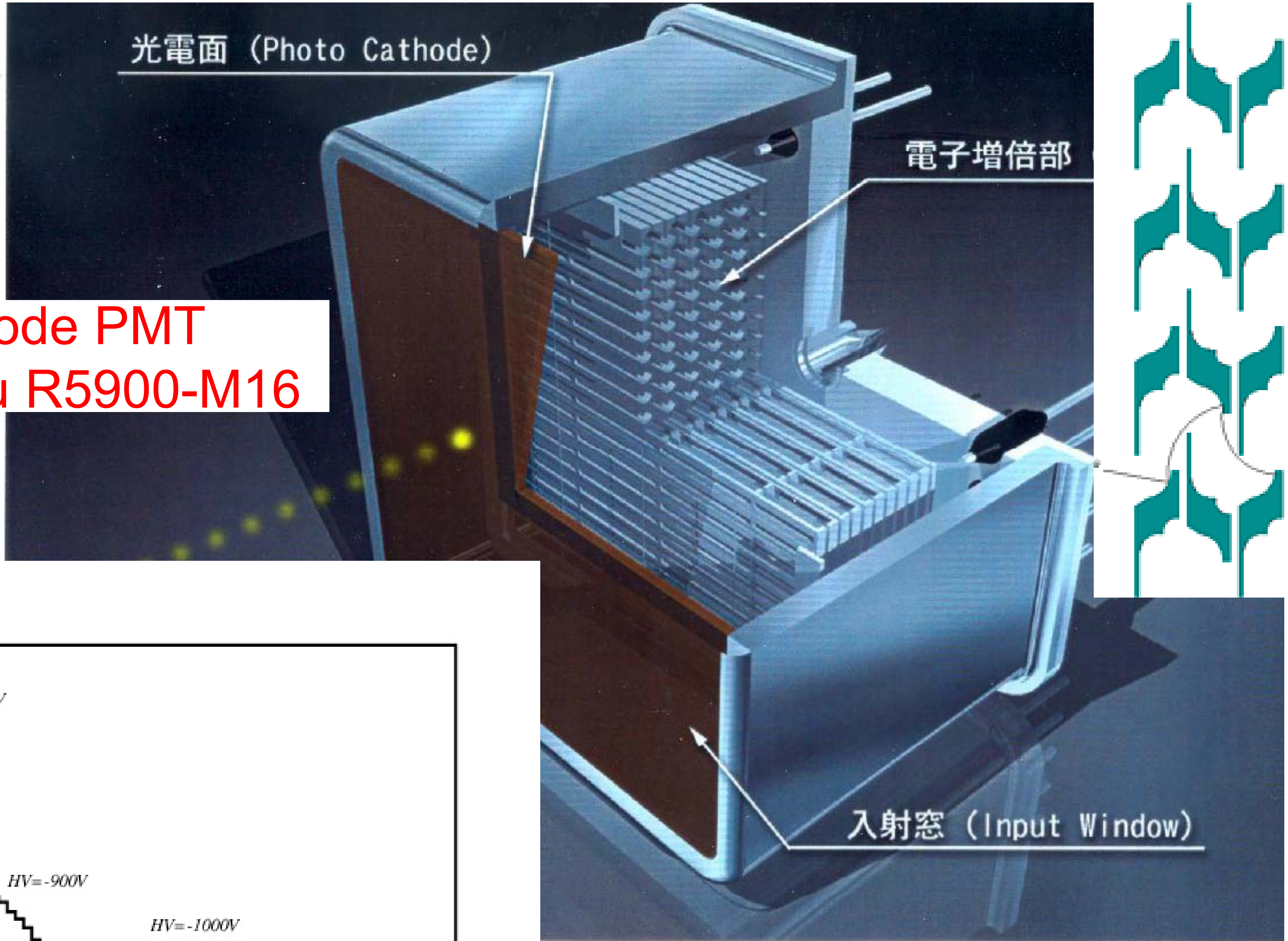

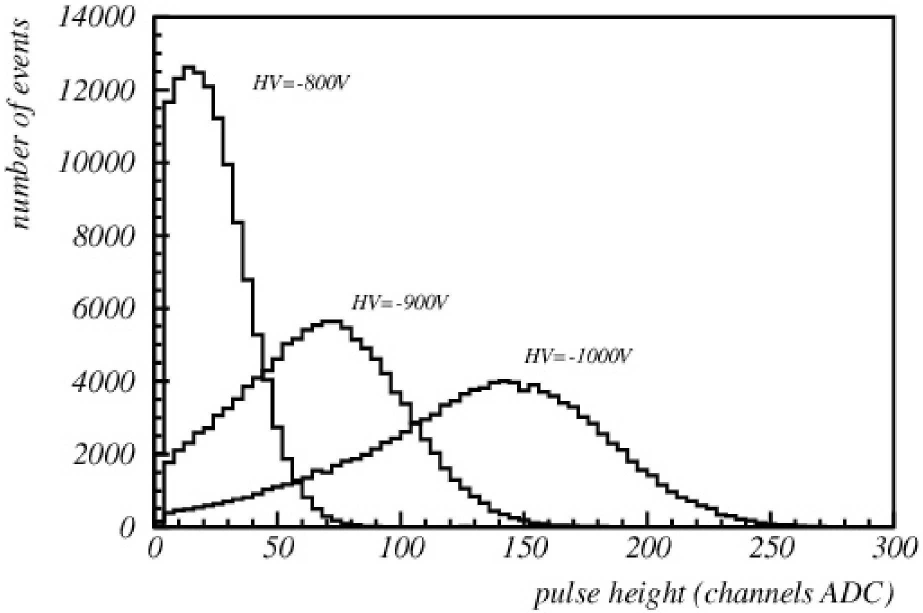

- Excellent single photon pulse height spectrum
- Low noise

Multiple radiators: LHCb RICHes

Need:

- Particle identification for momentum range ~2-100 GeV/c
- Cannot cover such a kinematic range with a single RICH

→3 radiators

(aerogel, CF_4, C_4F_{10})

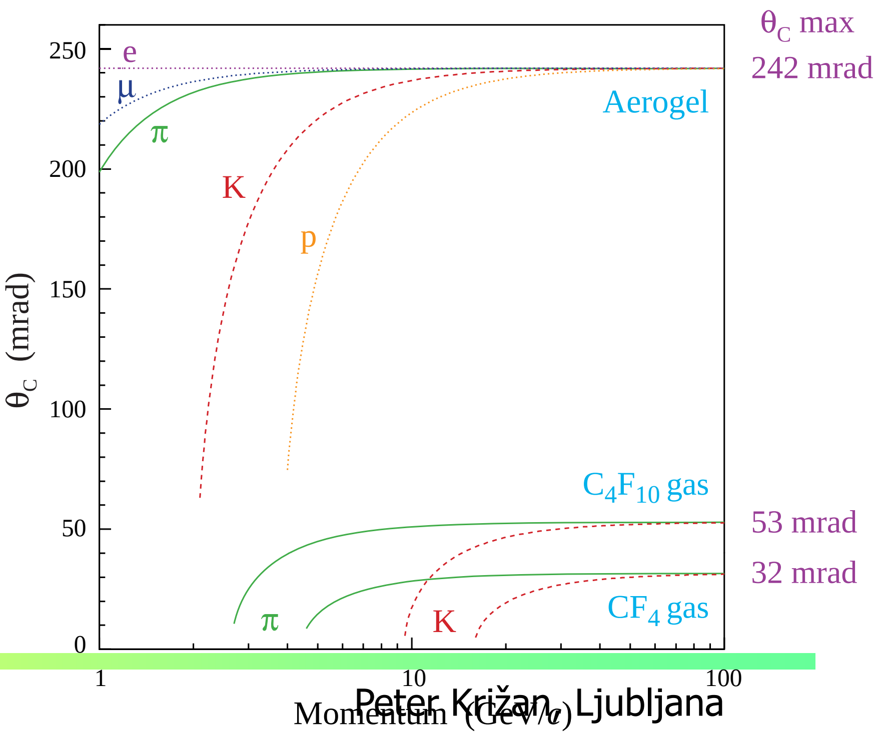

LHCb RICHes

RICH 1

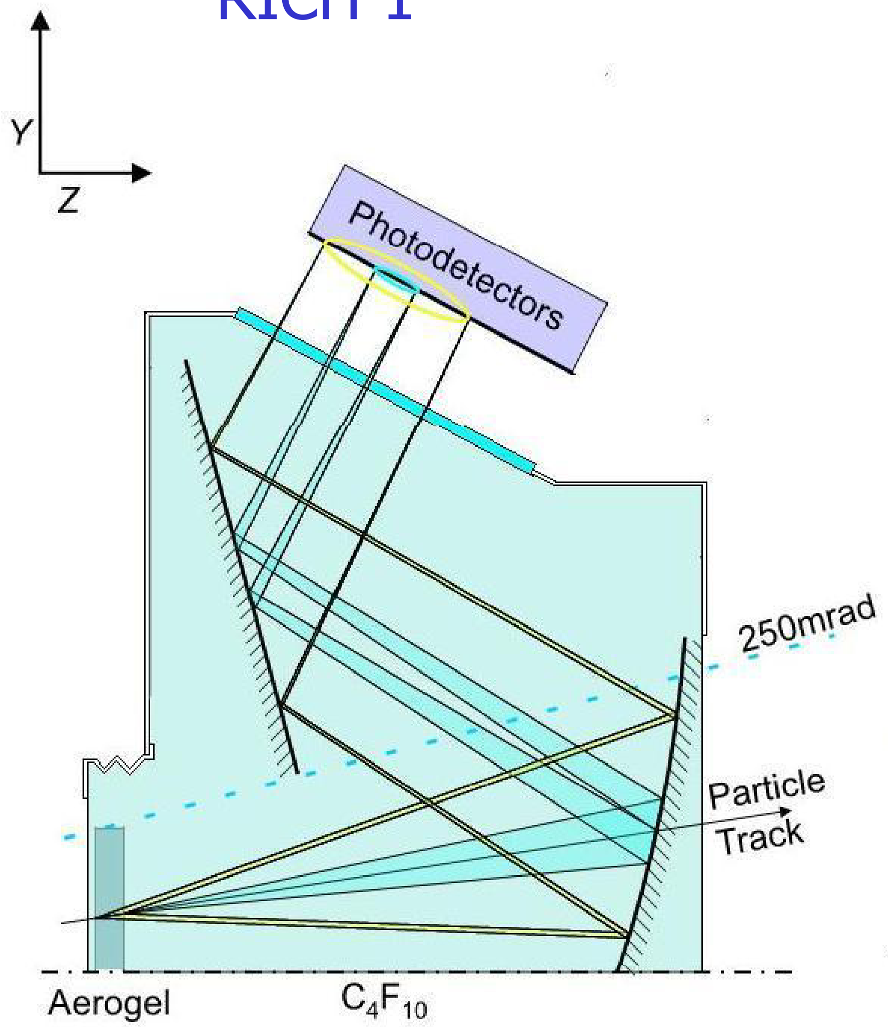

RICH 2

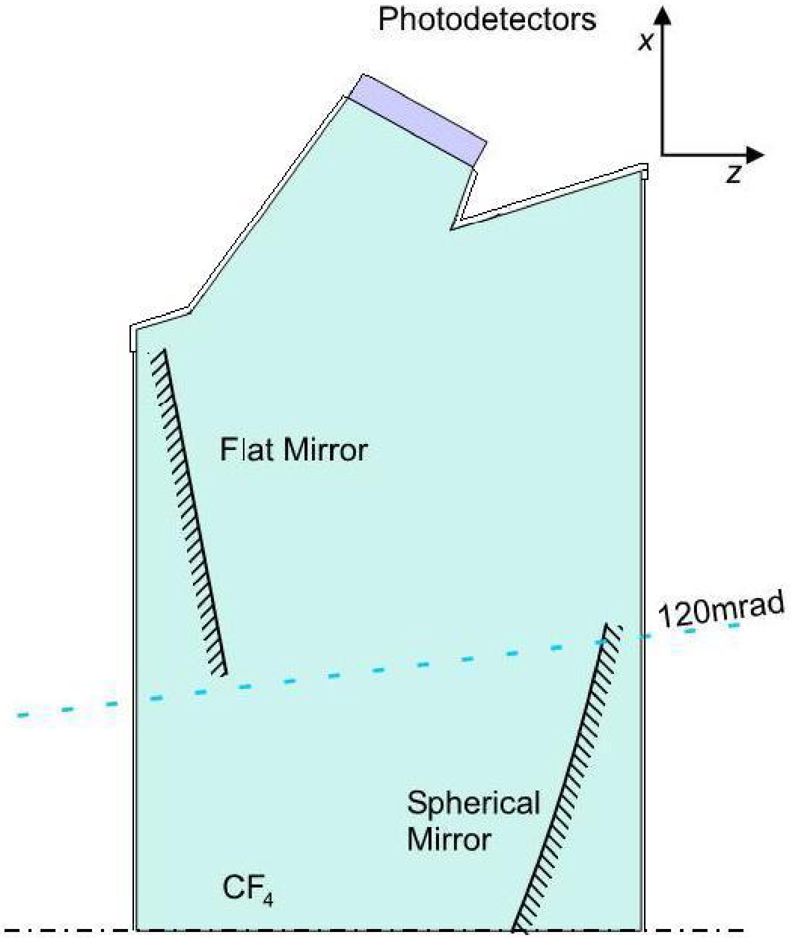

LHCb RICHes

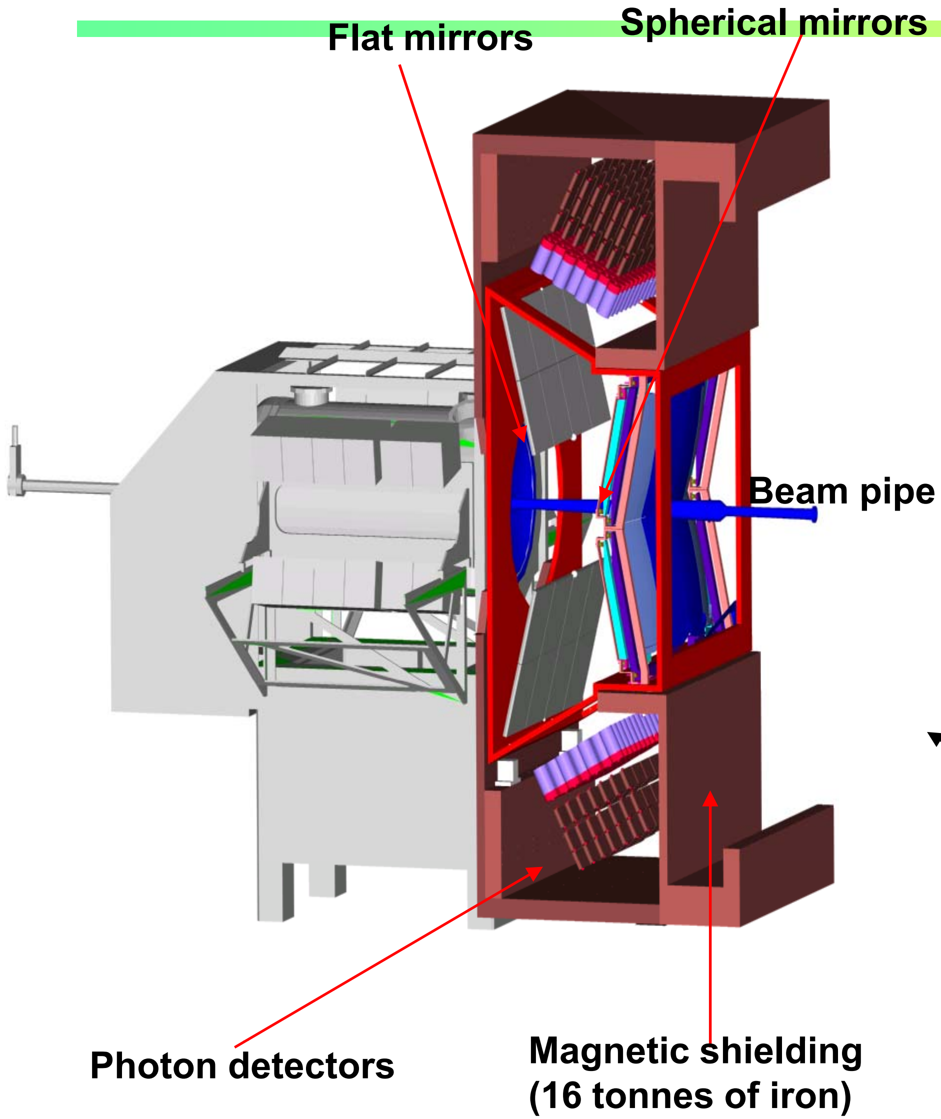

Flat mirrors
Spherical mirrors
Beam pipe
Photon detectors
Magnetic shielding
(16 tonnes of iron)

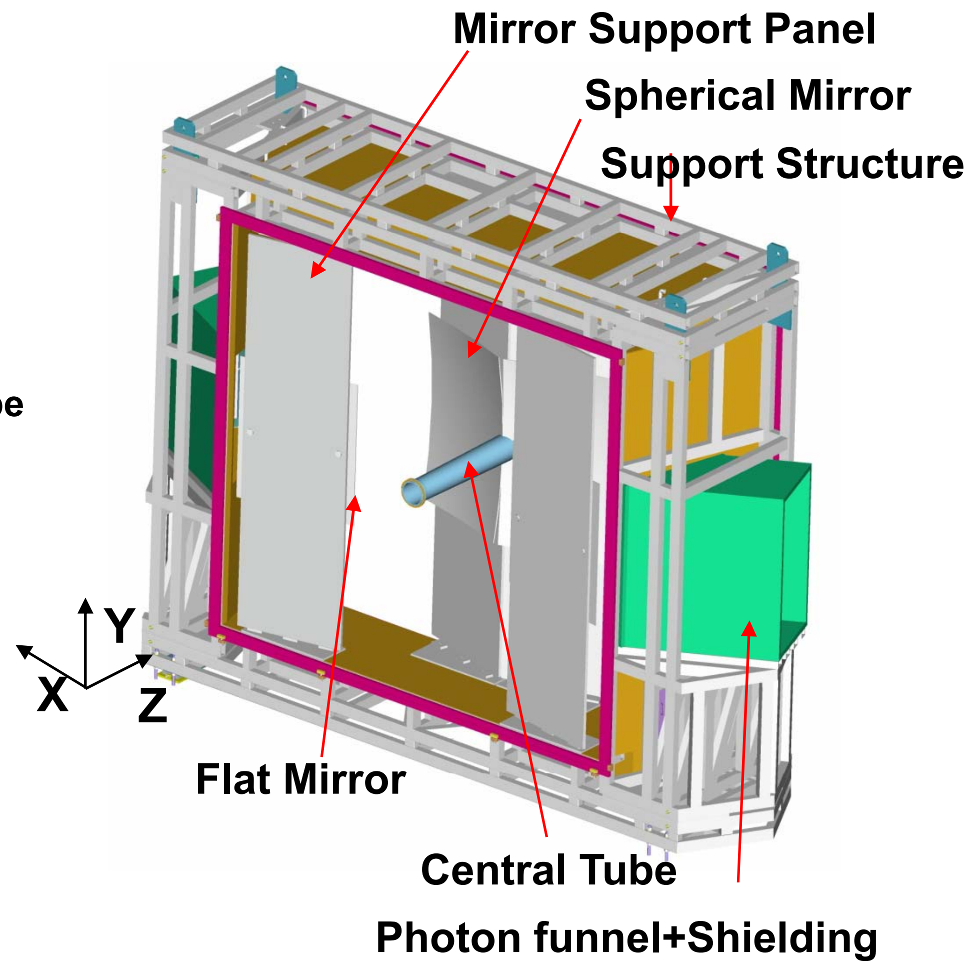

Mirror Support Panel
Spherical Mirror
Support Structure
Y
X
Z
Flat Mirror
Central Tube
Photon funnel+Shielding

Resolution of a RICH counter

•Photon impact point resolution (photon detector resolution

•Emission point uncertainty

•Dispersion: $n=n(\lambda)$ in $\cos\theta = 1/\beta n$

•Track parameters

•Errors of the optical system

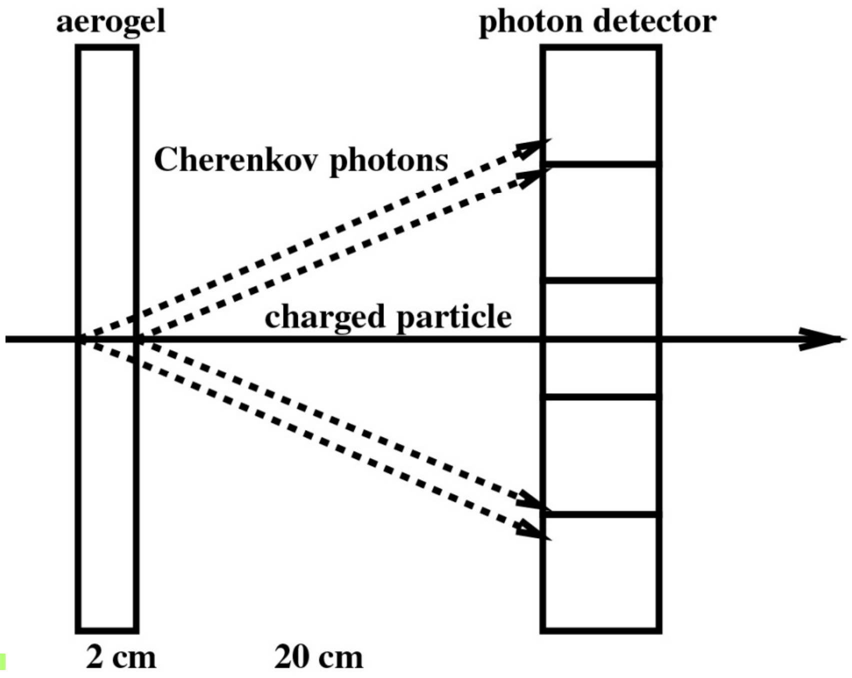

Radiator with multiple refractive indices

How to increase the number of photons without degrading the resolution?

normal

→ stack two tiles with different refractive indices: "focusing" configuration

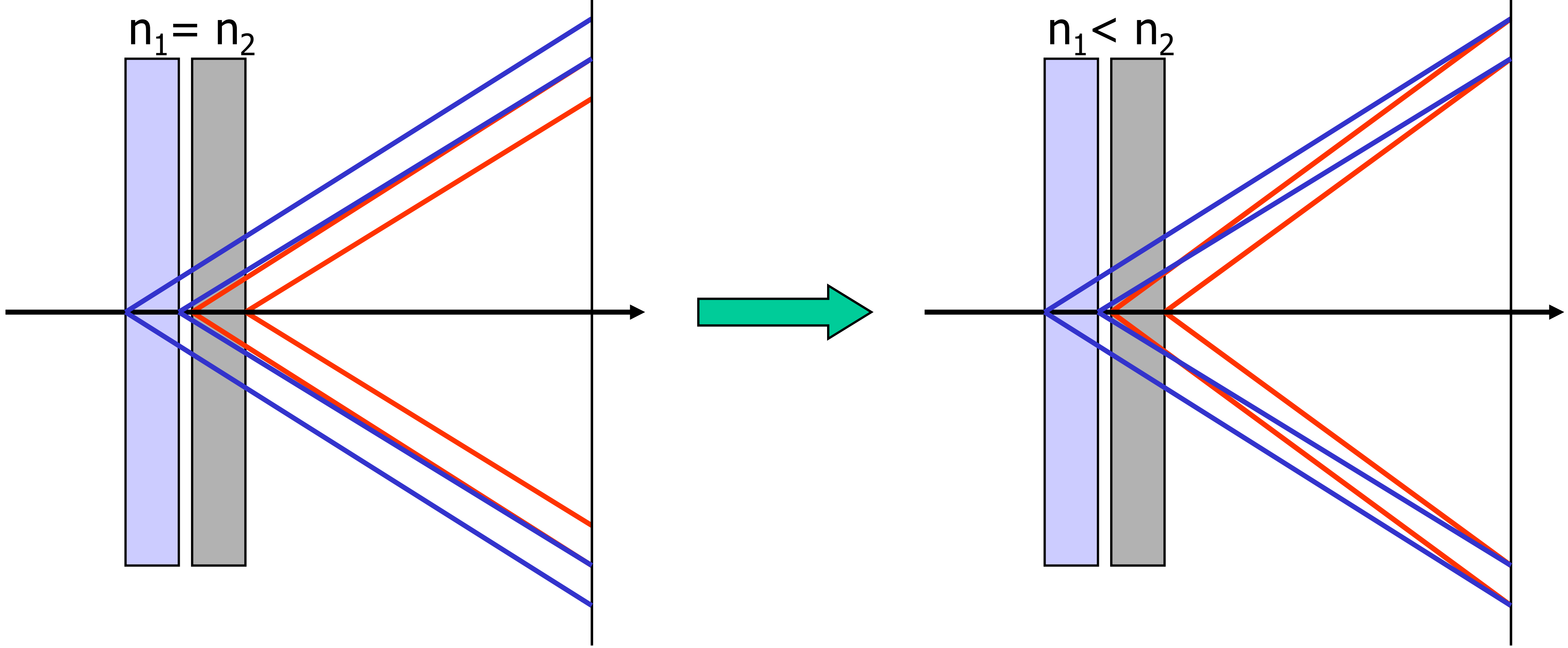

→ focusing radiator

Focusing configuration – data

4cm aerogel single index

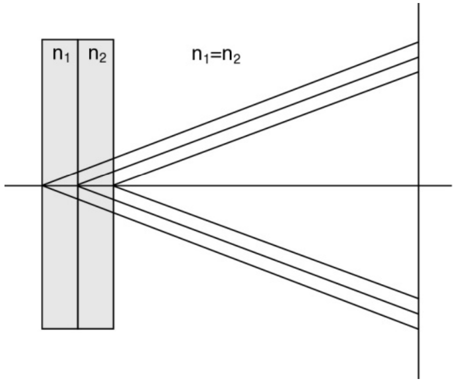

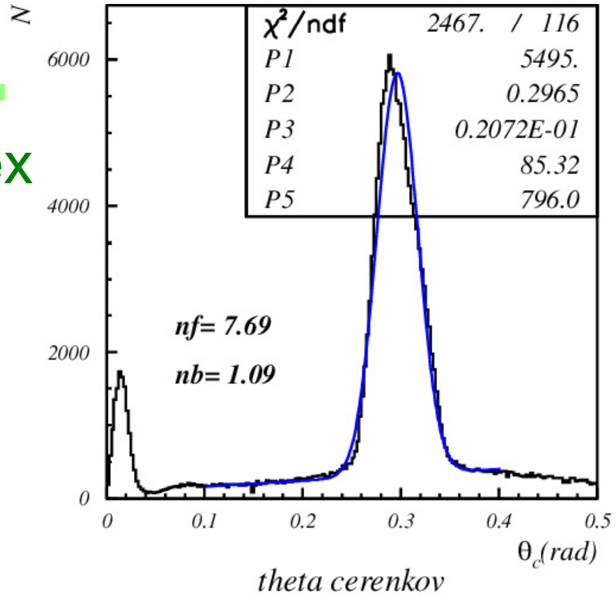

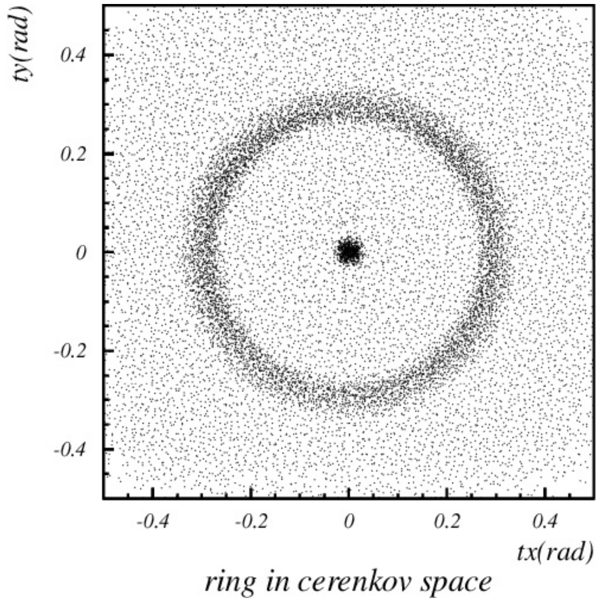

2+2cm aerogel

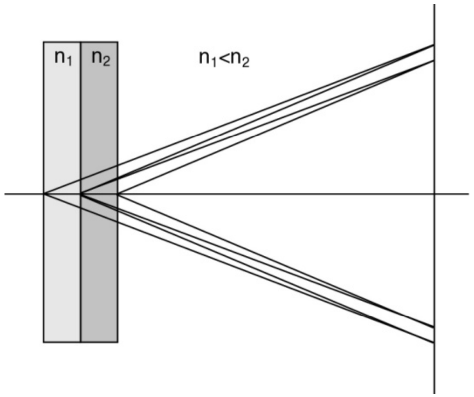

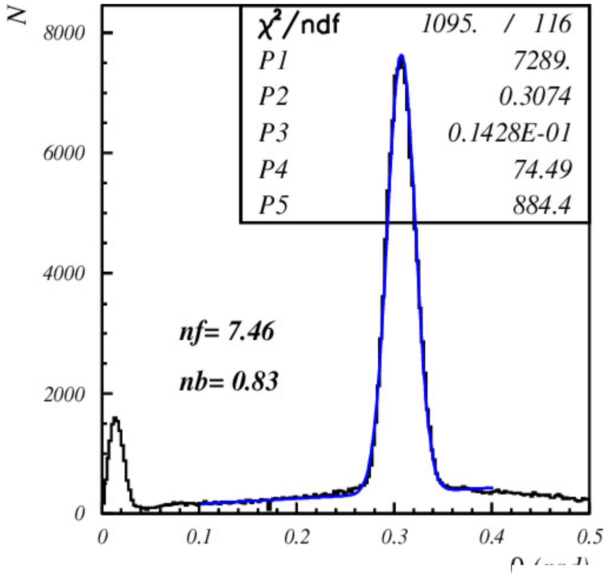

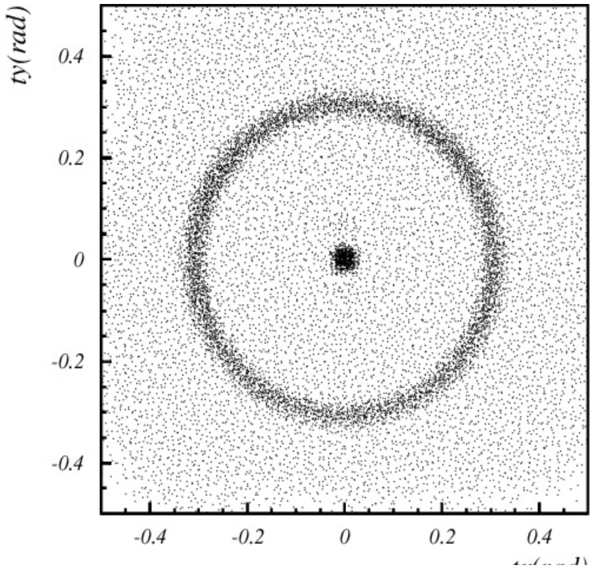

→NIM A548 (2005) 383

DIRC: Detector of Internally Reflected Cherekov photons

DIRC: a special kind of RICH (Ring Imaging Cherenkov counter) where Čerenkov photons trapped in a solid radiator (e.q. quartz) are propagated along the radiator bar to the side, and detected as they exit and traverse a gap.

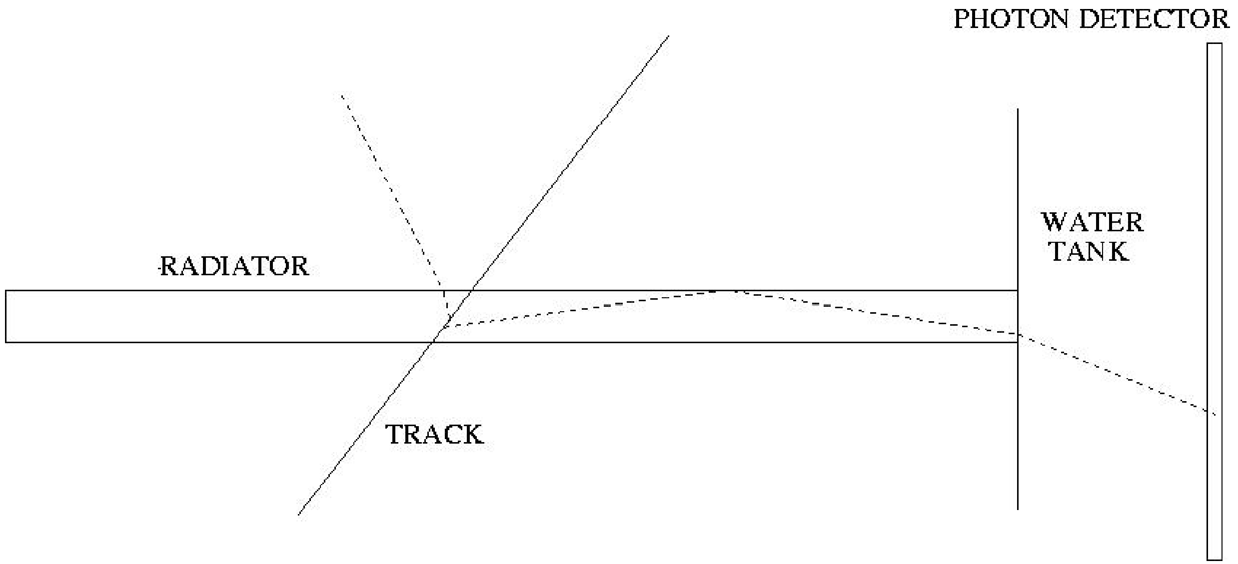

DIRC

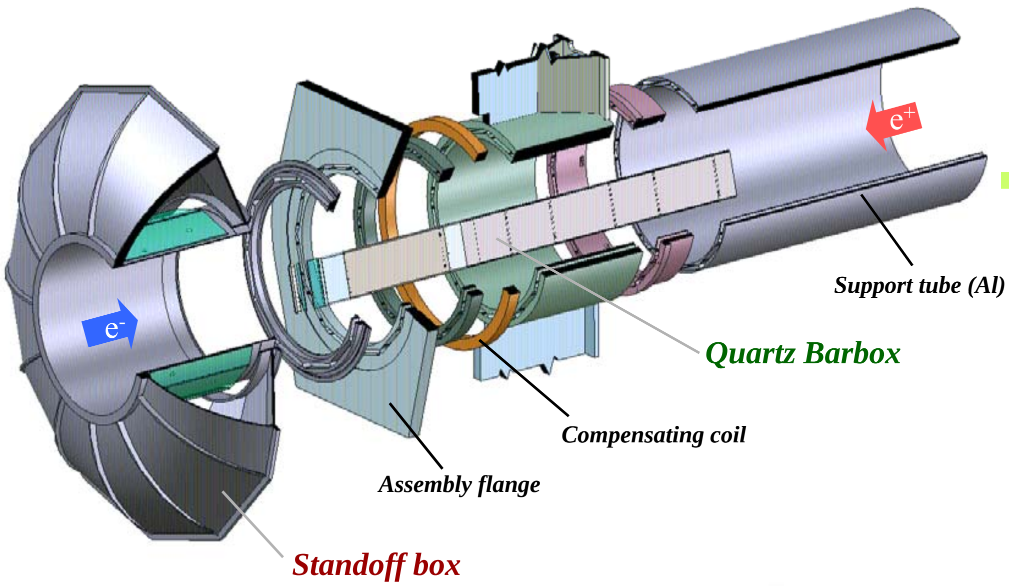

e-
e+
Support tube (Al)
Quartz Barbox
Compensating coil
Assembly flange
Standoff box

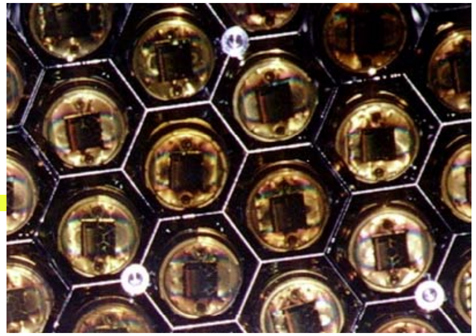

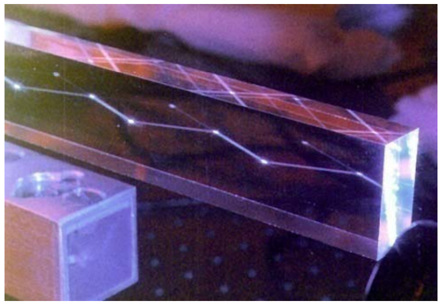

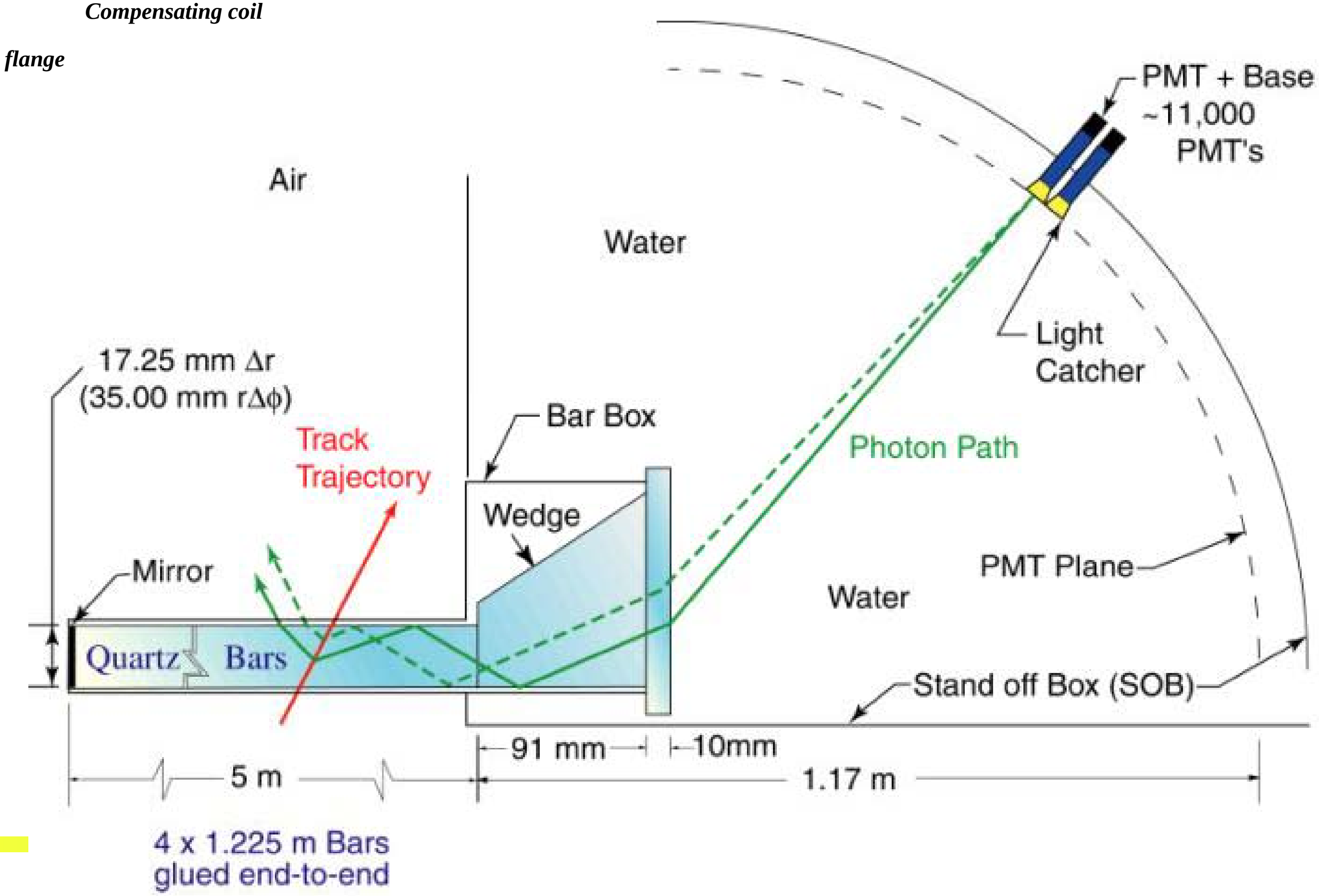

PMT + Base
~11,000
PMT's
Air
Water
Light
Catcher
17.25 mm Δr
(35.00 mm rΔϕ)
Track
Trajectory
Bar Box
Photon Path
Wedge
PMT Plane
Mirror
Water
Quartz
Bars
Stand off Box (SOB)
91 mm
10mm
5 m
1.17 m
4 x 1.225 m Bars
glued end-to-end

DIRC performance

Babar DIRC: a Bhabha event $e^+ e^- \to e^+ e^-$

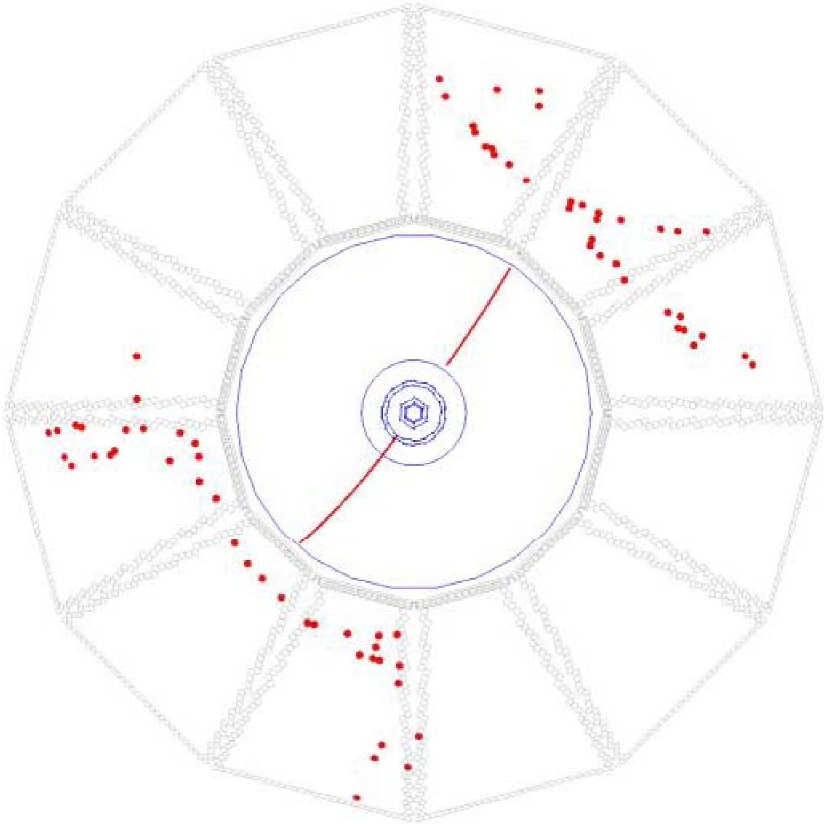

To check the performance, use kinematically selected decays: $D^{*+} \to \pi^+ D^0$, $D^0 \to K^- \pi^+$

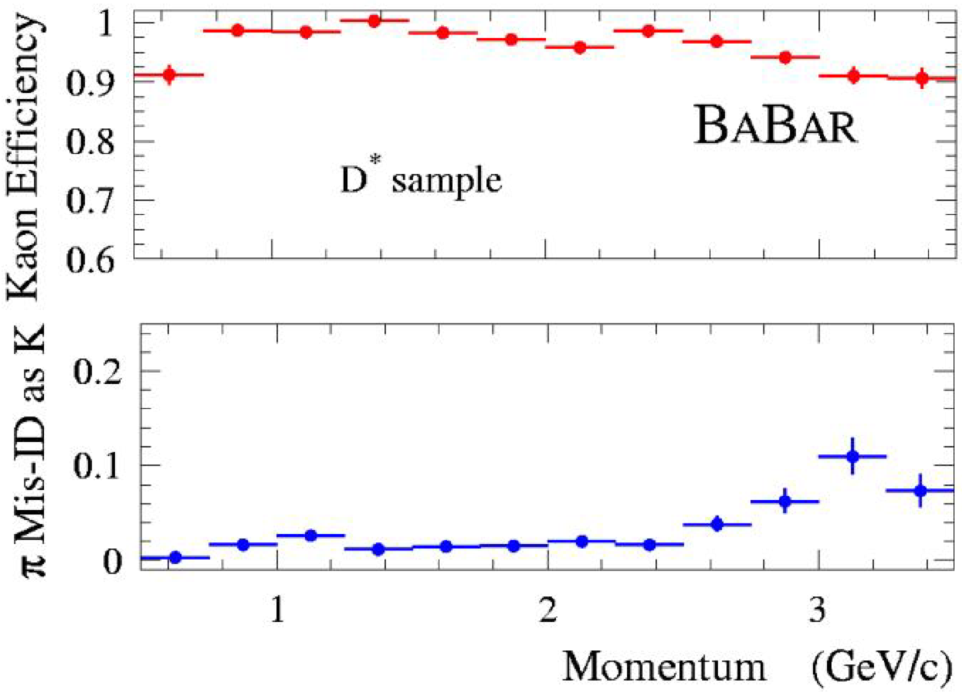

Time-Of-Propagation (TOP) counter

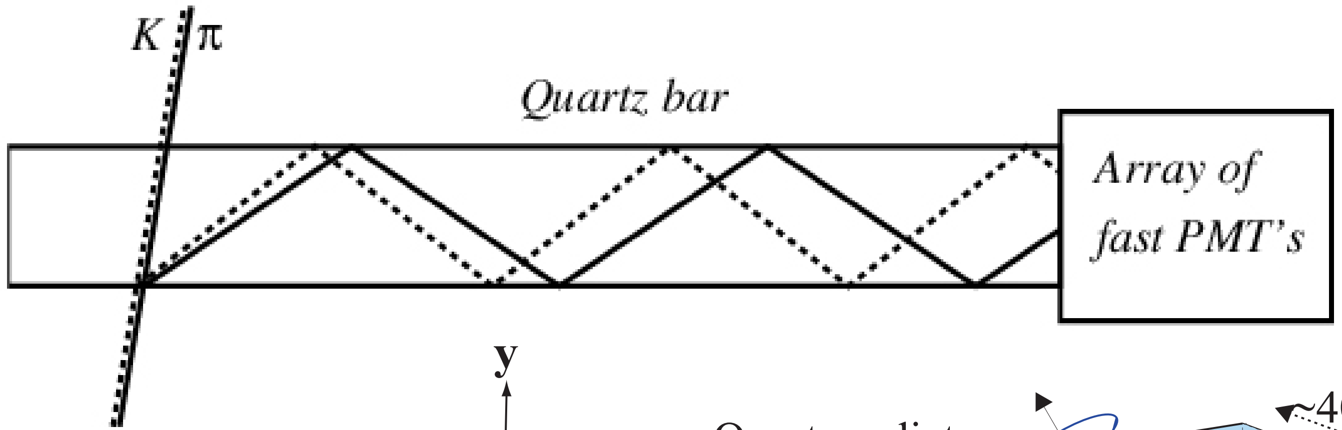

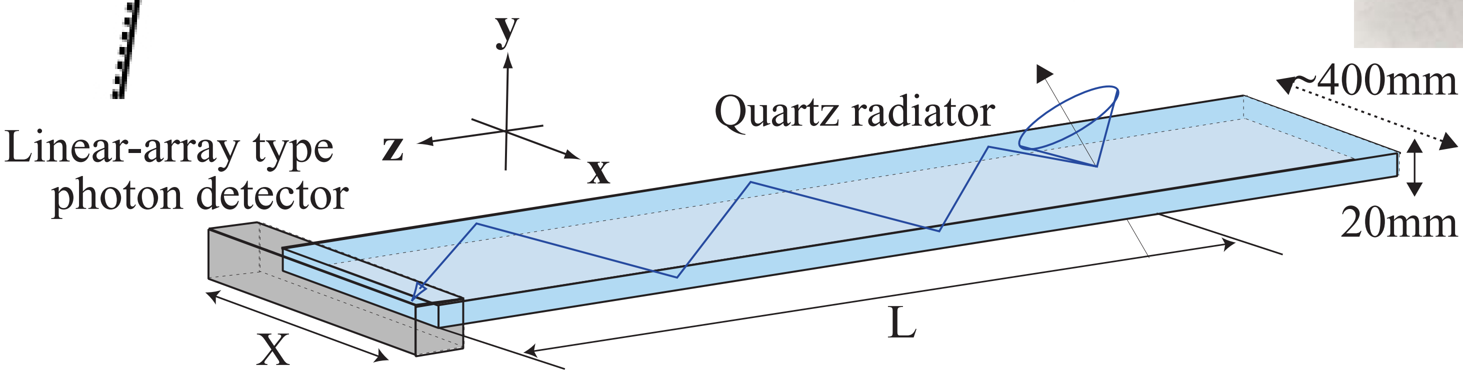

Similar to DIRC, but instead of two coordinates measure:

- One (or two coordinates) with a few mm precision
- Time-of-arrival

→ Excellent time resolution < ~40ps
required for single photons in 1.5T B field

TOP image

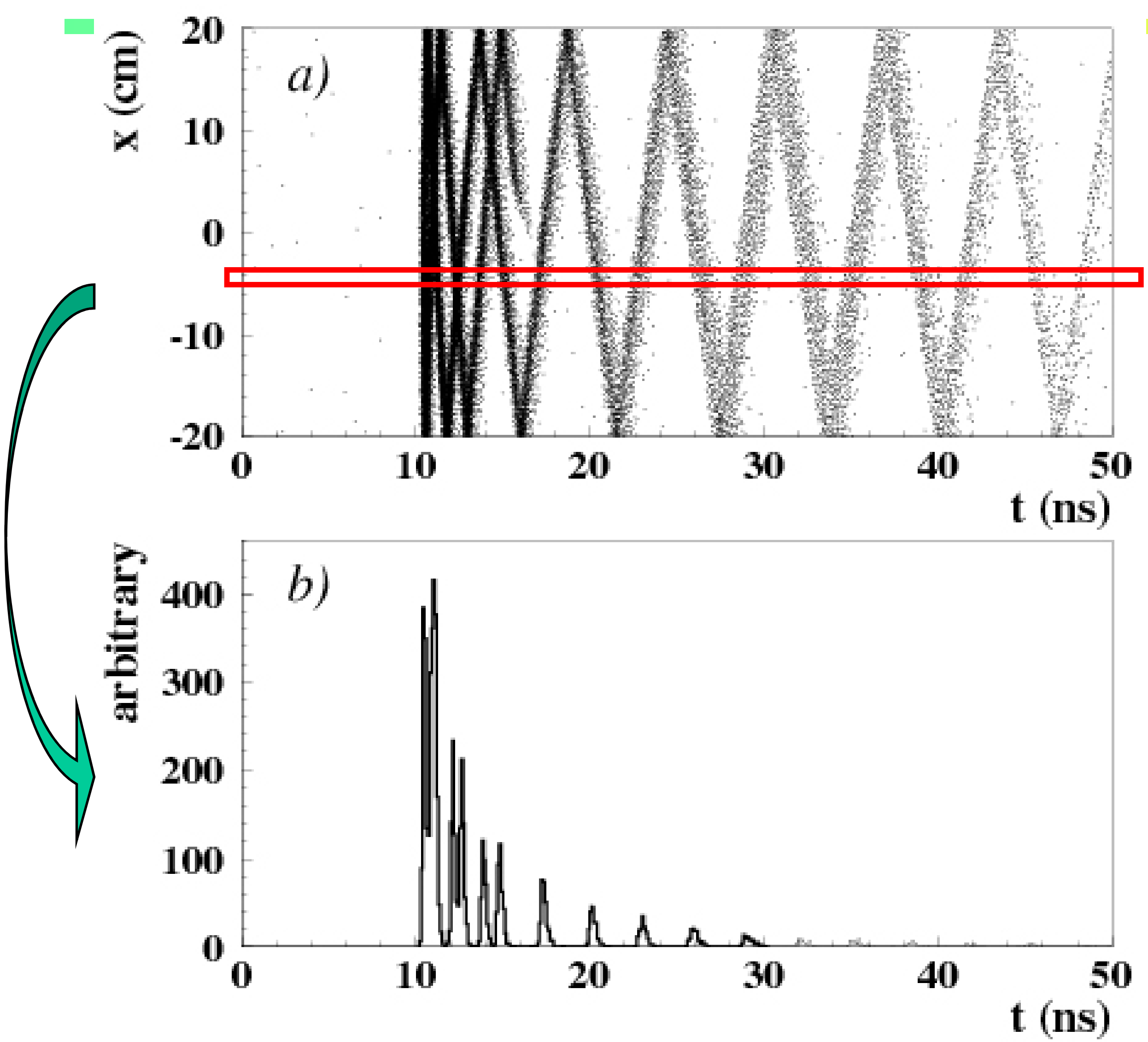

- Pattern in the coordinate-time space ('ring') of a pion hitting a quartz bar with ~80 MAPMT channels

Time distribution of signals recorded by one of the PMT channels: different for π and K

Transition radiation detectors

X rays emitted at the boundary of two media with different refractive indices, emission angle ~1/γ

Emission rate depends on γ (Lorentz factor): becomes important at γ~1000

- Electrons at 0.5 GeV
- Pions, muons above 100 GeV

In between: discrimination e vs pions, mions

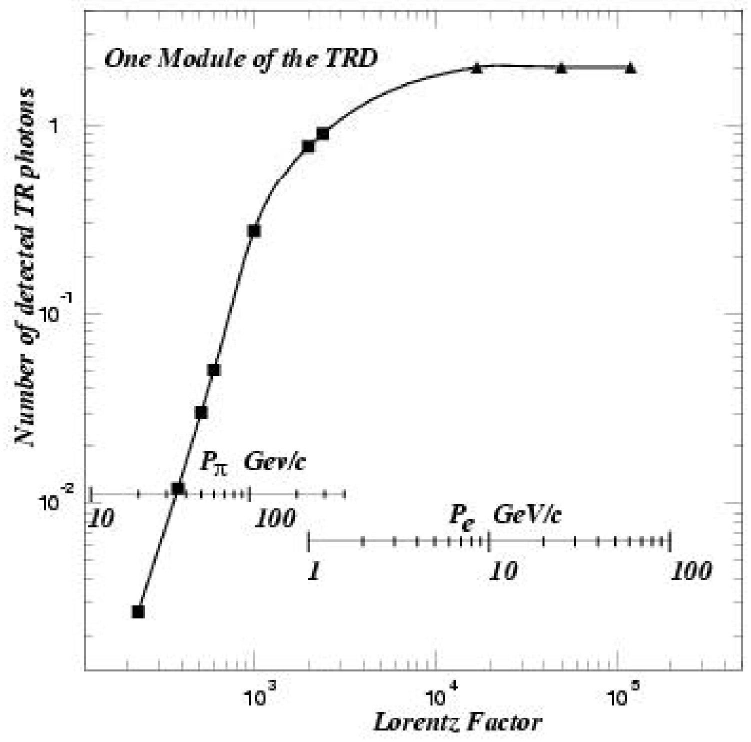

Detection of X rays: high Z gas – Xe

Few photons per boundary can be detected

Need many boundaries

- Stacks of thin foils or
- Porous materials – foam with many boundaries of individual 'bubbles'

Transition radiation - 1

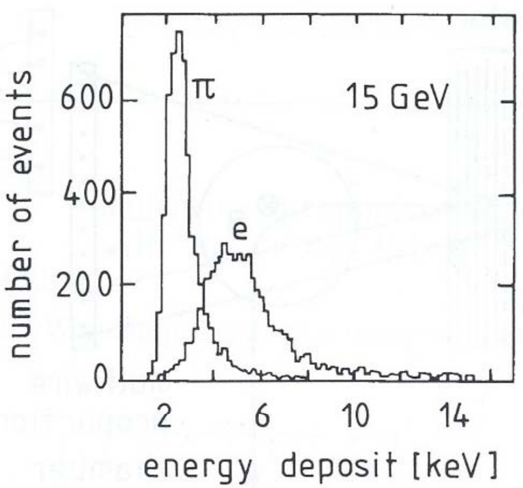

Fig. 6.25. Energy-loss distribution of 15 GeV electrons and pions in a transition radiation detector [467].

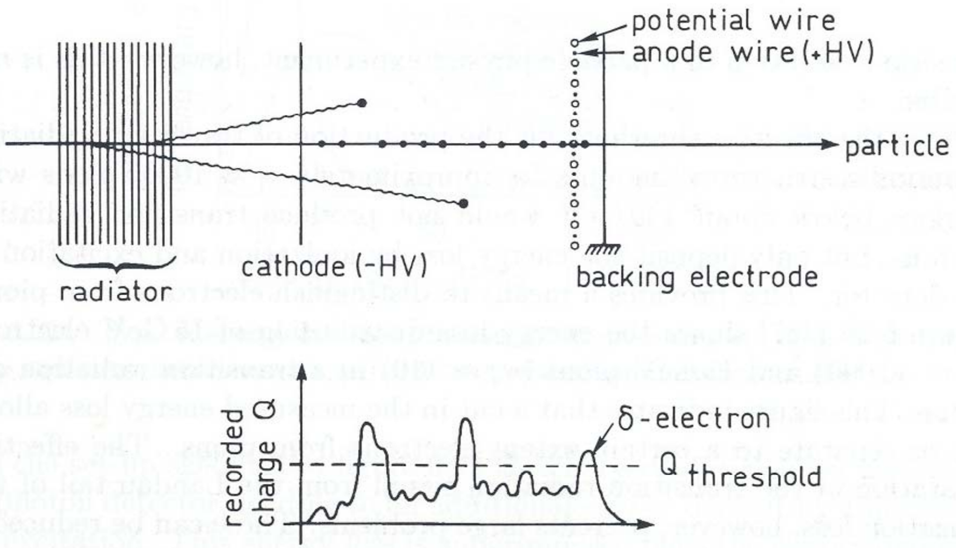

Fig. 6.26. Principle of separating ionization energy loss from the energy loss from emission of transition radiation photons.

Separation of X ray detection – high energy deposit on one place – against ionisation losses

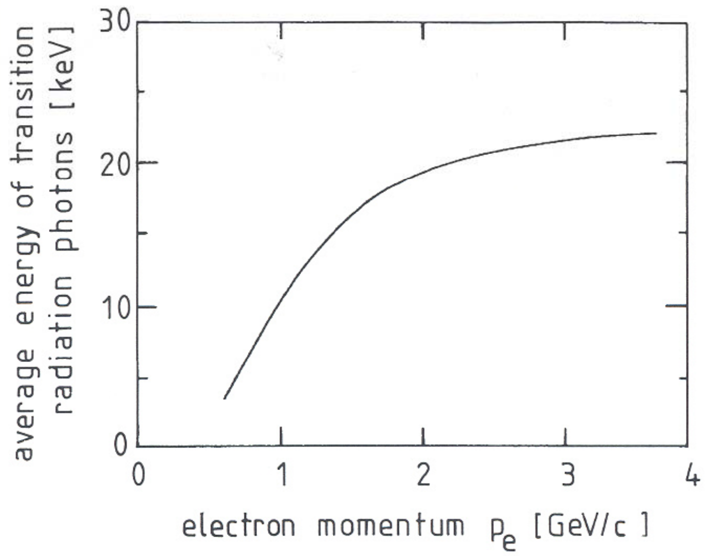

Transition radiation - 3

Example of performance 2

Radiator: organic foam
between the detector tubes
(straws made of capton
foil)

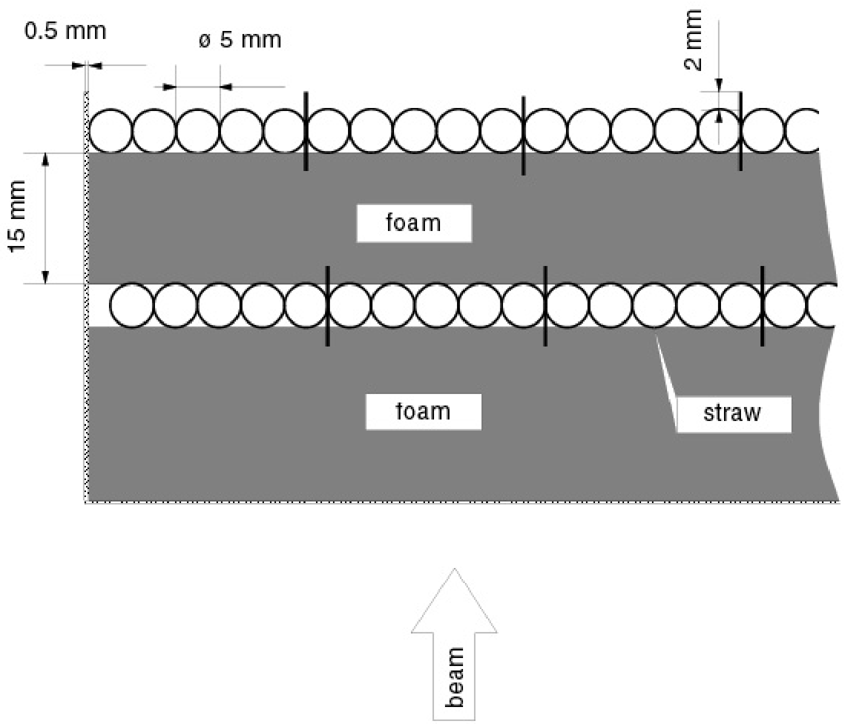

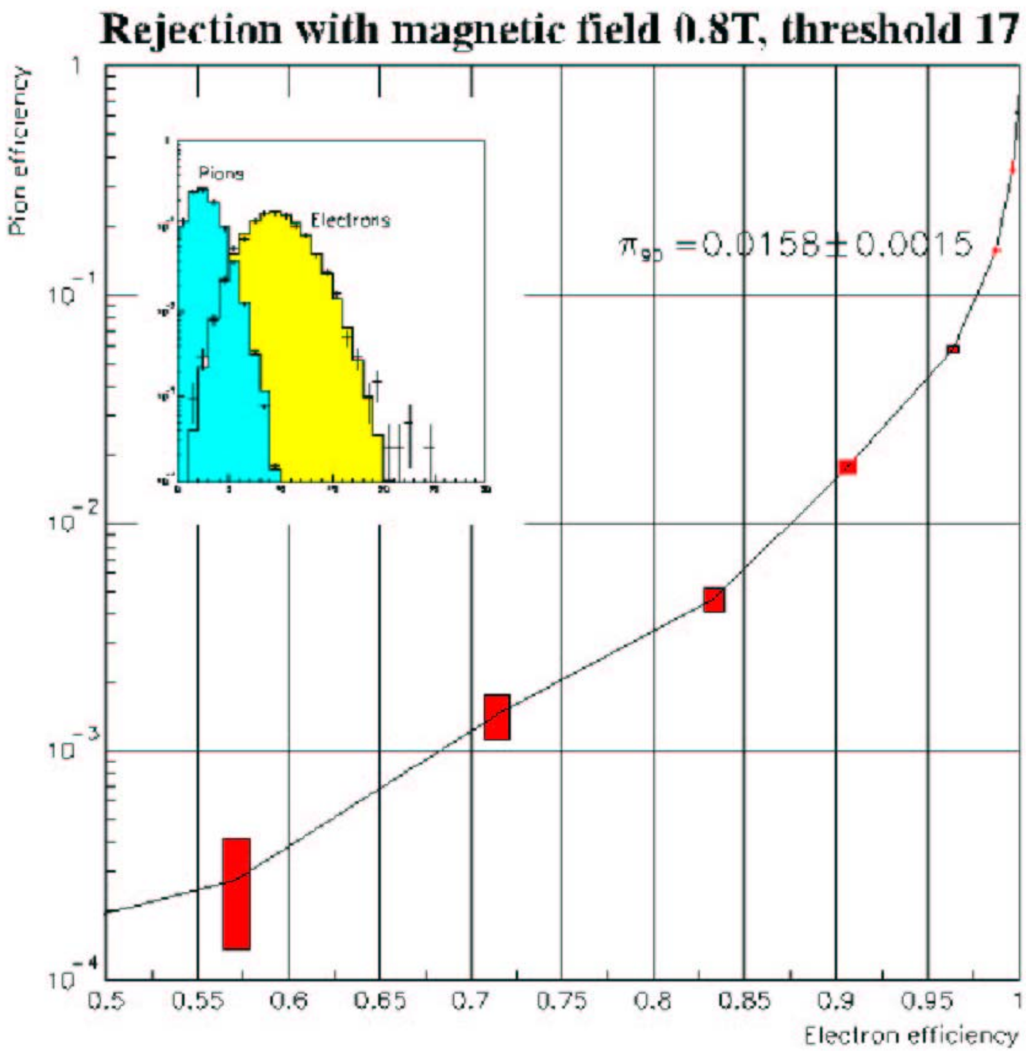

TRT: pion-electron separation

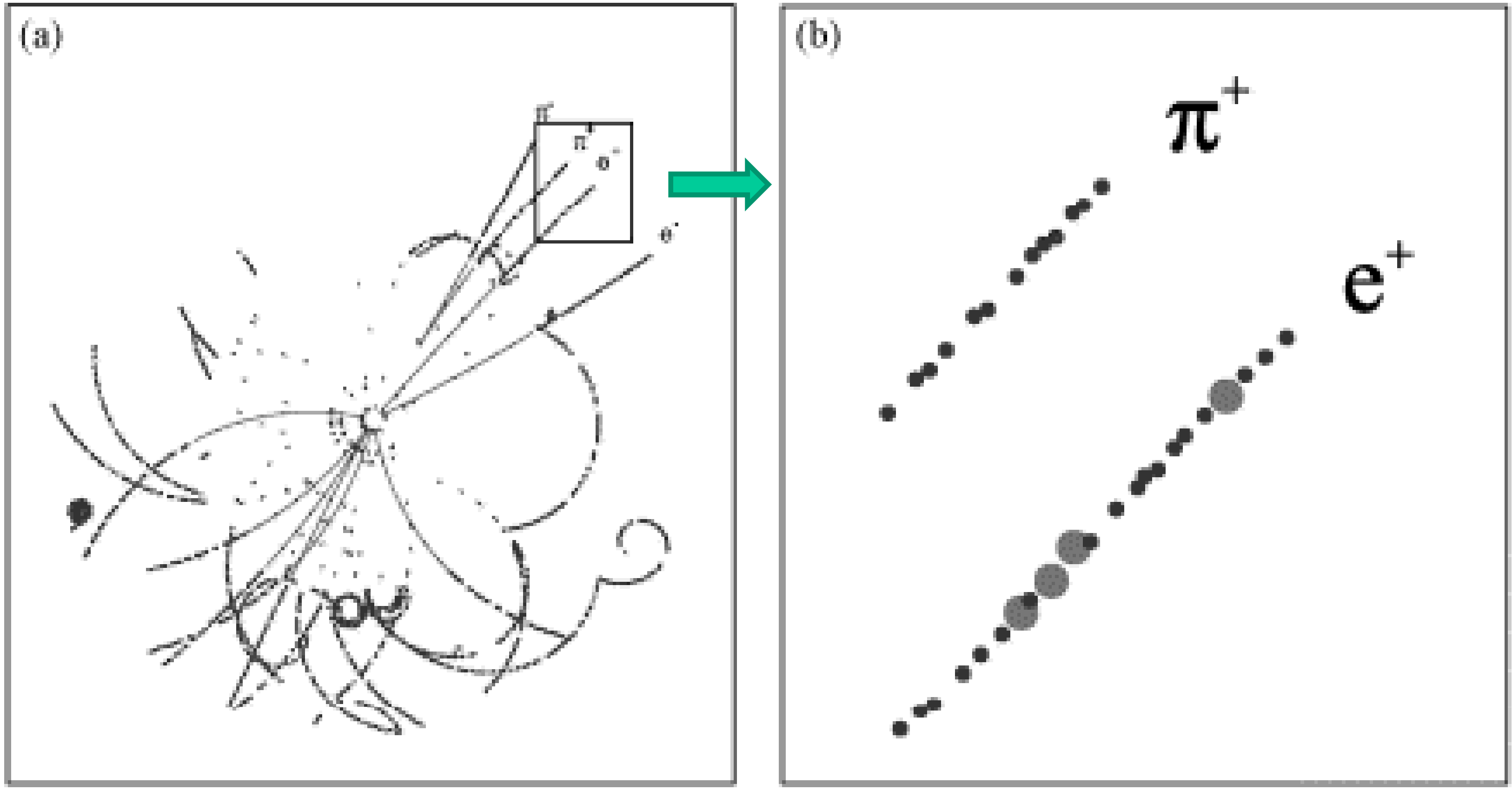

Small circles: low threshold (ionisation), big circles: high threshold (X ray detection)

Transition radiation detector in ATLAS: combination of a tracker and a transition radiation detector

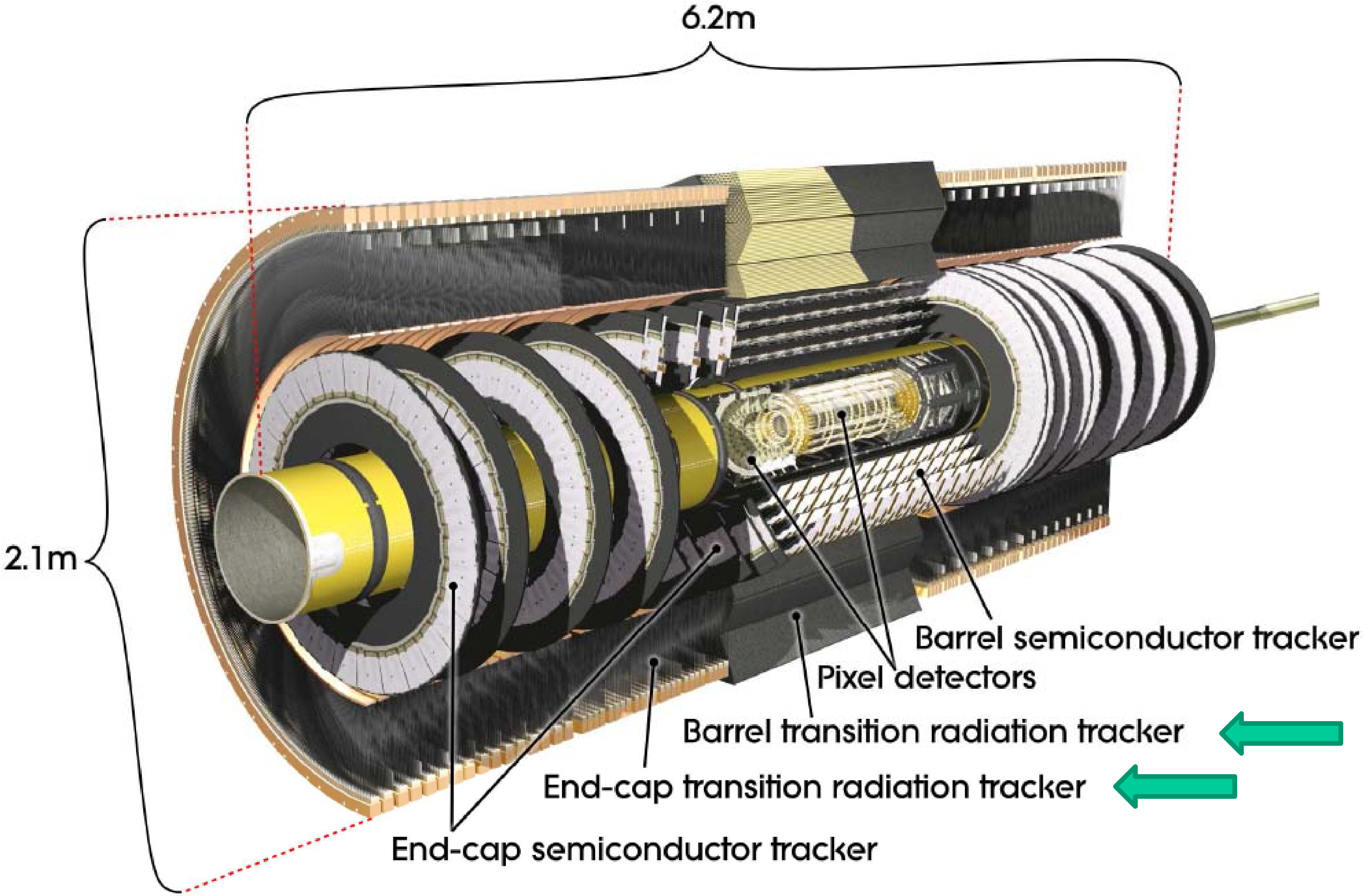

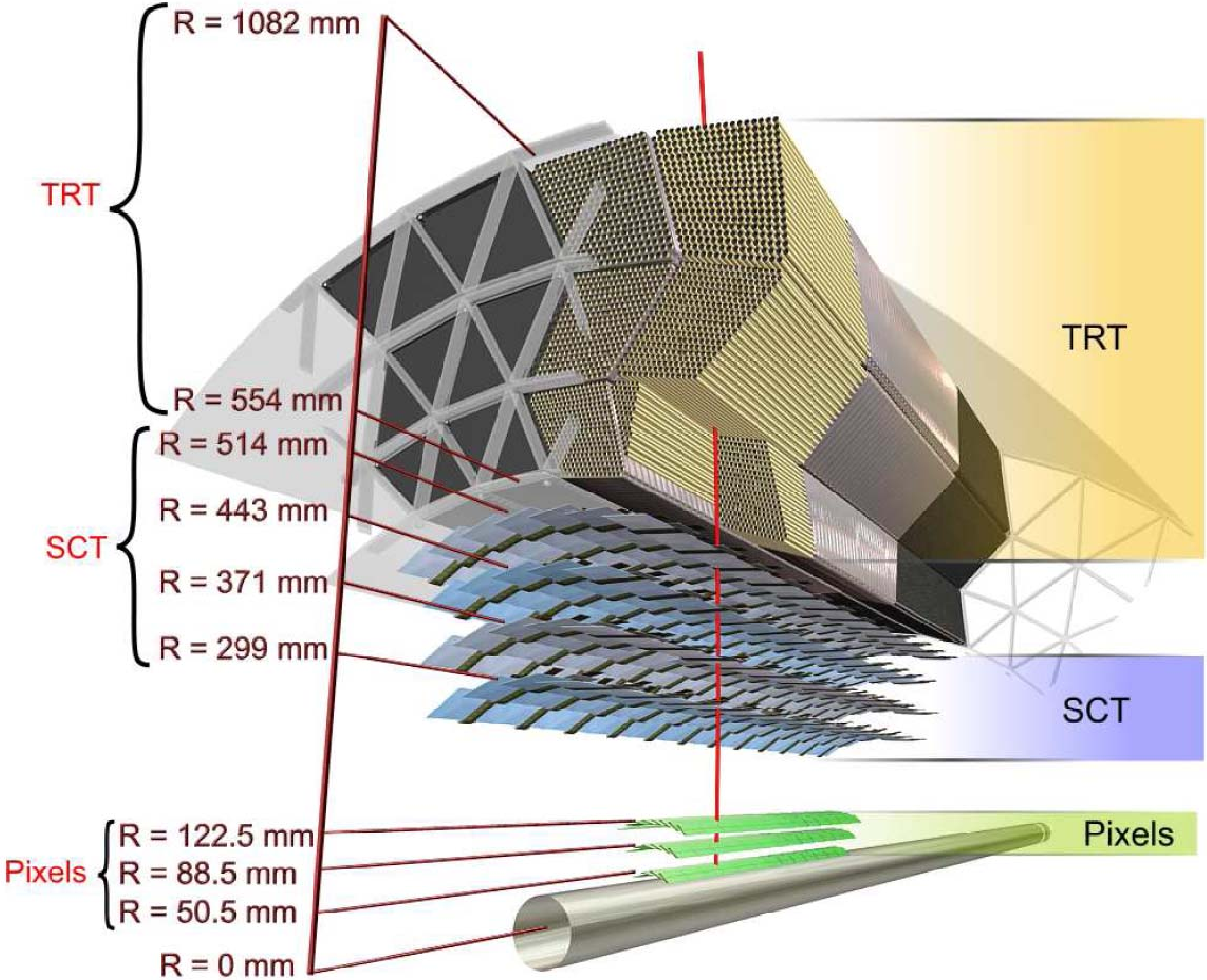
R = 1082 mm
TRT
R = 554 mm
R = 514 mm
R = 443 mm
SCT
R = 371 mm
R = 299 mm
R = 122.5 mm
Pixels
R = 88.5 mm
R = 50.5 mm
R = 0 mm
TRT
SCT
Pixels

ATLAS TRT: combination of Transition Radiation detector and a Tracker

Radiator: 3mm thick layers made of polypropylene-polyethylene fibers with ~19 micron diameter, density: 0.06 g/cm^3

Straw tubes: 4mm diameter with 31 micron diameter anode wires, gas: 70% Xe, 27% CO_2, 3% O_2.

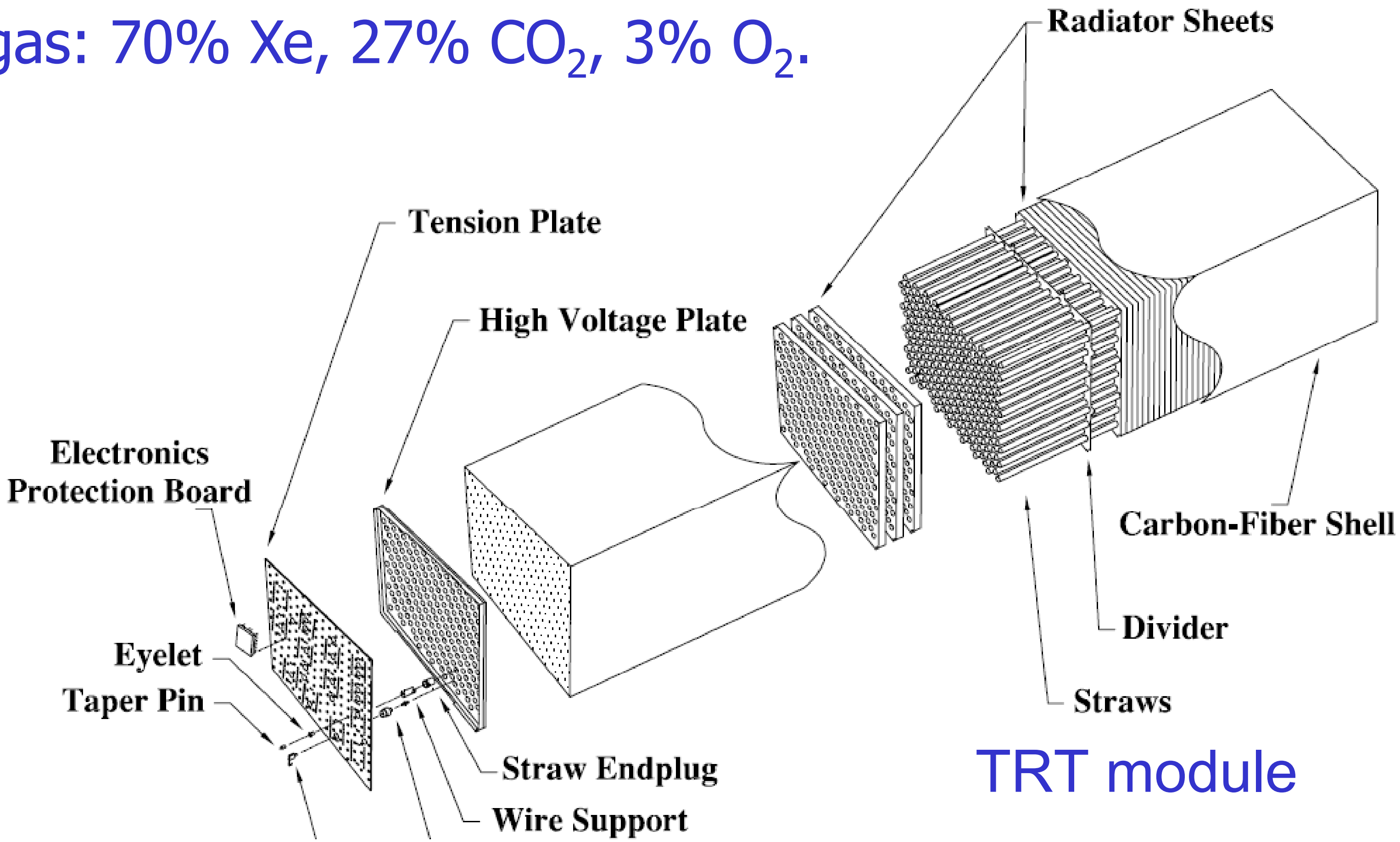

TRT module

Particle identification: Comparison of methods

Time-of-flight

dE/dx measurement

Čerenkov counters

Transition radiation counters

Compare by calculating the length of detector needed for a given separation (3σ)

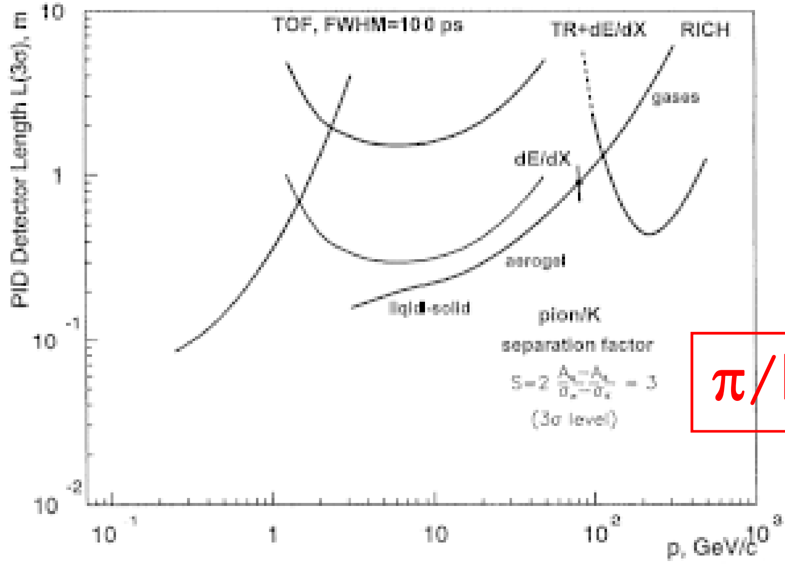

π/K

Fig. 14. Pion–kaon separation by different PID methods: the length of the detectors needed for 3 sigma separation.

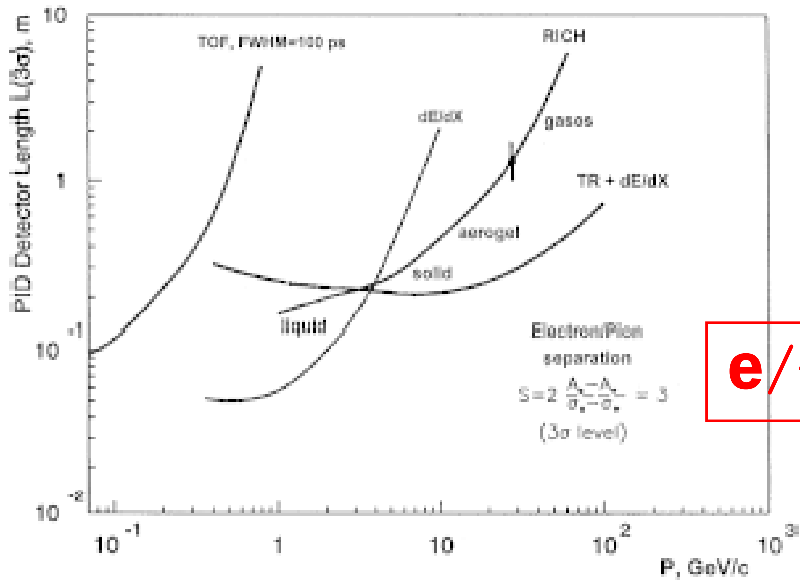

e/π

Fig. 15. The same as Fig. 14 for electron–pion separation.

PID coverage of kaon/pion spectra

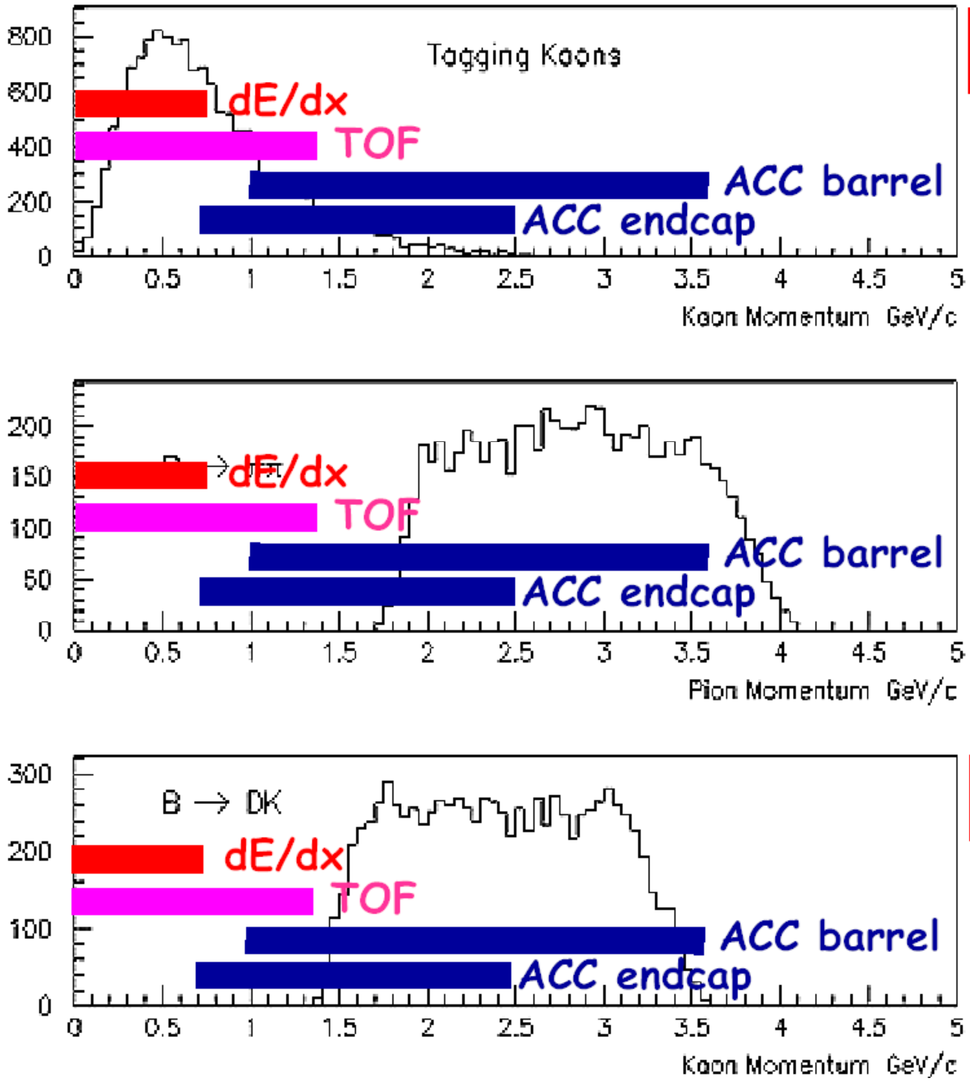

Tagging Kaons

B $\rightarrow \pi\pi$

B $\rightarrow$ DK

PID coverage of kaon/pion spectra

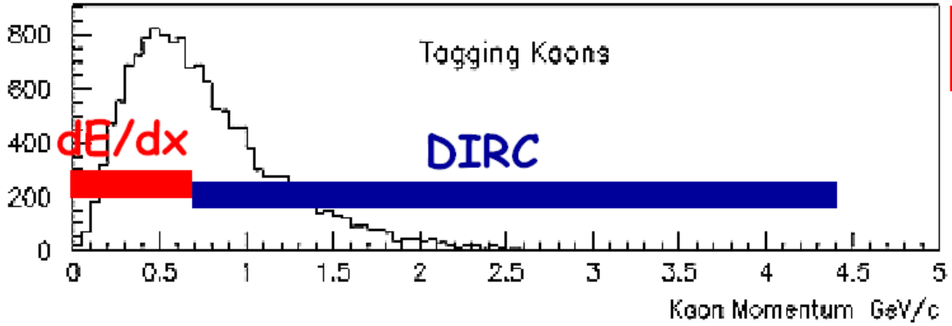

Tagging Kaons

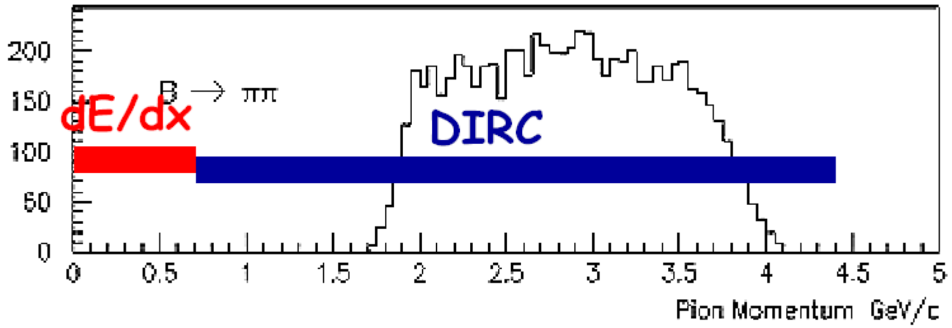

$B \to \pi\pi$

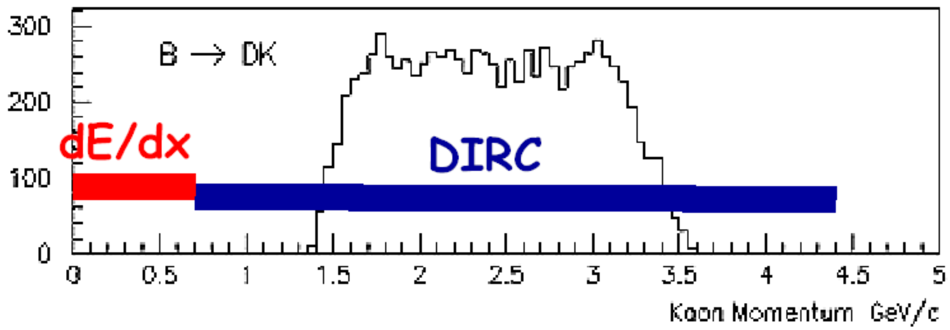

$B \to DK$

Muon and K_L detector at B factories

Separate muons from hadrons (pions and kaons): exploit the fact that muons interact only electromag., while hadrons interact strongly → need a few interaction lengths to stop hadrons (interaction lengths = about 10x radiation length in iron, 20x in CsI). A particle is identified as muon if it penetrates the material.

Detect K_L interaction (cluster): again need a few interaction lengths.

Some numbers: 0.8 interaction length (CsI) + 3.9 interaction lengths (iron)

Interaction length: iron 132 g/cm^2, CsI 167 g/cm^2

$(dE/dx)_{min}$: iron 1.45 MeV/(g/cm^2), CsI 1.24 MeV/(g/cm^2)

→ ΔE_{min} = (0.36+0.11) GeV = 0.47 GeV → reliable identification of muons possible above ~600 MeV

Example: Muon and K_L detection at Belle

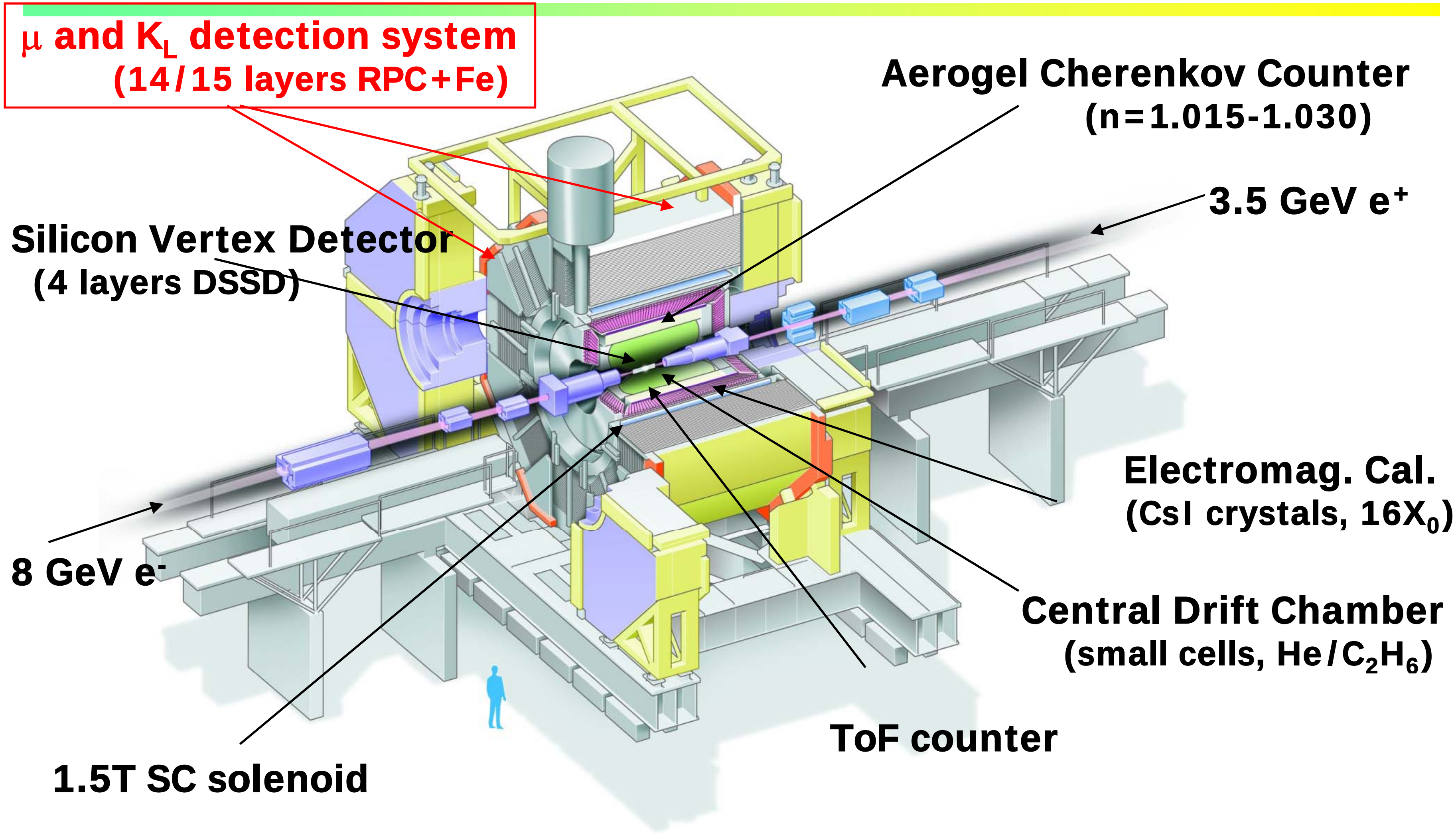

Muon and K_L detector

Up to 21 layers of resistive-plate chambers (RPCs) between iron plates of flux return

Bakelite RPCs at BABAR

Glass RPCs at Belle

(better choice)

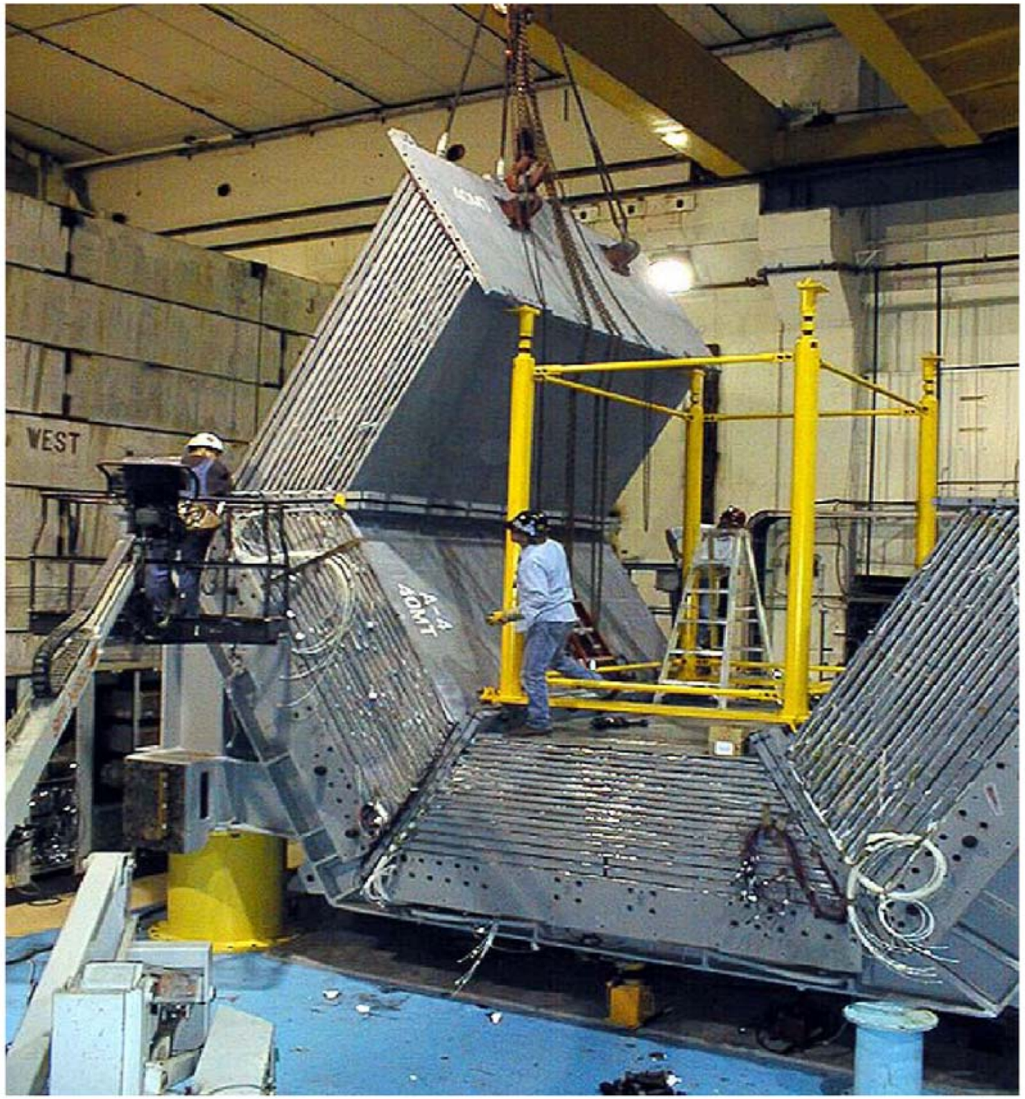

Muon and K_L detector

Example:

event with

- **two muons and a**
- **K_L**

and a pion that partly penetrated

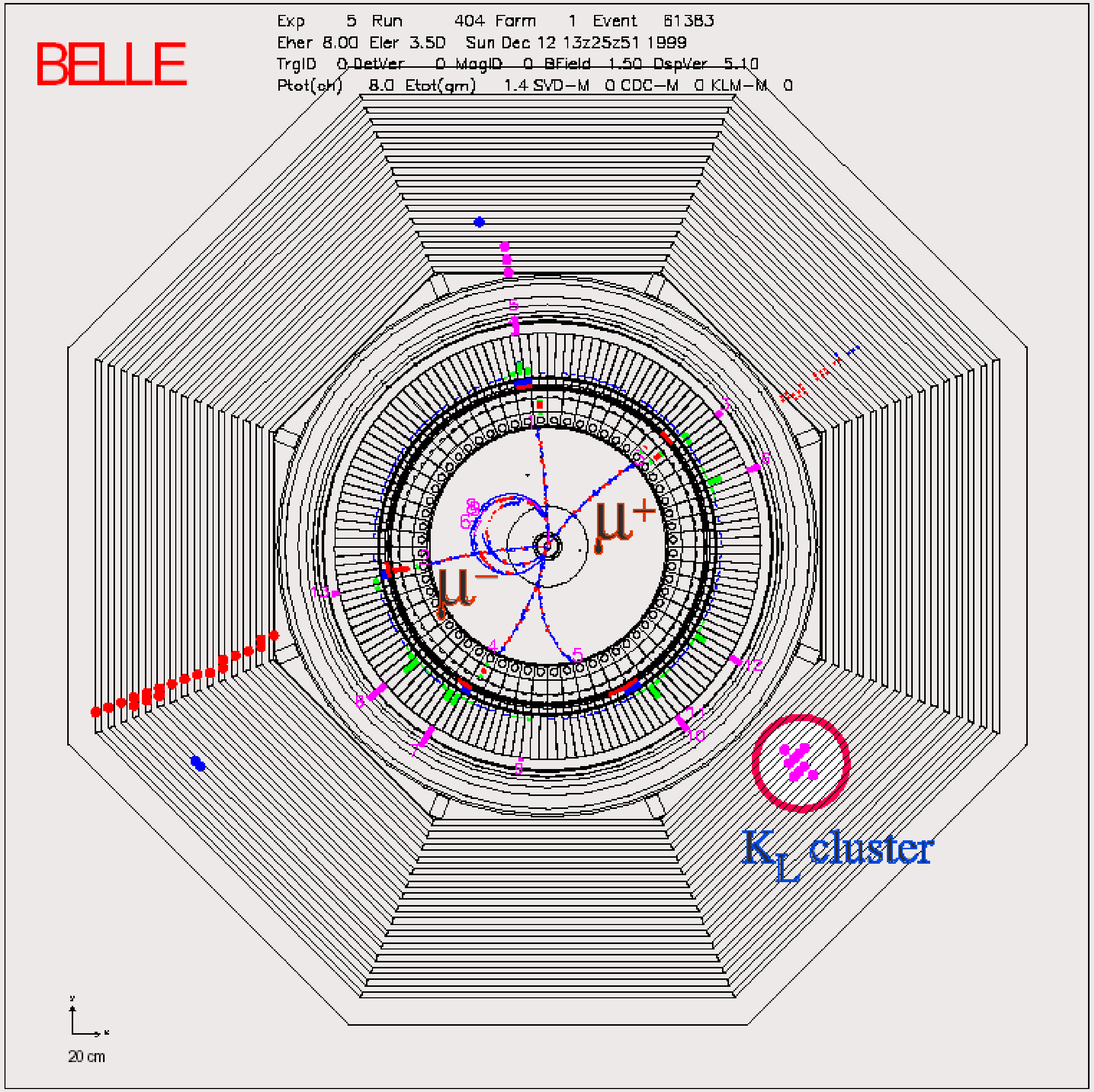

Muon and K_L detector performance

Muon identification: efficient for p>800 MeV/c

efficiency

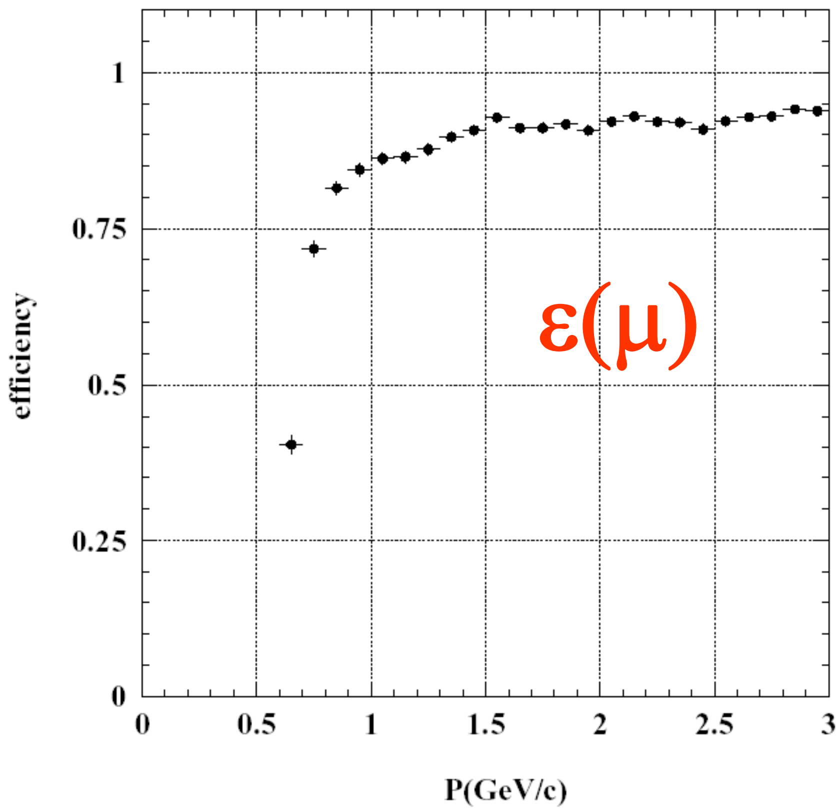

Fig. 109. Muon detection efficiency vs. momentum in KLM.

fake probability

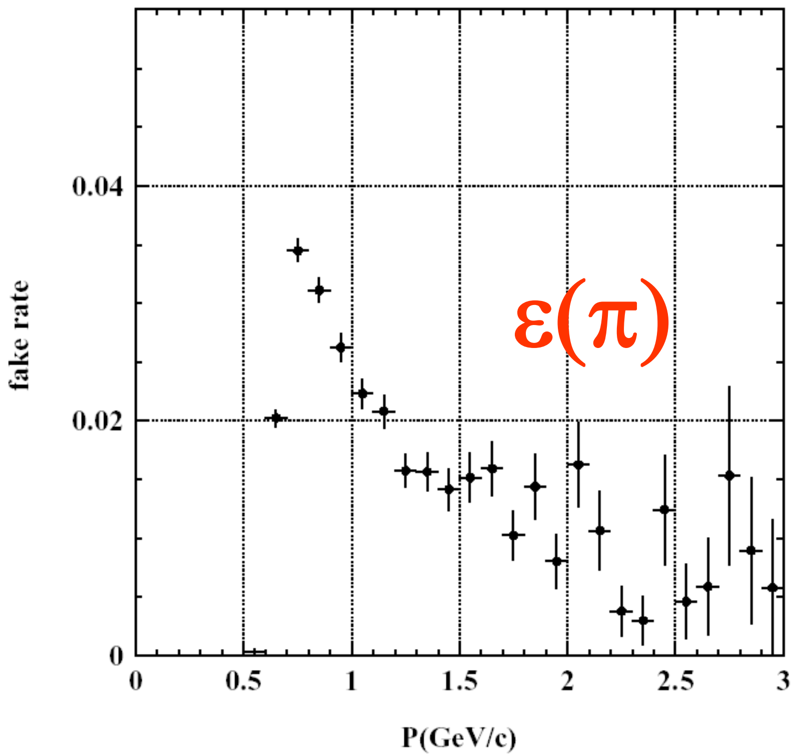

Fig. 110. Fake rate vs. momentum in KLM.

Muon and K_L detector performance

K_L detection: resolution in direction →

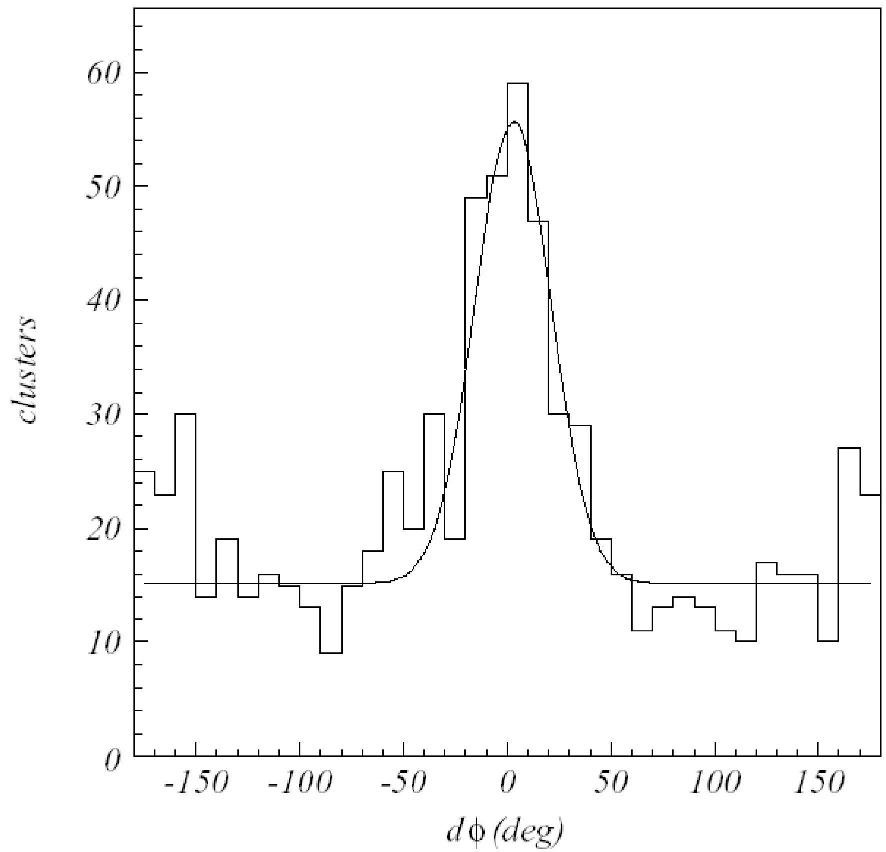

Fig. 107. Difference between the neutral cluster and the direction of missing momentum in KLM.

K_L detection: also with possible with electromagnetic calorimeter (0.8 interactin lengths)

Identification of muons at LHC - example ATLAS

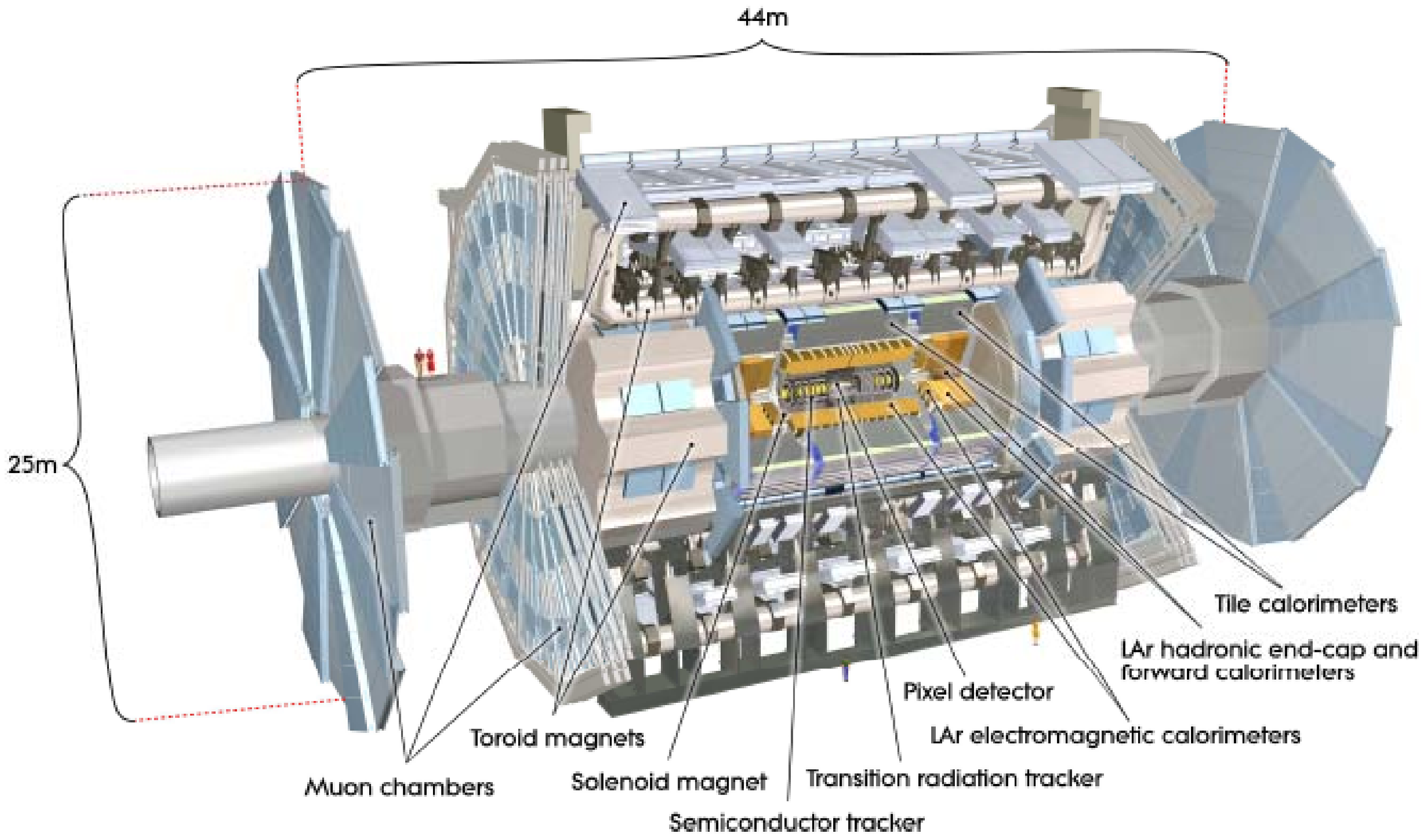

Identification of muons in ATLAS

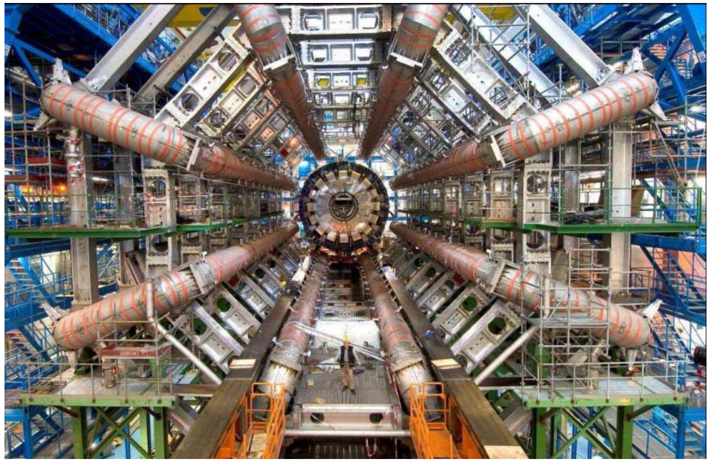

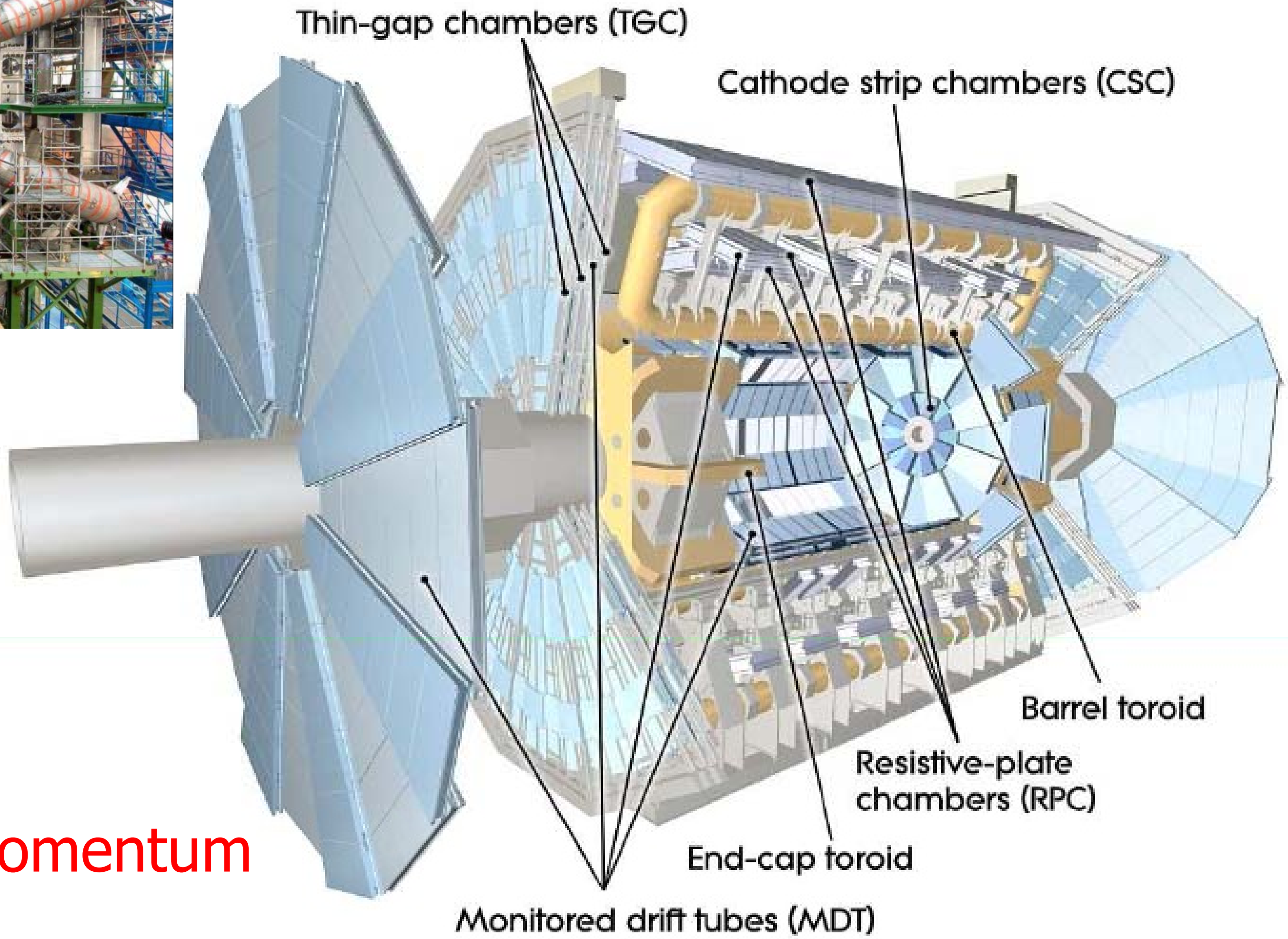

- Identify muons
- Measure their momentum

Muon spectrum

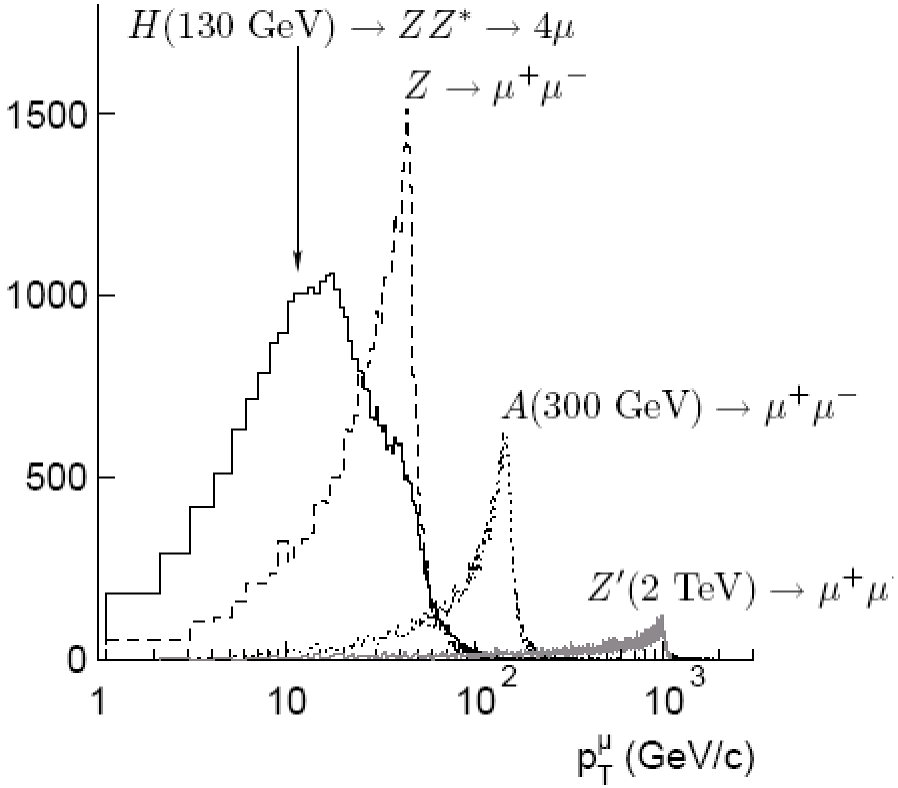

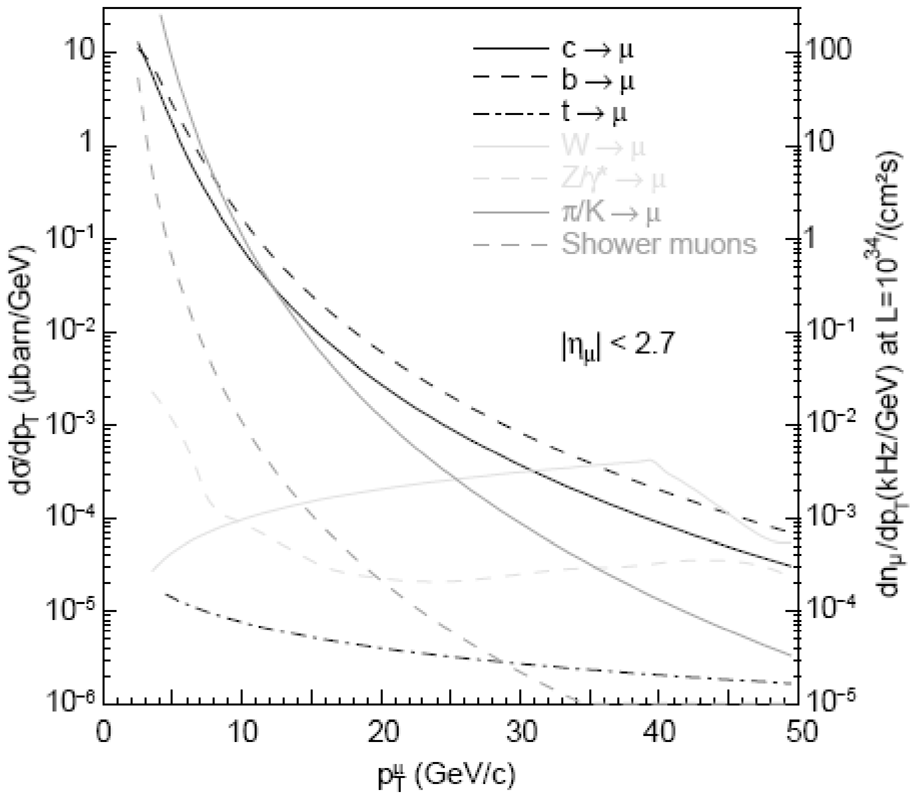

Muon identification in ATLAS

Material in front of the muon system

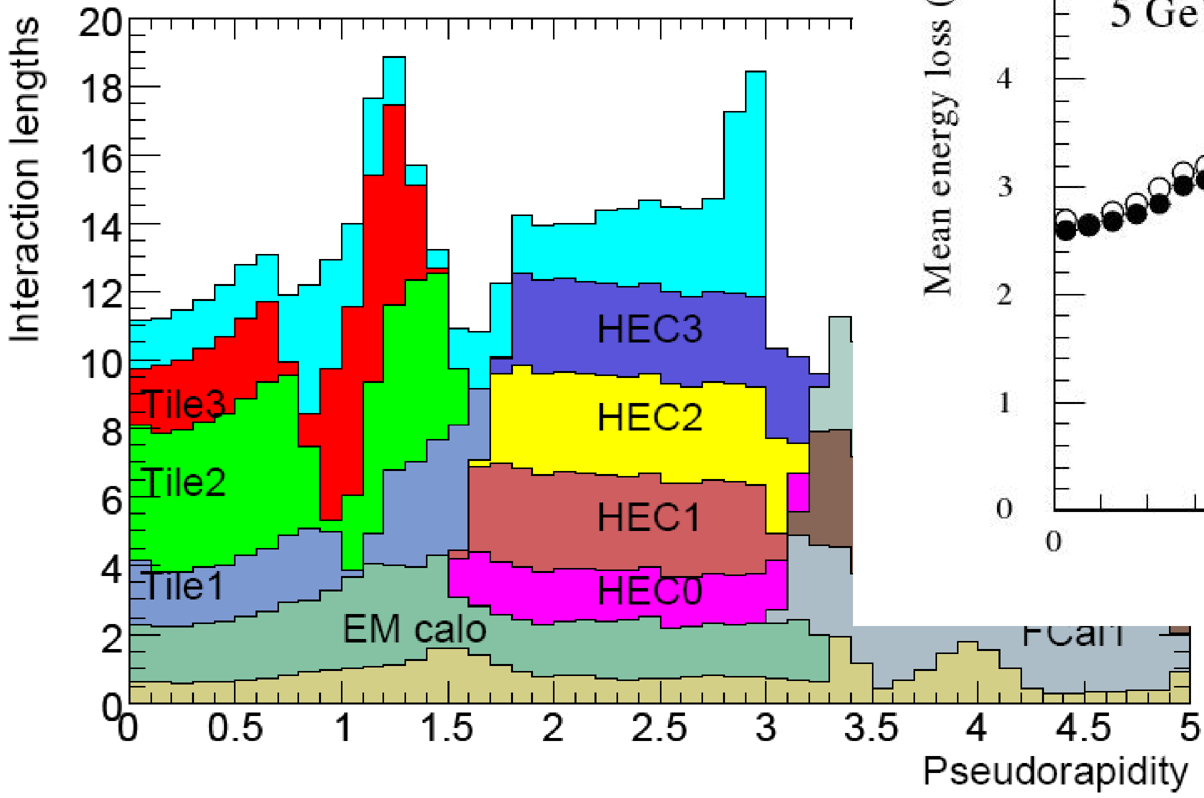

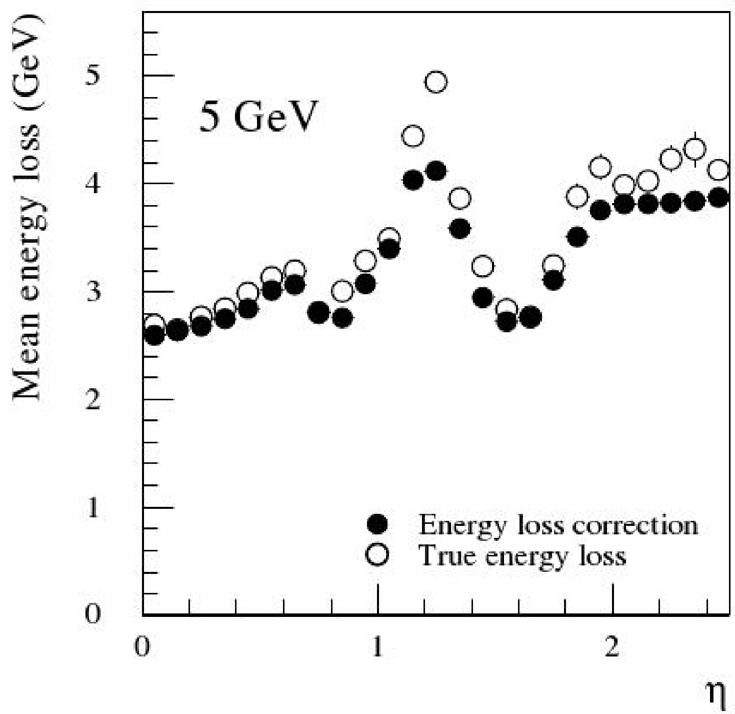

Figure 5.2: Cumulative amount of material, in units of interaction length, as a function of $|\eta|$, in front of the electromagnetic calorimeters, in the electromagnetic calorimeters themselves, in each hadronic layer, and the total amount at the end of the active calorimetry. Also shown for completeness is the total amount of material in front of the first active layer of the muon spectrometer (up to $|\eta| < 3.0$).

Muon identification efficiency

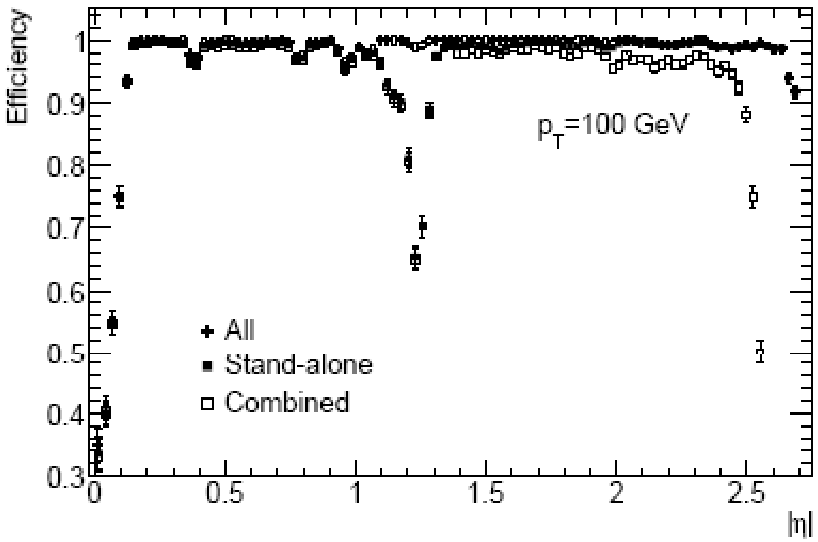

Figure 10.37: Efficiency for reconstructing muons with $p_T = 100\,\text{GeV}$ as a function of $|\eta|$. The results are shown for stand-alone reconstruction, combined reconstruction and for the combination of these with the segment tags discussed in the text.

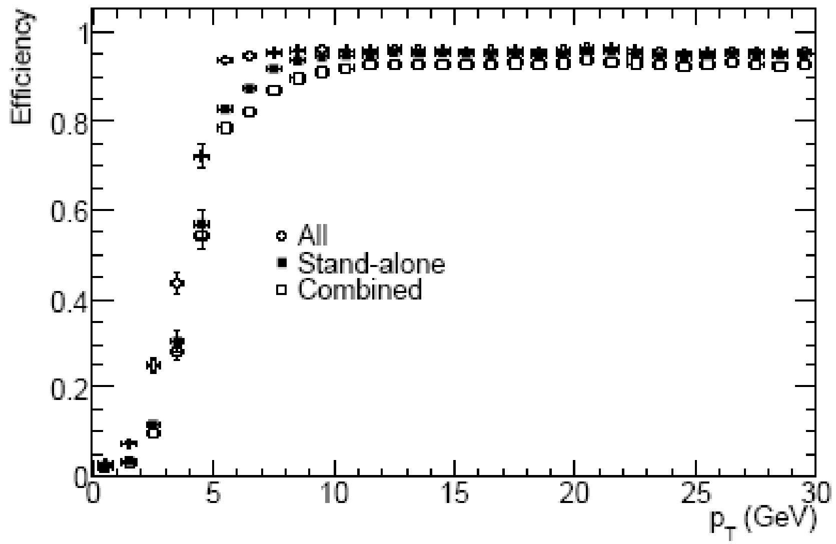

Figure 10.38: Efficiency for reconstructing muons as a function of p_T. The results are shown for stand-alone reconstruction, combined reconstruction and for the combination of these with the segment tags discussed in the text.

Neutrino detection

Use inverse beta decay

$\nu_e + n \rightarrow p + e^-$

$\bar{\nu}_e + p \rightarrow n + e^+$

$\nu_\mu + n \rightarrow p + \mu^-$

$\bar{\nu}_\mu + p \rightarrow n + \mu^+$

$\nu_\tau + n \rightarrow p + \tau^-$

$\bar{\nu}_\tau + p \rightarrow n + \tau^+$

However: cross section is very small!

$6.4\ 10^{-44}\ \mathrm{cm}^2$ at 1MeV

Probability for interaction in 100m of water = $4\ 10^{-16}$

Not much better at high energies:

$0.67\ 10^{-38}\ E/1\mathrm{GeV}\ \mathrm{cm}^2$ per nucleon

At 100 GeV, still 11 orders below the proton-proton cross section

Superkamiokande: an example of a neutrino detector

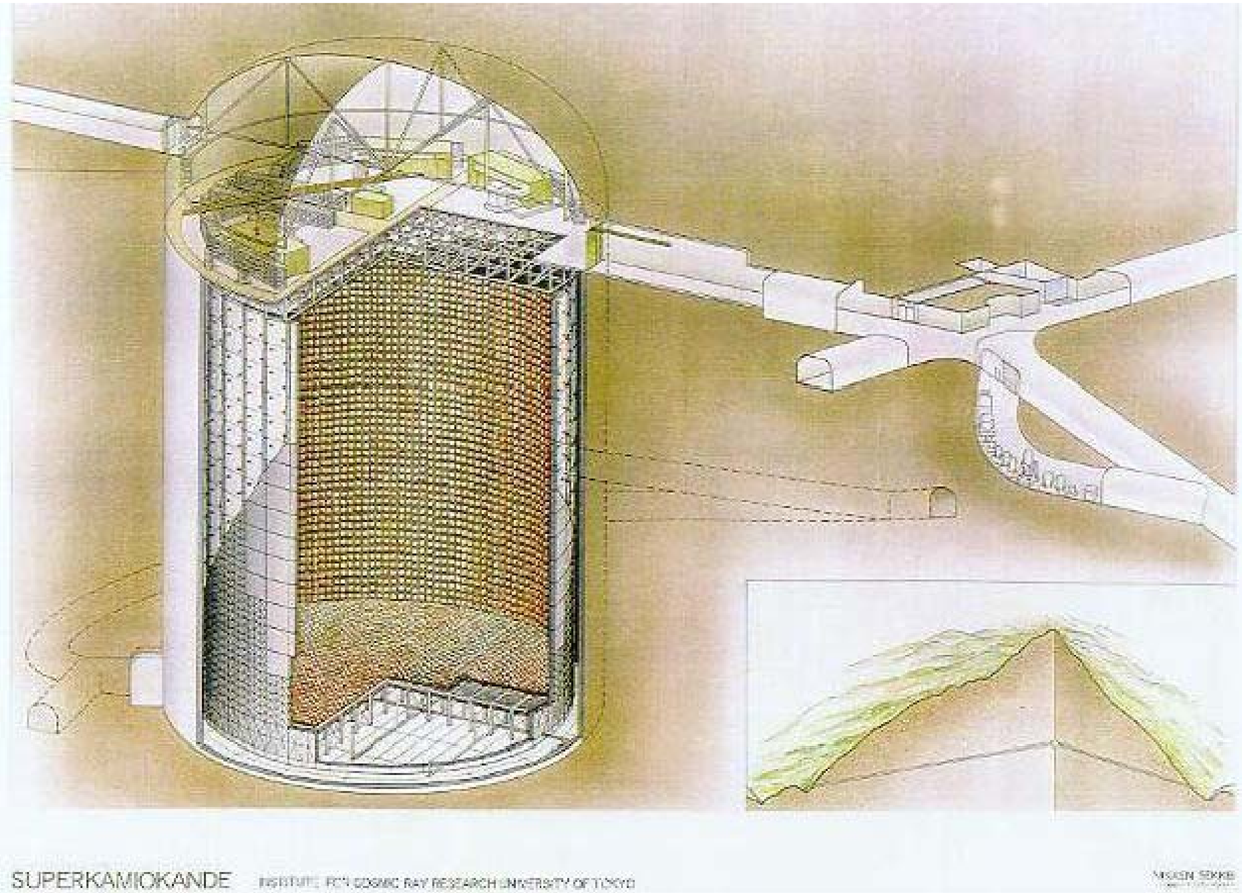

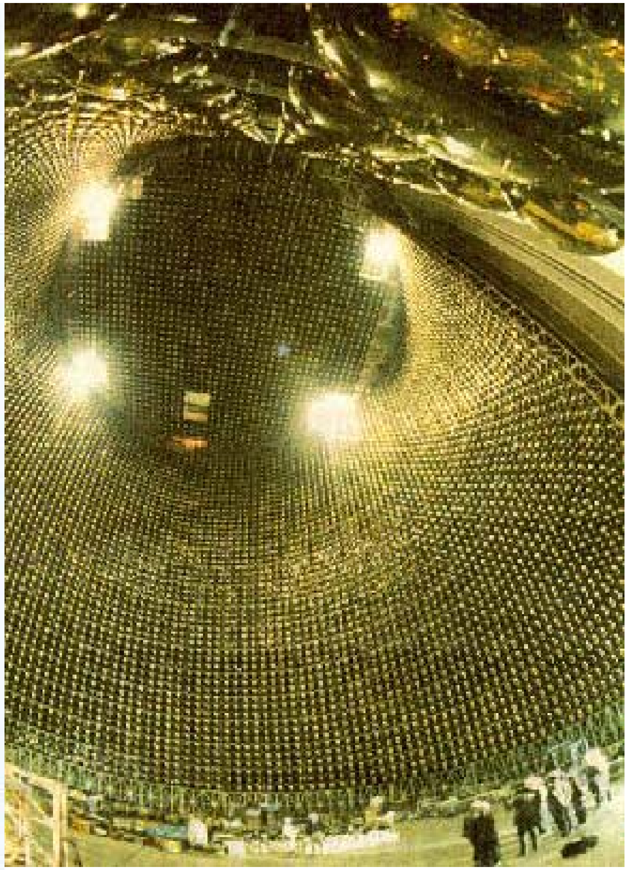

MC simulation: H → 4 μ (ATLAS)

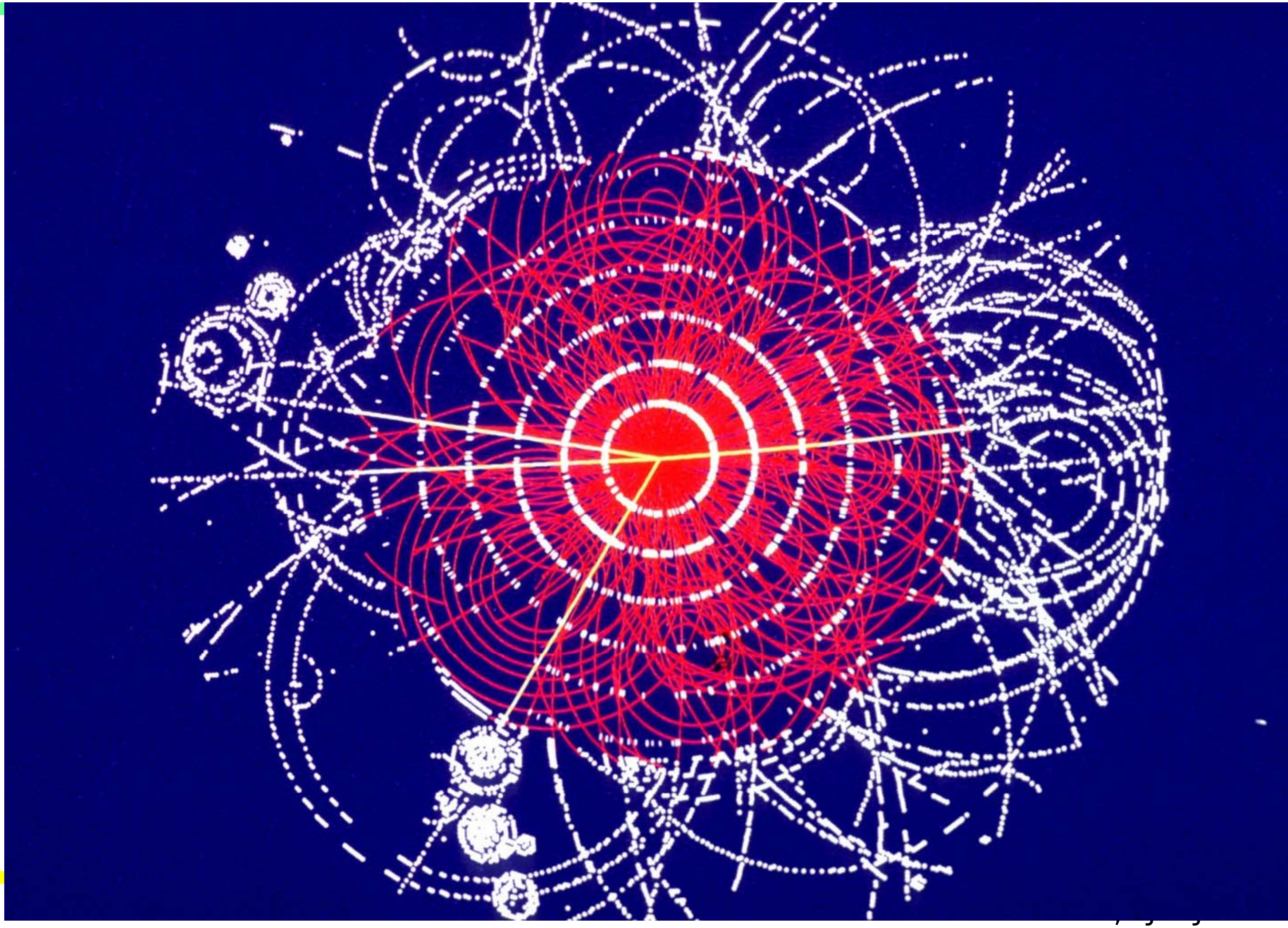

Superkamiokande: detection of electrons and muons

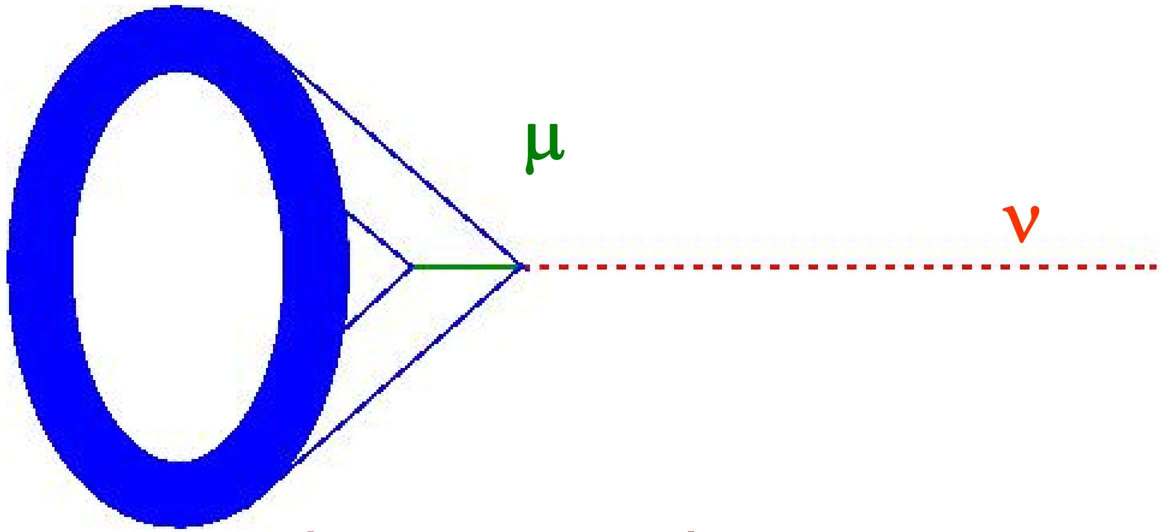

The muon or electron emits Cerenkov light
→ ring at the detector walls

- Muon ring: sharp edges
- Electron ring: smeared

Superkamiokande: detection of neutrinos by measureing Cherenkov photons

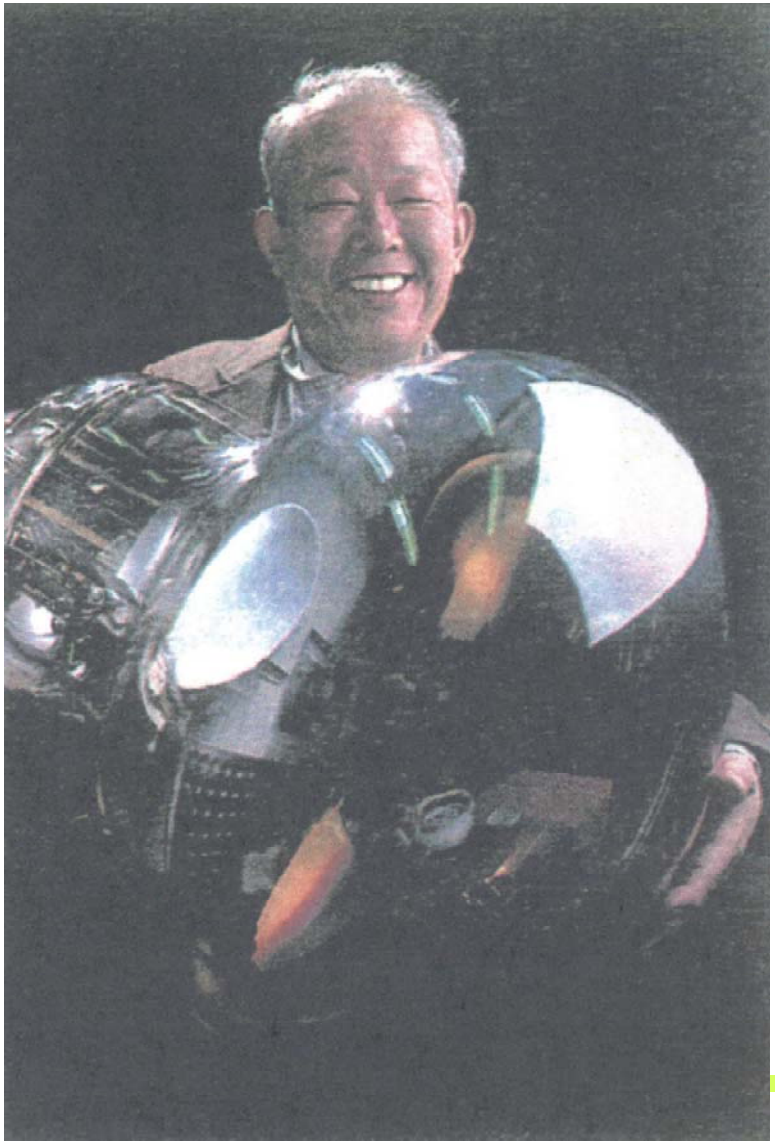

Light detectors: HUGE photomultiplier tubes

M. Koshiba

Muon vs electron

Cherenkov photons from a muon track:

Example: 1GeV muon neutrino

Track length of the resulting muon: L=E/(dE/dx)= =1GeV/(2MeV/cm)=5m

→ a well defined "ring" on the walls

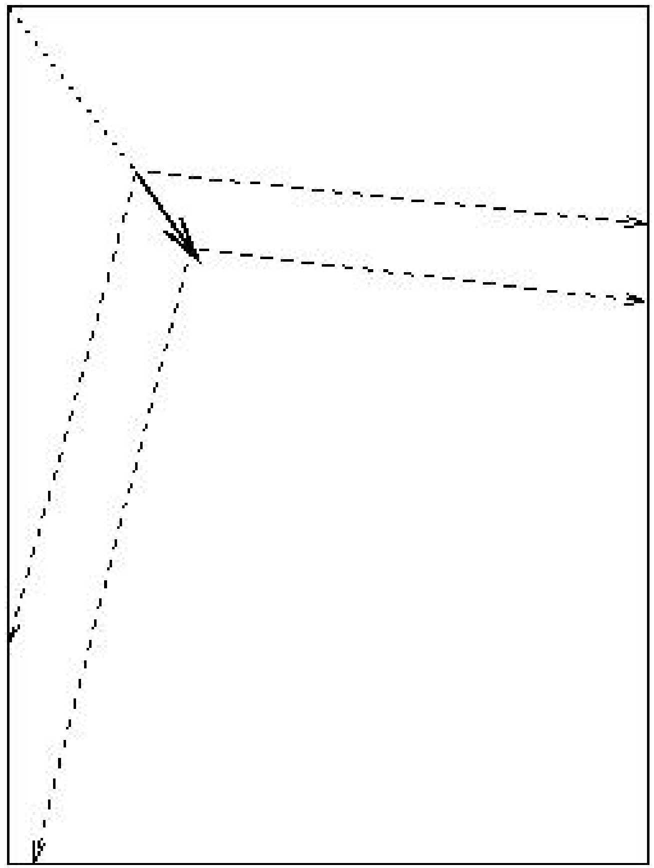

Superkamiokande: muon event

Muon 'ring' as seen by the photon detectors

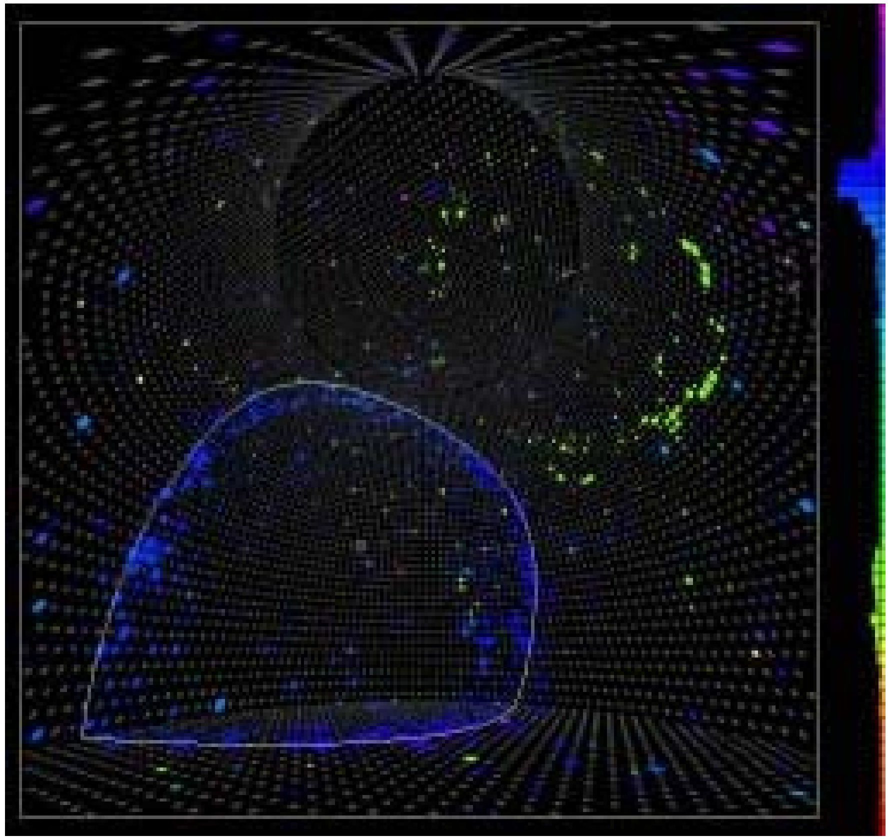

Muon event: photon detector cillinder walls

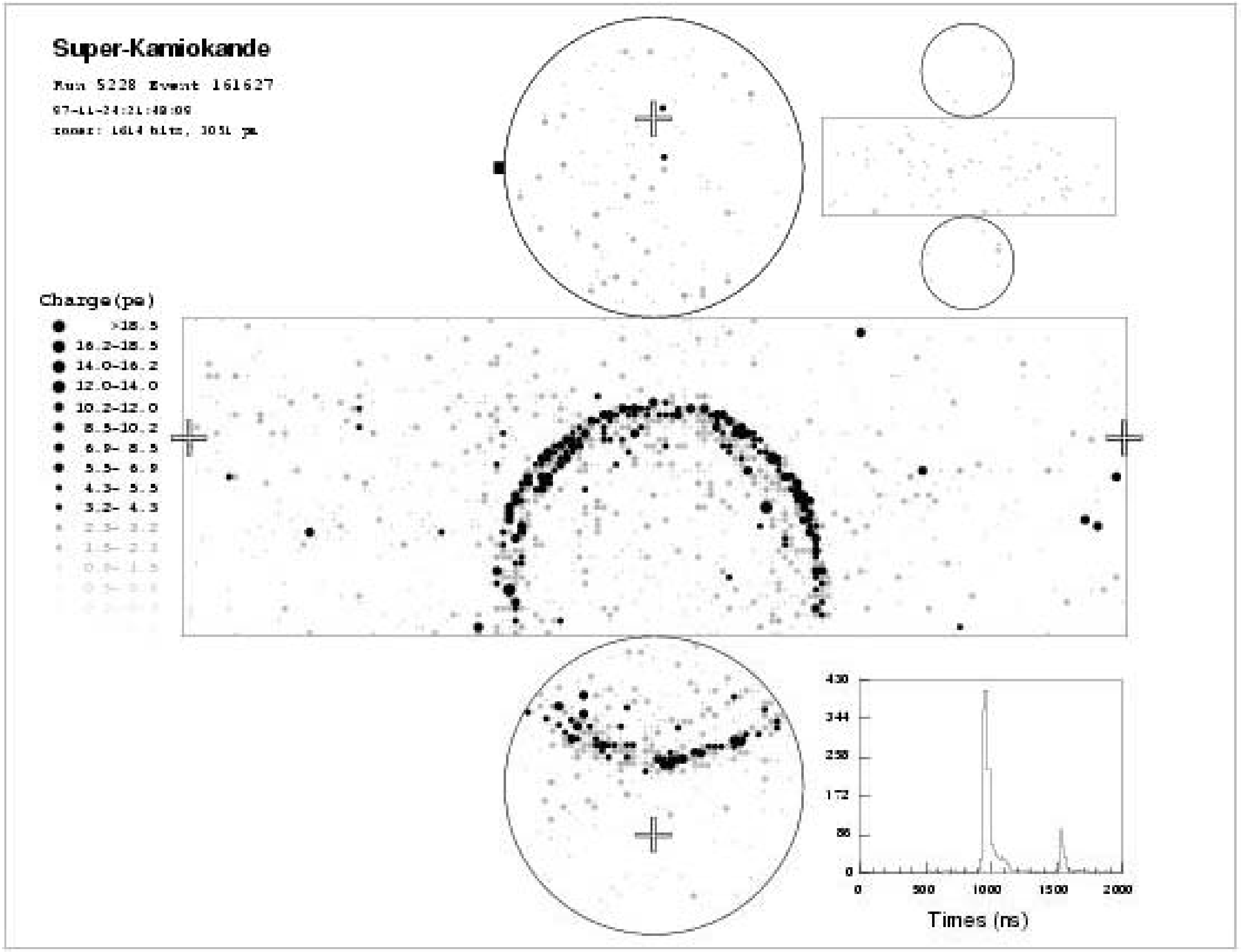

Cherenkov photons from an electron track

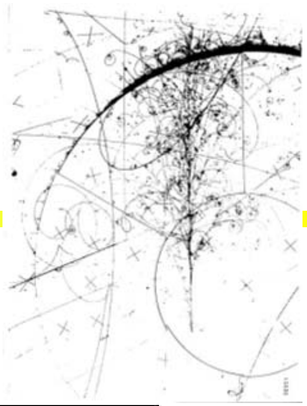

Electron starts a shower!

Cherenkov photons from an electron generated shower

Example: 1GeV el. neutrino

Shower length:

$L=X_0*\log_2(E/E_{crit})= 36cm*\log_2(1GeV/10MeV) =2.5m$

Shower particles are not parallel to each other

-> a blurred, less well defined "ring" on the walls

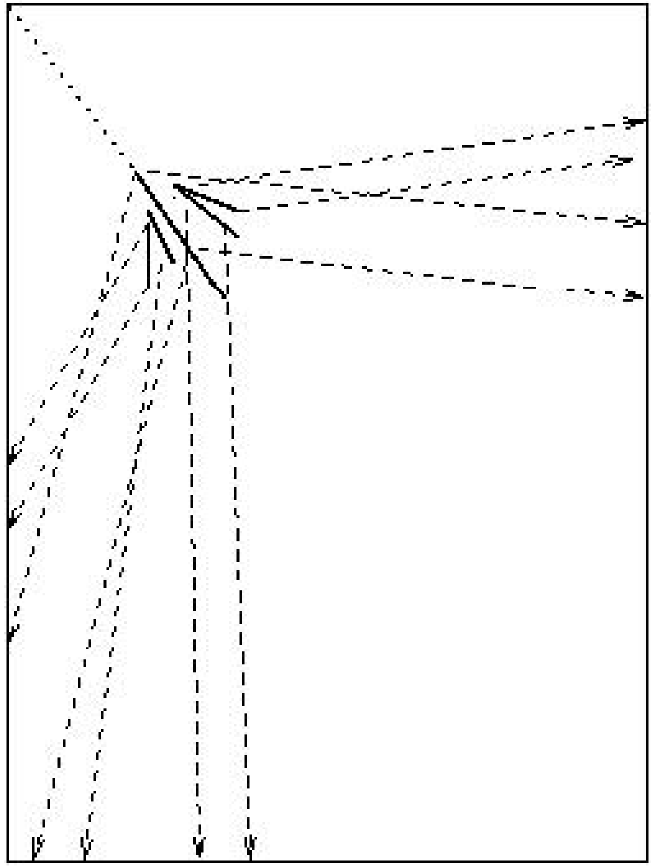

Electron event: blurred ring

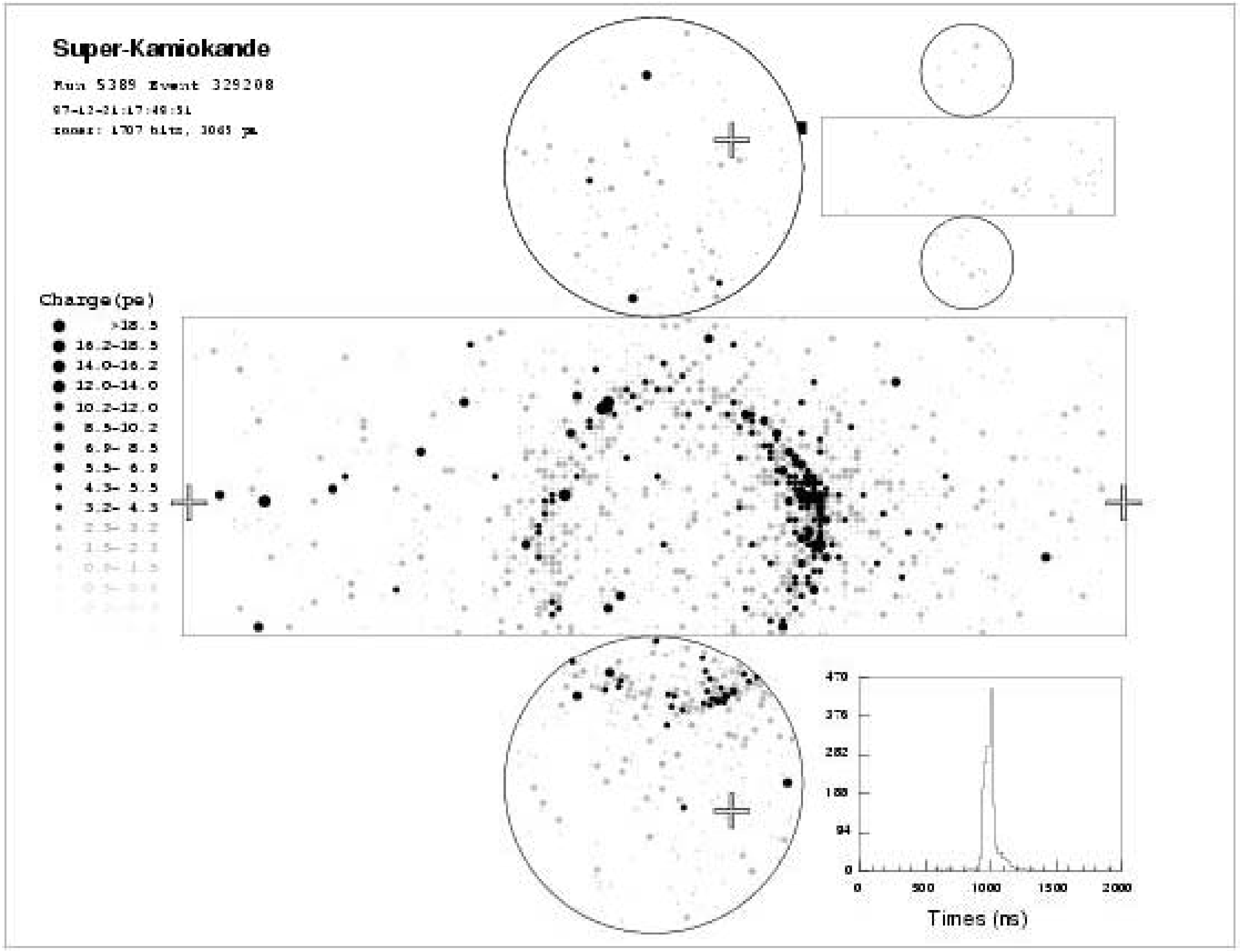

Detection of τ neutrinos

ν_τ **+ n → p +** τ^- τ^- **→** $\mu^- \nu_\mu \nu_\tau$

- Detect and identifiy mion
- Extrapolate back
- Check for a ‘kink’ in the sensitive volume – e.g. a thick photographic emulsion

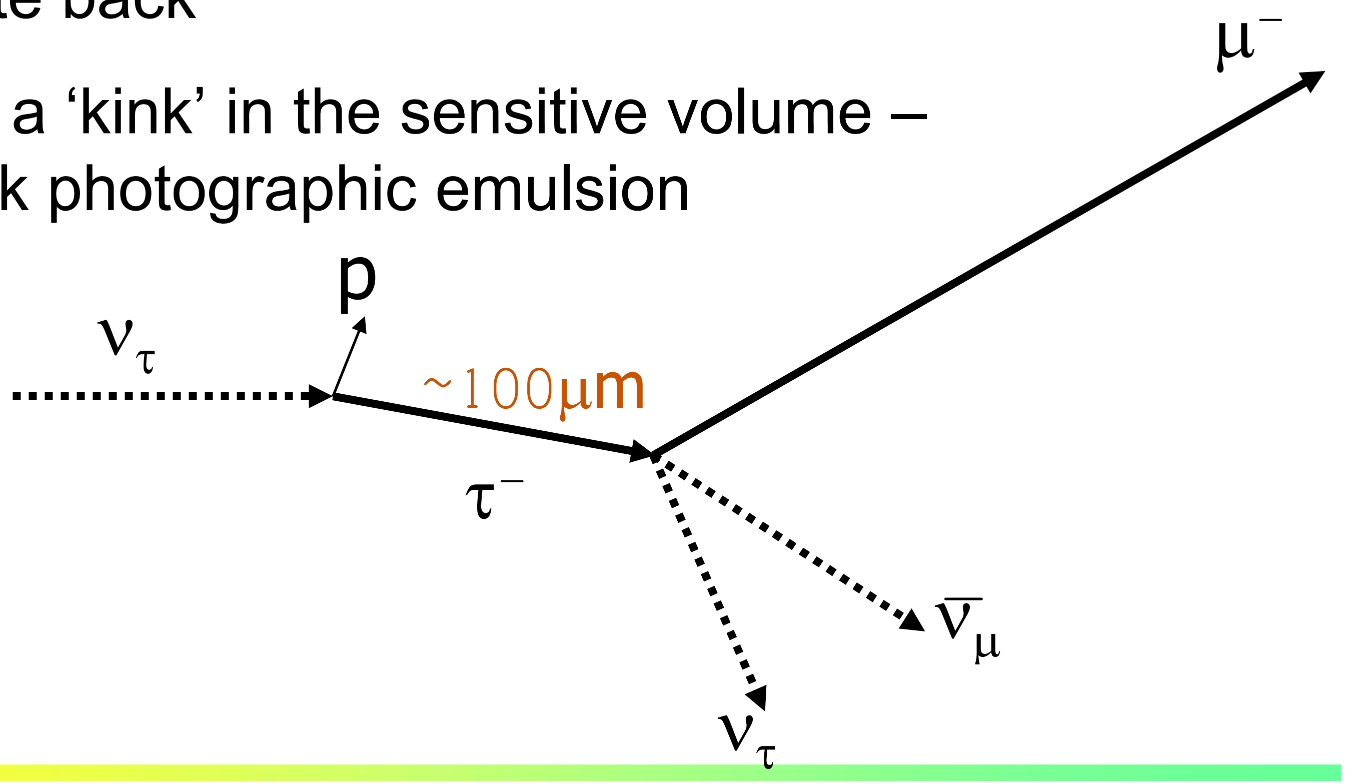

Detection of τ neutrinos: OPERA

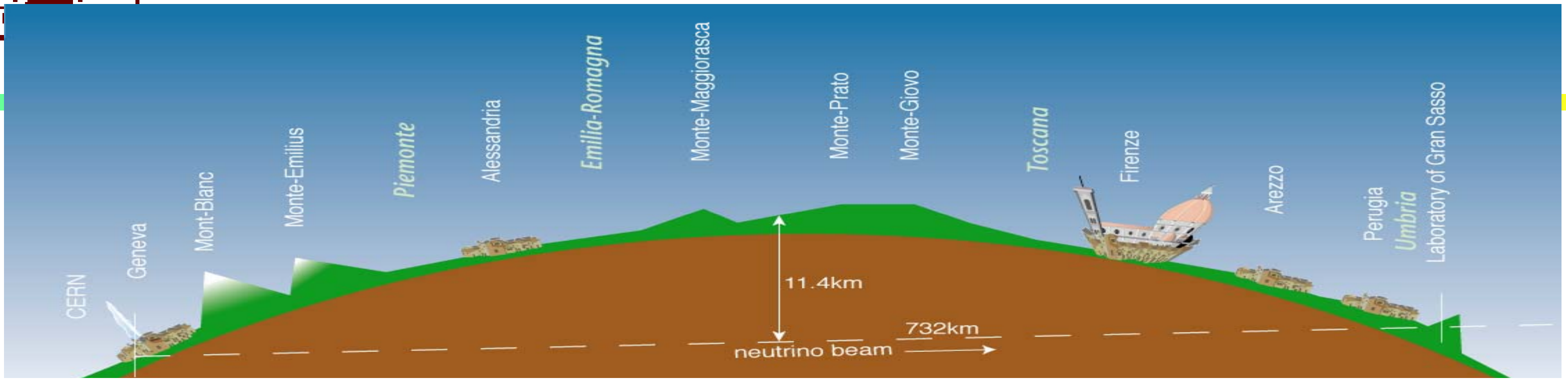

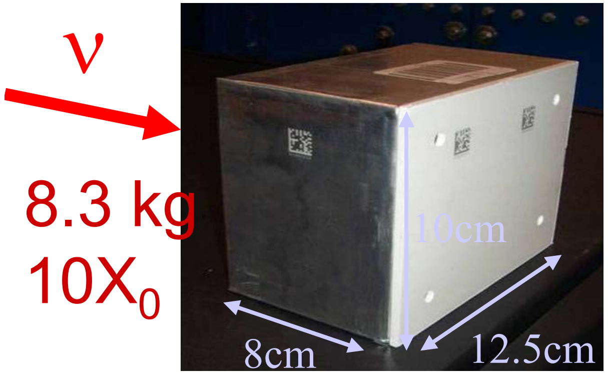

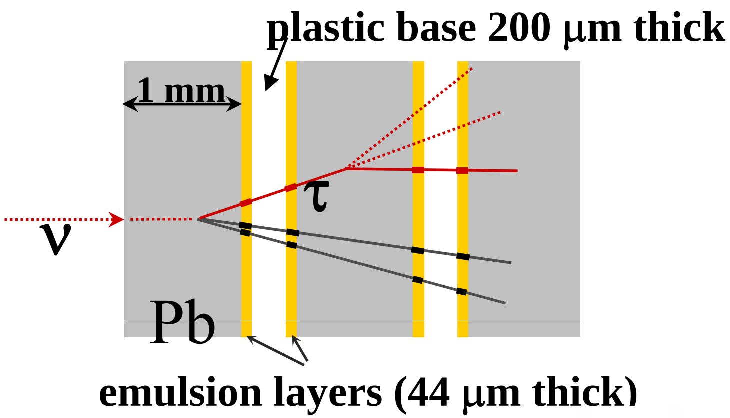

Detection unit: a brick with 56 Pb sheets (1mm) + 57 emulsion films

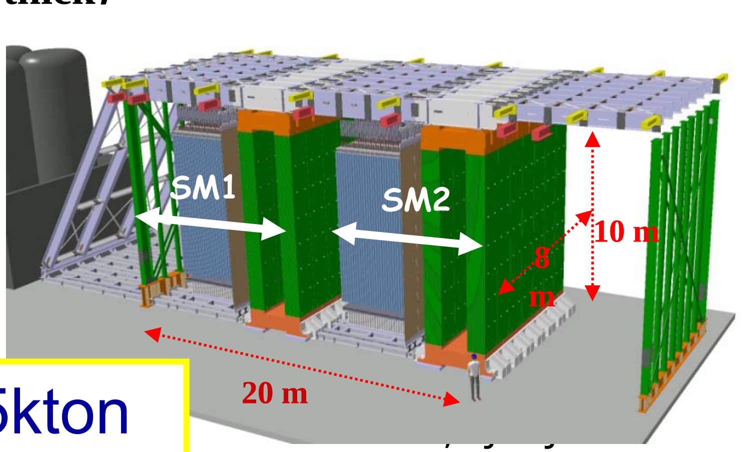

155000 bricks, detector tot. mass = 1.35kton

Detection of very high energy neutrinos (from galactic sources)

The expected fluxes are very low:

Need really huge volumes of detector medium!

What is huge? From $(100m)^3$ to $(1km)^3$

Also needed: directional information.

Again use: $\nu_\mu + n \rightarrow p + \mu^-$; μ direction coincides with the direction of the high energy neutrino.

AMANDA: use the Antarctic ice instead of water

- Normal ice is not transparent due to Rayleigh scattering on inhomogenuities (air bubbles)
- At high pressures (large depth) there is a phase transition, bubbles get partly filled with water-> transparent!
- Originally assumed: below 800m OK; turned out to be much deeper.

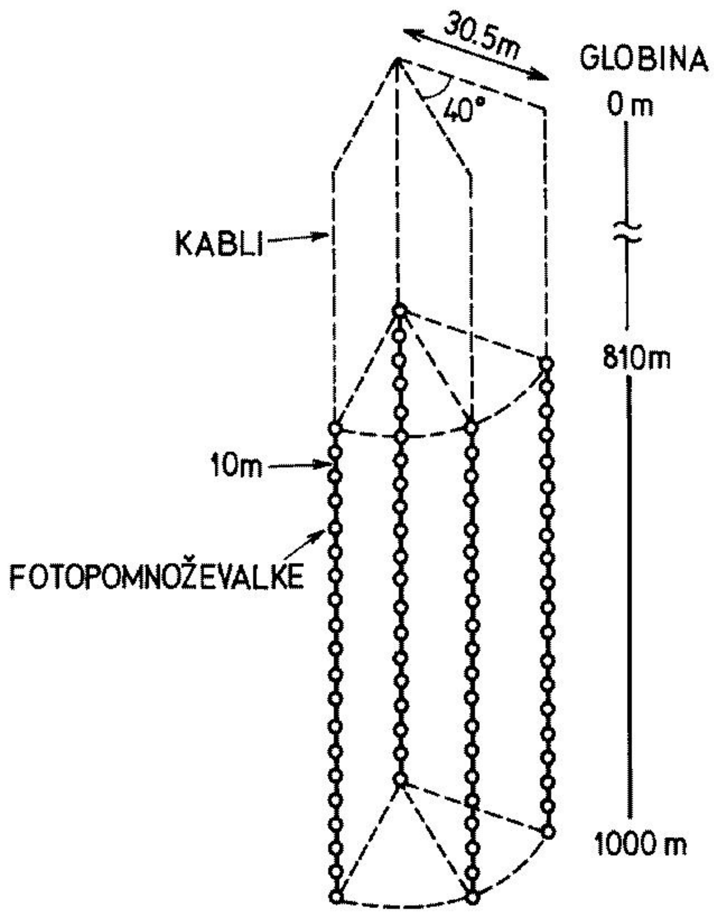

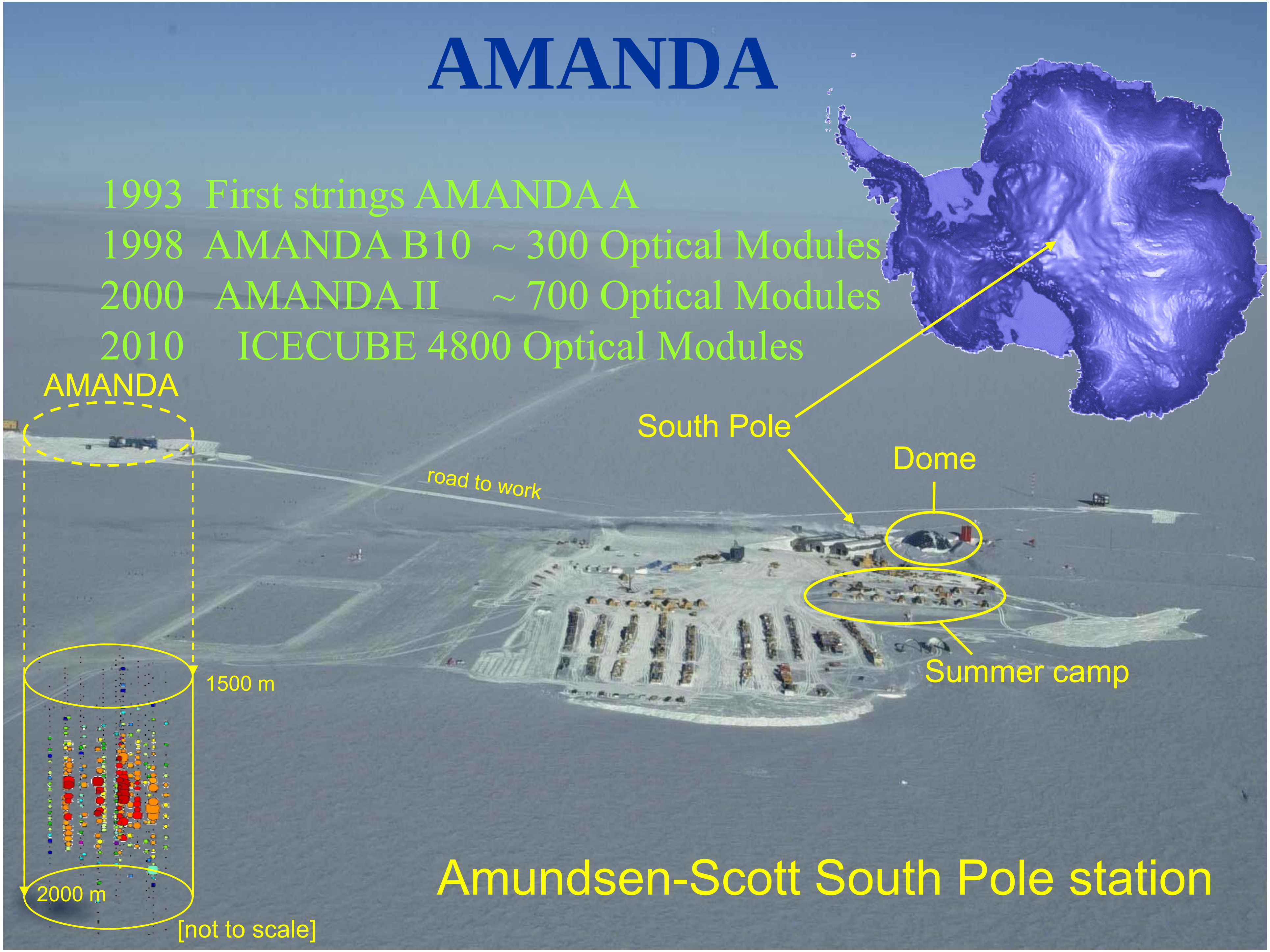
AMANDA
1993 First strings AMANDA A
1998 AMANDA B10 ~ 300 Optical Modules
2000 AMANDA II ~ 700 Optical Modules
2010 ICECUBE 4800 Optical Modules
AMANDA
road to work
South Pole
Dome
Summer camp
1500 m
2000 m
[not to scale]
Amundsen-Scott South Pole station

Reconstruction of direction and energy of incident high energy muon netrino

For each event:

Measure time of arrival on each of the tubes

Cherenkov angle is known: $\cos\theta=1/n$

Reconstruct muon track

Track direction -> neutrino direction

Track length -> neutrino energy

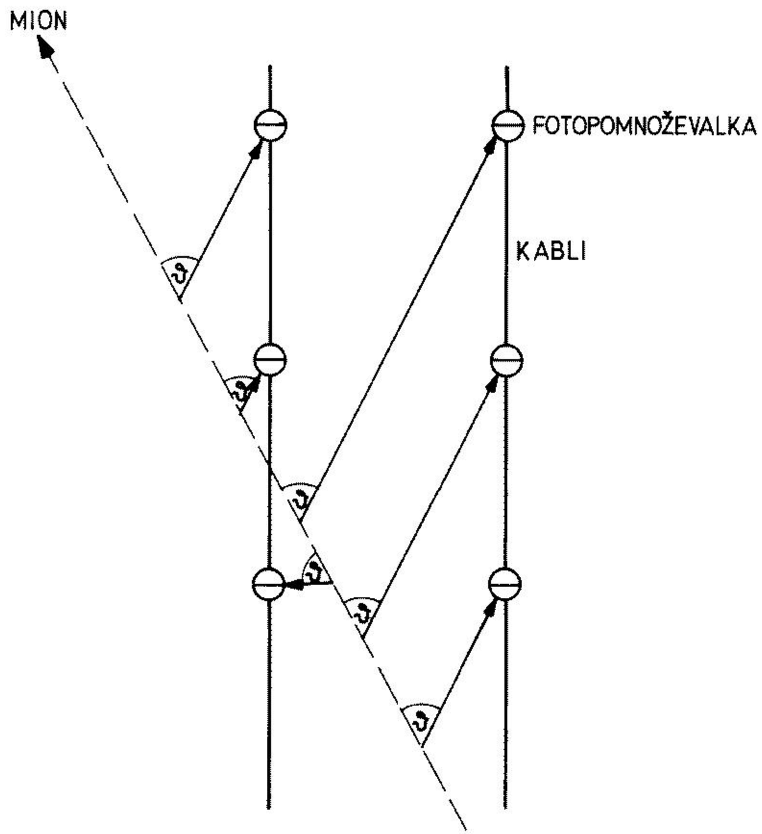

AMANDA

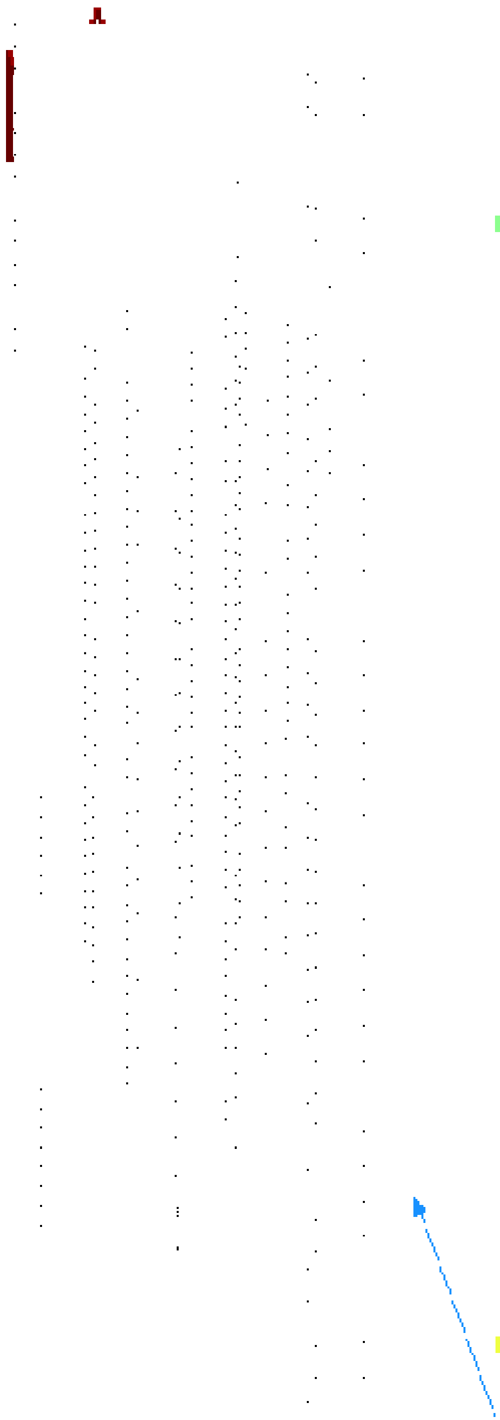

Example of a detected event, a muon entering the PMT array from below

Analysis of data

If we have N independent (unbiased) measurements x_i of some unknown quantity μ with a common, but unknown, variance σ^2, then

$$\widehat{\mu} = \frac{1}{N}\sum_{i=1}^{N} x_i$$

$$\widehat{\sigma^2} = \frac{1}{N-1}\sum_{i=1}^{N}(x_i - \widehat{\mu})^2$$

are unbiased estimates of μ and σ^2. The errors of the estimates are

- for μ: $\sigma/\sqrt{N}$
- for σ: $\sigma/\sqrt{(2N)}$ (for Gaussian distributed x_i and large N)

Analysis of data 2: unbinned likelihood fit

Assume now that we have N independent (unbiased) measurements x_i that come from a probability density function (p.d.f.) f(x; θ), where θ **= (**θ_1**, ...** θ_m**)** is a set of m parameters whose values are unknown. The method of maximum likelihood takes the estimators θ **to be those values of** θ **that maximize the likelihood function,**

$$L(\boldsymbol{\theta}) = \prod_{i=1}^{N} f(x_i; \boldsymbol{\theta}) \ .$$

It is easier to minize ln*L* (same minimum) → a set of m equations

$$\frac{\partial \ln L}{\partial \theta_i} = 0 \ , \qquad i = 1, \ldots, n \ .$$

Analysis of data 3

The errors and correlations between parameters $\theta=(\theta_1,....\theta_m)$ can be found from the inverse of the covariance matrix

$$(\widehat{V}^{-1})_{ij} = - \left.\frac{\partial^2 \ln L}{\partial\theta_i \partial\theta_j}\right|_{\widehat{\theta}}$$

The variance σ^2 on the paramter θ_i is V_{ii}

Analysis of data 4: binned likelihood fit

If the sample is large (high n), data can be grouped in a histogram. The content of each bin, n_i, is distributed according to the Poisson distribution with mean $\nu_i(\theta)$,

$$f(\nu_i(\theta), n_i) = \nu_i(\theta)^{n_i} \exp(-\nu_i(\theta)) / n_i!$$

The parameters θ are determined by maximizing a properly normalized likelihood function

$$-2\ln\lambda(\boldsymbol{\theta}) = 2\sum_{i=1}^{N}\left[\nu_i(\boldsymbol{\theta}) - n_i + n_i \ln\frac{n_i}{\nu_i(\boldsymbol{\theta})}\right]$$

In the limit of zero bin width, maximizing this expression is equivalent to maximizing the unbinned likelihood function.

Analysis of data 5: least squares method

If we have N independent measurements of variable $\mathbf{y_i}$ at points $\mathbf{x_i}$, and if y_i are Gaussian distributed around a mean $F(x_i, \theta)$ with variance σ_i^2 , the log likelihood function yields

$$\chi^2(\boldsymbol{\theta}) = -2\ln L(\boldsymbol{\theta}) + \text{ constant } = \sum_{i=1}^{N} \frac{(y_i - F(x_i;\boldsymbol{\theta}))^2}{\sigma_i^2}$$

and the parameters θ are determined by minimizing this expression.

This weighted sum of squares can be used in a general case of a non-Gaussian distribution → Least squares method

Analysis of data 6: least squares method

The value of χ^2 at the minimum is an indication of the goodness of fit. The mean of χ^2 should be equal to the number of degrees of freedom, n = N-m, where m is the number of parameters. Popular: quote χ^2/n

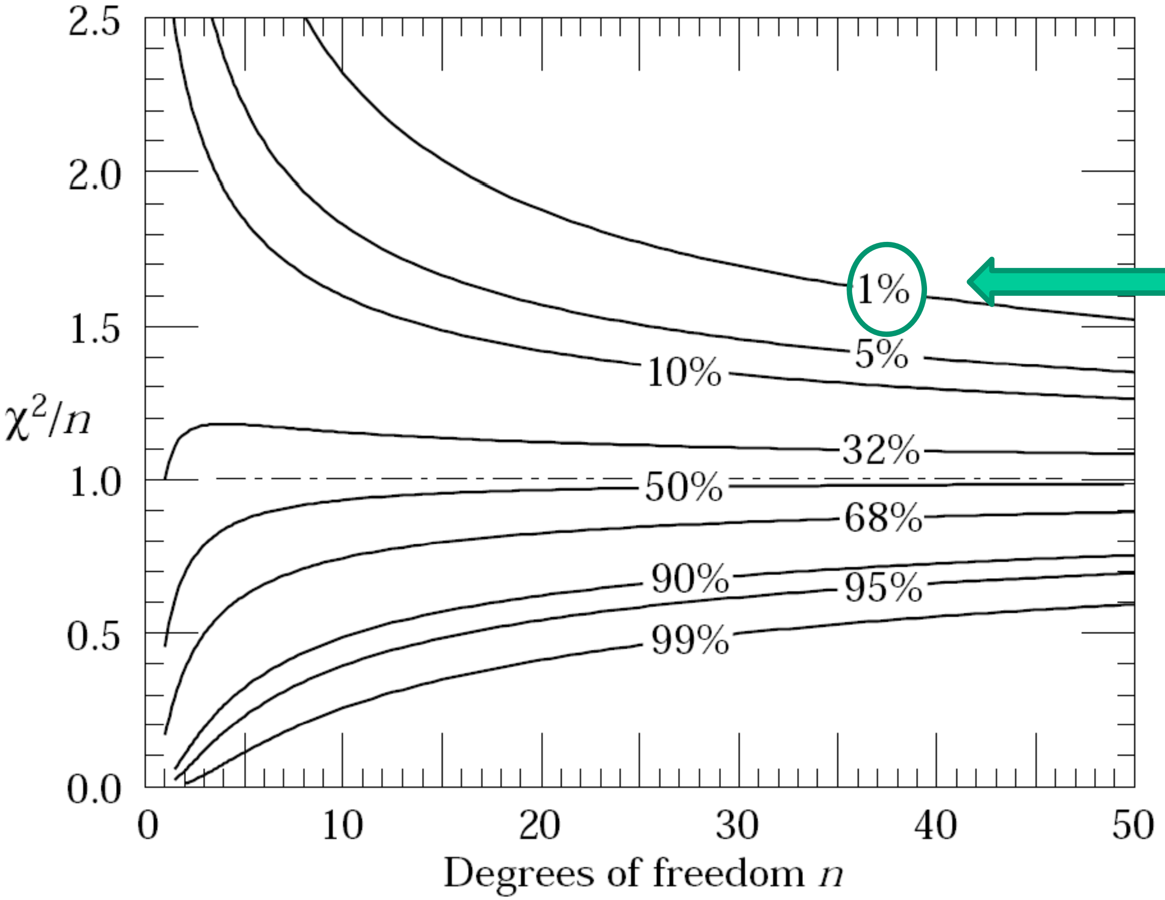

Probability that the fit would give χ^2/n bigger than the observed value

Contents of this course

- Lecture 1: Introduction, experimental methods, detectors, data analysis
- Lecture 2: Selection of particle physics experiments

http://www-f9.ijs.si/~krizan/sola/nagoya-ise/

- Slides
- Literature

Backup slides

Gas mixtures for drift chambers and MWPCs

Main component: a gas with a low average ionisation energy W_i - nobel gases have less degrees of freedom.

Add to this:

- A component which absorbs photons ('quencher') produced in the avalanche (deexcitation of atoms and ions) – an organic molecule with a lot of degrees of freedom: isobutane, methane, CO_2, ethane
- A component which prevents that ionized organic molecules would travel to the cathode, stop there, and polymerize to form poorly conductive layers: a gas which has a low ionisation energy - methylal
- A small concentration of an electronegative gas (freon, ethylbromide) which prevents the electrons travel too far (to prevent that electrons which escaped from the cathode start new avalanches) allows to work at high gains (10^7)

'Magic mixture': 72% Ar, 23.5% isobutane, 4% methylal, 0.5% freon

Time-of-flight measurement 3

Resolution of a PMT: transient time spread (TTS), time variation for single photons

Tubes for TOF have to be optimized for small TTS.

Main contribution after the optimisation: photoelectron time spread before it hits the first dynode.

Estimate: take two cases, one with T=1eV and the other with T=0 after the photoelectron leaves the photocathode; take U=200V and d=10mm

T=1eV: $v_0 = \sqrt{(2T/m)} = 0.002\ c$, $a=F/m=200eV/(10mm\ 0.5\ 10^6 eV/c^2)$

$d = v_0 t + at^2/2 \rightarrow t = \sqrt{(2d/a+(v_0/a)^2)} - v_0/a$

T=0eV : $v_0 = 0 \rightarrow t=\sqrt{(2d/a)}=2.3ns$

Time difference: 170ps is a typical value.

Good tubes: σ(TTS)=100ps

For N photons: $\sigma \sim \sigma(TTS) / \sqrt{(N)}$

TOF capability: window photons

Expected number of detected Cherenkov photons emitted in the PMT window (2mm) is ~15

→ Expected resolution ~35 ps

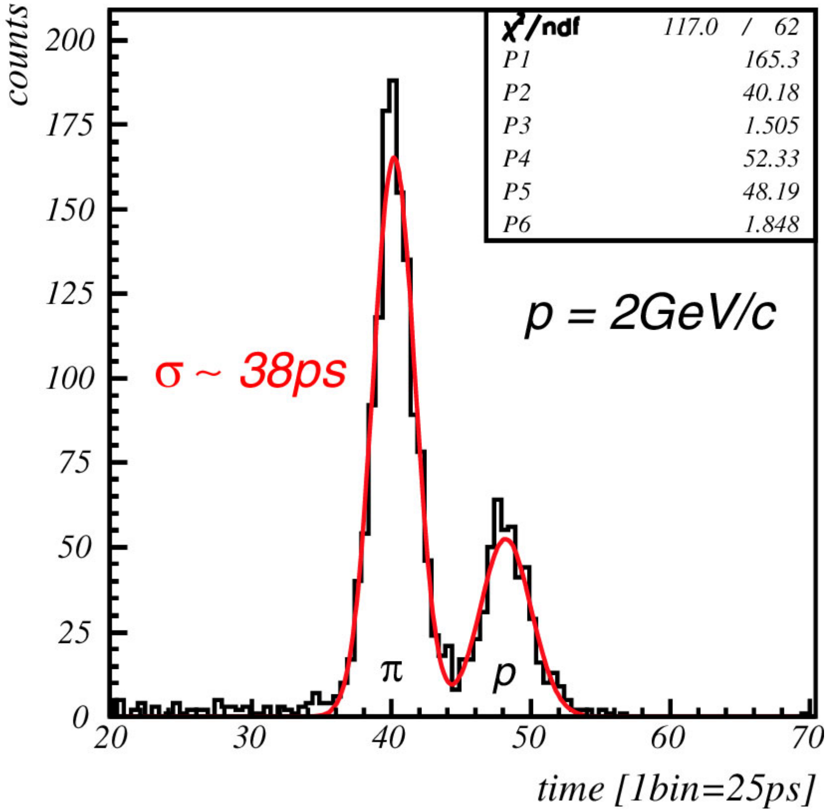

TOF test with pions and protons at 2 GeV/c.
Distance between start counter and MCP-PMT is 65cm

→ In the real detector ~2m
→ 3x better separation

Components of an experimental apparatus (‘spectrometer’)

- Tracking and vertexing systems
- Particle identification devices
- Calorimeters (measurement of energy)

Calorimetry Design: B factories

Requirements

•Best possible energy and position resolution: 11 photons per Y(4S) event; 50% below 200 MeV in energy

•Acceptance down to lowest possible energies and over large solid angle

•Electron identification down to low momentum

Constraints

•Cost of raw materials and growth of crystals

•Operation inside magnetic field

•Background sensitivity

Implementation

Thallium-doped Cesium-Iodide crystals with 2 photodiodes per crystal

Thin structural cage to minimize material between and in front of crystals

Calorimetry: BaBar

6580 CsI(Tl) crystals with photodiode readout

About 18 X_0, inside solenoid

$$\frac{\sigma(E)}{E} = \frac{(2.32 \pm 0.03 \pm 0.3)\%}{\sqrt[4]{E}} \oplus (1.85 \pm 0.07 \pm 0.1)\%$$

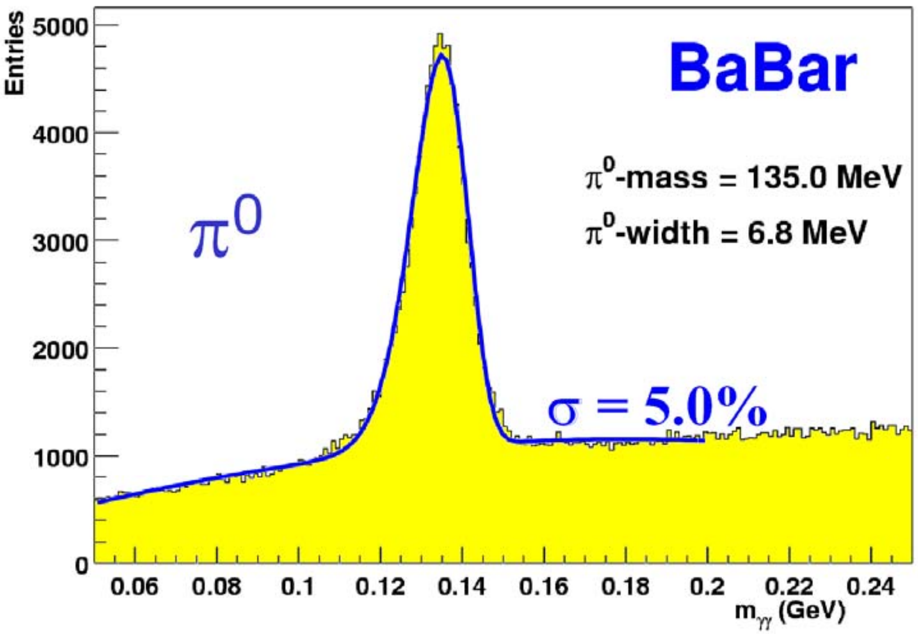

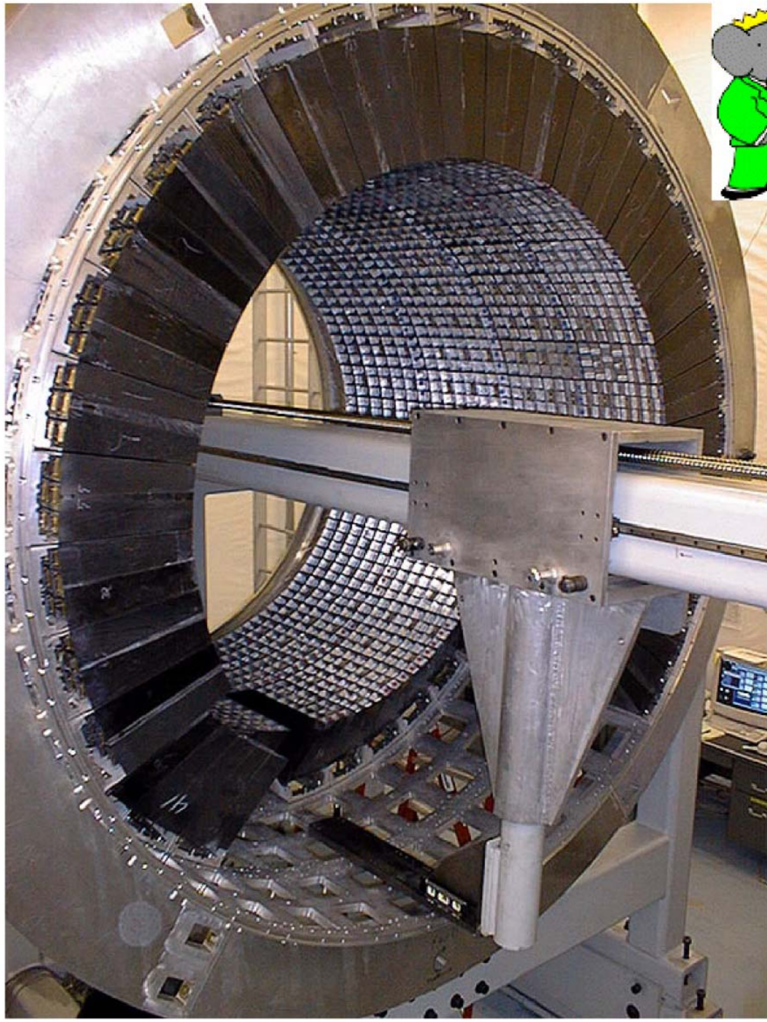

Belle central drift chamber

- 50 layers of wires (8400 cells) in 1.5 Tesla magnetic field
- Helium:Ethane 50:50 gas, Al field wires, CF inner wall with cathodes, and preamp only on endplates
- Particle identification from ionization loss (5.6-7% resolution)

$$\frac{\sigma(p_T)}{p_T} = 0.19\% \times p_T \oplus \frac{0.30\%}{\beta}$$

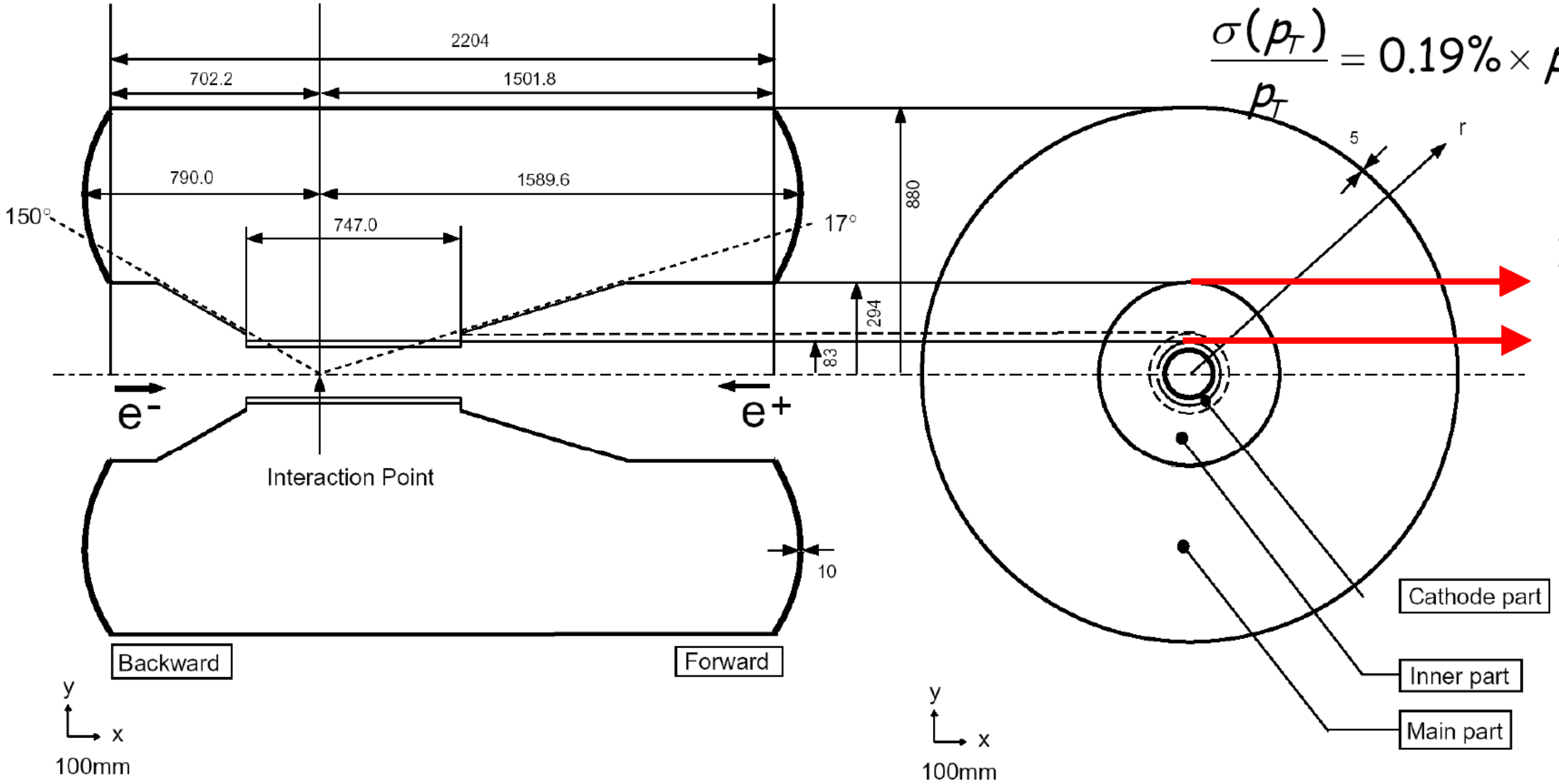

15 layers:
8.8-22.4
cm radius

Tracking: BaBar drift chamber

40 layers of wires (7104 cells) in 1.5 Tesla magnetic field

Helium:Isobutane 80:20 gas, Al field wires, Beryllium inner wall, and all readout electronics mounted on rear endplate

Particle identification from ionization loss (7% resolution)

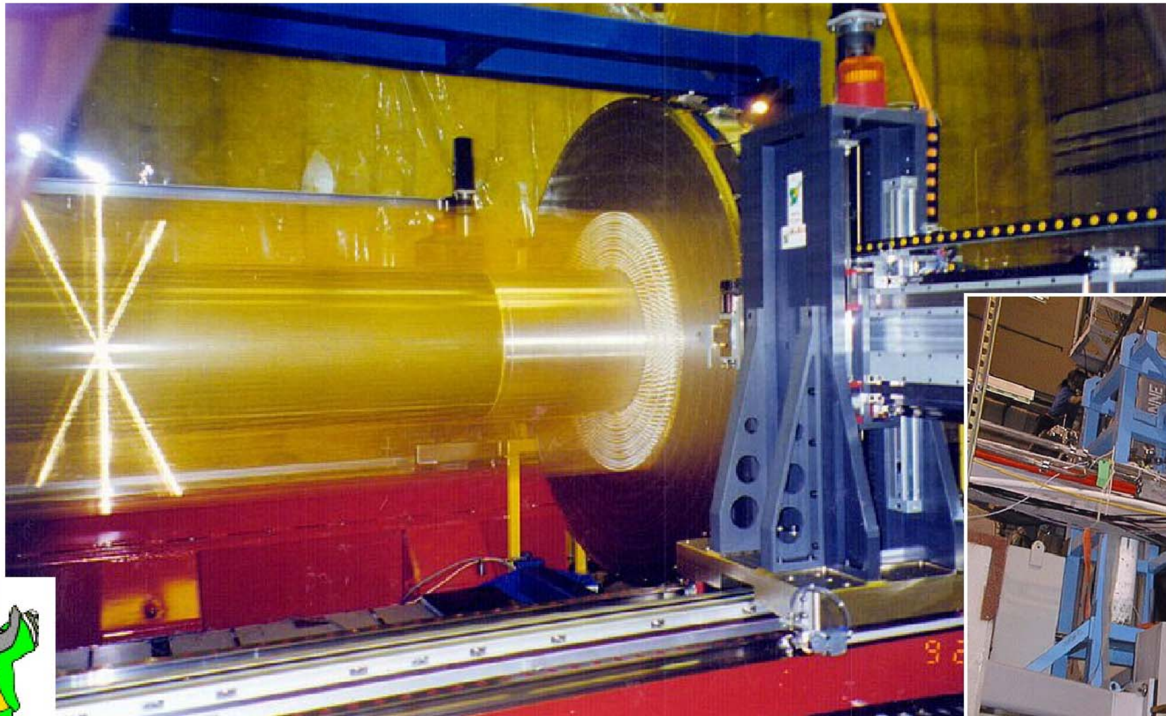

16 axial, 24 stereo layers

$$\frac{\sigma(p_T)}{p_T} = 0.13\% \times p_T + 0.45\%$$

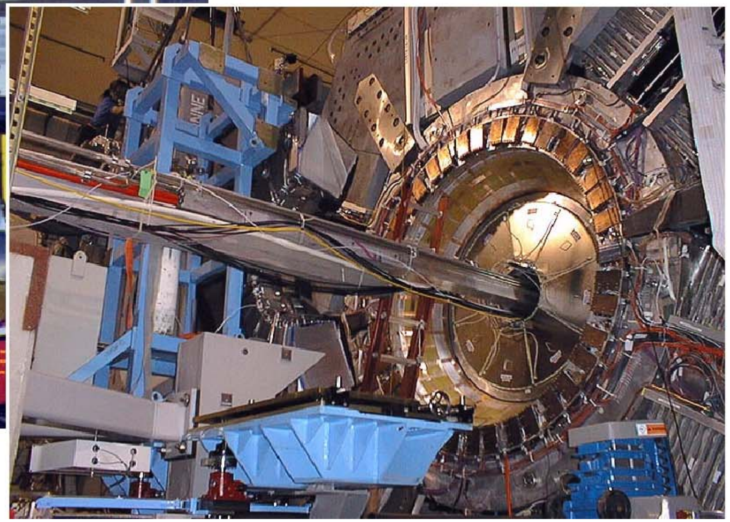

TRT performance

at 90% electron efficiency

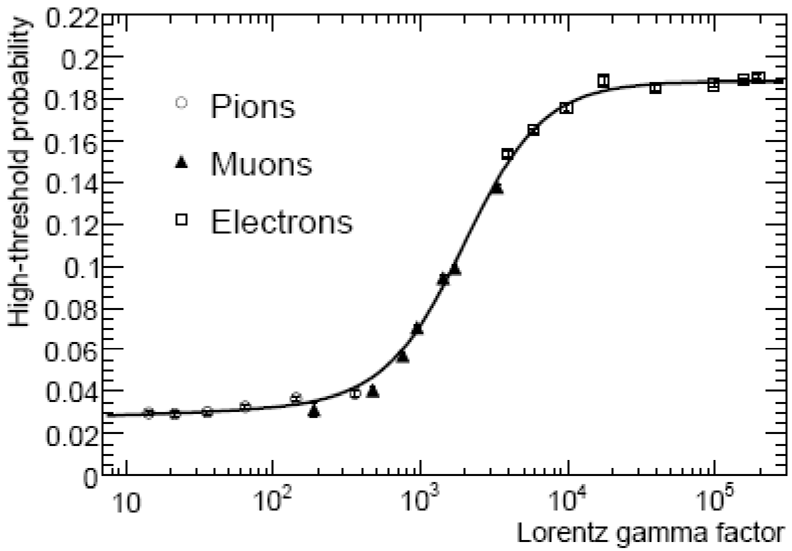

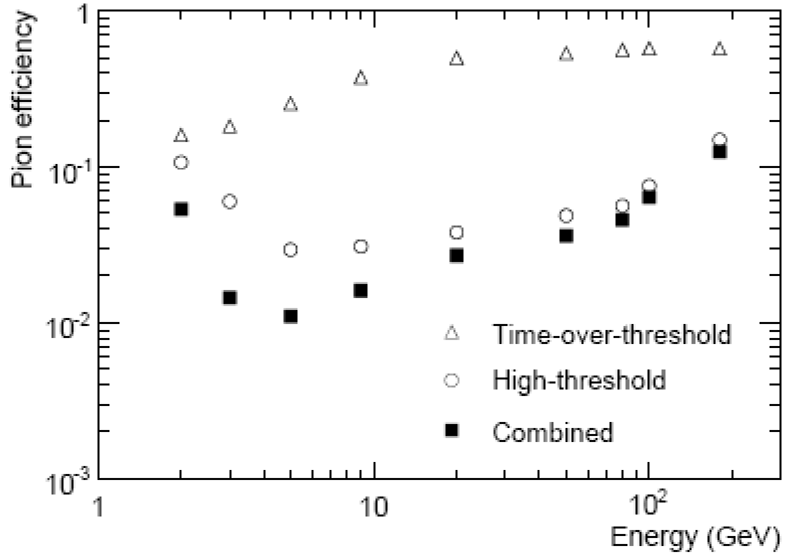

Figure 10.25: Average probability of a high-threshold hit in the barrel TRT as a function of the Lorentz γ-factor for electrons (open squares), muons (full triangles) and pions (open circles) in the energy range 2–350 GeV, as measured in the combined test-beam.

Figure 10.26: Pion efficiency shown as a function of the pion energy for 90% electron efficiency, using high-threshold hits (open circles), time-over-threshold (open triangles) and their combination (full squares), as measured in the combined test-beam.

ATLAS: muon fake probability

Sources of fakes:

-Hadrons: punch through negligible, >10 interaction legths of material in front of the muon system (remain: muons from pion and kaon decays)

-Electromagnetic showers triggered by energetic muons traversing the calorimeters and support structures lead to low-momentum electron and positron tracks, an irreducible source of fake stand-alone muons. Most of them can be rejected by a cut on their transverse momentum (pT > 5 GeV reduces the fake rate to a few percent per triggered event); can be almost entirely rejected by requiring a match of the muon-spectrometer track with an inner-detector track.

- Fake stand-alone muons from the background of thermal neutrons and low energy g-rays in the muon spectrometer ("cavern background"). Again: pT > 5 GeV reduces this below 2% per triggered event at 10^{33} cm^{-2} s^{-1}. Can be reduced by almost an order of magnitude by requiring a match of the muon-spectrometer track with an inner-detector track.